Protecting Our Investment: Solving Fast Response Cutter Corrosion

by

Isabelle Claire Patnode
B.S., U.S. Coast Guard Academy (2016)

Submitted to the Department of Mechanical Engineering
in partial fulfillment of the requirements for the degree of
Master of Science in Mechanical Engineering
at the
MASSACHUSETTS INSTITUTE OF TECHNOLOGY
June 2023

Author .....
Isabelle Claire Patnode
Department of Mechanical Engineering
May 12, 2023

Certified by .....
Steven B. Leeb
Professor
Thesis Supervisor

Certified by .....
Erik K. Saathoff
Doctoral Candidate
Thesis Supervisor

Accepted by .....
Nicolas G. Hadjiconstantinou
Chairman, Mechanical Engineering Committee on Graduate Studies

Protecting Our Investment: Solving Fast Response Cutter Corrosion

by

Isabelle Claire Patnode

Submitted to the Department of Mechanical Engineering
on May 12, 2023, in partial fulfillment of the
requirements for the degree of
Master of Science in Mechanical Engineering

Abstract

The USCG Fast Response Cutter (FRC) fleet is experiencing corrosion at an alarming rate in the propulsion shaft tunnels. An investigation into this problem was conducted from the perspectives of "root cause" and "prevention." Root causes for the corrosion stem from an interaction in a complex, two-stage galvanic protection system onboard the ship that uses both passive zinc protection and impressed current cathodic protection (ICCP) from an active, feedback-controlled power supply. By using custom measuring instruments and applying them on an in service FRC in order to better understand the complications with galvanic protection on the FRC, crucial insights were discovered. The ICCP power supply unit is intended to prevent corrosion by actively injecting current through anodes in order to raise the magnitude of the voltage measured between the reference electrode and the hull. When designing the FRC, it was expected that a combination of ICCP and passive zincs would protect the hull steel in tandem; however, this has not been the case along the entirety of the ship. The ICCP system is unable to accurately determine the reference potential, a useful indicator for whether the hull steel is adequately protected from corrosion, in every area of the ship, allowing some areas to corrode at an accelerated rate. This report details a full summary of analysis and results, along with a review of laboratory experiments and field experiments with several FRCs in the USCG fleet concluding with specific, actionable suggestions for mitigating corrosion in the FRC stern tube. Additionally, this report outlines how non-intrusive load monitoring, which has a proven track record for preemptively recognizing faults in shipboard equipment, analyzed the ICCP system and how this relates to shipboard microgrids.

Thesis Supervisor: Steven B. Leeb
Title: Professor

Thesis Supervisor: Erik K. Saathoff
Title: Doctoral Candidate

Acknowledgments

First and foremost, I want to thank my husband Frank for being by my side and guiding me through the past 2 years. Thank you for believing in me even when I did not believe in myself. Your constant support and love kept me going through every tough day and I could not have done this without you. I would also like to acknowledge the constant support from all of my family and friends. To my parents, thank you for encouraging me and setting me up throughout life to be able to reach this accomplishment. You always pushed to "do what is hard" and go for my biggest dreams. To Garrett and Caroline, I am so proud of the people you have grown into and am grateful for the constant facetime calls, visits, and laughs the past two years. I would like to thank the US Coast Guard for allowing me to continue my academic pursuits, as well as the American Society of Naval Engineers (ASNE), The Grainger Foundation, and the Office of Naval Research NEPTUNE program for their financial assistance. Thank you Professor Leeb for challenging me and pushing me beyond what I thought was possible. I am so grateful you saw potential in me and pushed me and the team to accomplish this monumental task. Being able to share our research with the Coast Guard in Norfolk, VA was one of the most exciting days of my Coast Guard career and the importance of our contribution will follow with us for years to come. Thank you Erik for painstakingly guiding me through all things electrochemistry. Your knowledge and expertise was the glue that held our team together and I am so grateful. Thank you to all of my fellow LEES-GEM students: Mike, Jake, and Aaron. Thank you to all of the crews of STURGEON, WILLIAM CHADWICK, CHARLES SEXTON, and MARGARET NORVELL. I want to give special thanks to CDR DiPace, LT Luebke, and CWO Maddex for all of your technical shipboard expertise that helped make this project possible.

THIS PAGE INTENTIONALLY LEFT BLANK

Contents

THIS PAGE INTENTIONALLY LEFT BLANK

List of Figures

List of Tables

THIS PAGE INTENTIONALLY LEFT BLANK

Acronyms

AIO "All-In-One".

COMDTINST Commandant Instruction.

DAQ Data Acquisition Unit.

DCMS Deputy Commandant for Mission Support.

DFT Discrete Fourier Transform.

ECC Engineering Control Center.

ESD Engineering Services Division.

FDD Fault Detection & Diagnostics.

GUI Graphical User Interface.

IEPE Integrated Electronics Piezoelectric.

IoT Internet of Things.

MES Mean Envelope Spectrum.

MPDE Main Propulsion Diesel Engine.

MPG Main Propulsion Generator.

NILM Nonintrusive Load Monitor.

PSD Power Spectral Density.

SF Ship's Force.

SFLC Surface Forces Logistics Center.

SHP Shaft Horsepower.

SSDG Ship Service Diesel Generator.

TCP Transmission Control Protocol.

UDP User Datagram Protocol.

USCGC United States Coast Guard Cutter.

WPA2 Wi-Fi Protected Access II.

Chapter 1

USCG Fast Response Cutter Corrosion and Cathodic Protection Schemes

The United States Coast Guard commissioned their first Sentinel Class Fast Response Cutter in April of 2012 [1]. An image of this class of cutter is seen below in Figure 1-1. These cutters each wear the name of an instrumental Coast Guard member who has performed an act of great valor. The Sentinel class of ships is intended to replace the legacy patrol boat class cutters and simplify the fleet of patrol boats used by the US Coast Guard. Each ship costs nearly $74 million and is a very important investment to the Department of Homeland Security [1]. This class of ship is 154 ft long and has a crew of about 30 people. With a semi-planning hull, it can reach speeds much greater than the patrol boats the FRC is replacing. These cutters are located in every Coast Guard district and it is estimated that over 100 ships will be delivered in the following century [1]. The FRC is one of the Coast Guard's largest investments and ensuring the cutters can last for their entire life cycle is critical to operators, engineers, and the Department of Homeland Security. (This chapter is co-written with Michael Bishop.)

By having the capability to "semi-plane", the shape of the FRC hull is uniquely designed; specifically, the location where the shaft exits the hull is much further forward than a typical displacement hull. A carbon steel stern tube encompasses the

Figure 1-1: Newly Commissioned Fast Response Cutter [1]

stainless steel shaft from the point of exit, called the shaft seal, to the propeller. The area between the shaft and the stern tube is filled with seawater which is necessary to lubricate two water film bearings. Soon after this cutter was deployed, excessive hull degradation was noticed by dry dock availability managers. Quickly those charged with depot-level maintenance recognized a problem specifically located in the stern tube bearing housings; excessive corrosion with deep pits. This corrosion seemed more severe than typical corrosion related to steel hulls. This Chapter focuses on discussing the problem statement of corrosion in the stern tube, the various methods attempting to prevent corrosion onboard the FRC, and the problems that can stem from overusing these protective measures [2].

1.1 Problem Statement

Figure 1-2 is an up close image of the FRC stern tube bearing housing after being taken out of the water, but before it has been sand blasted. This image clearly highlights the intense corrosion this area is experiencing and how much metal has subsequently disappeared.

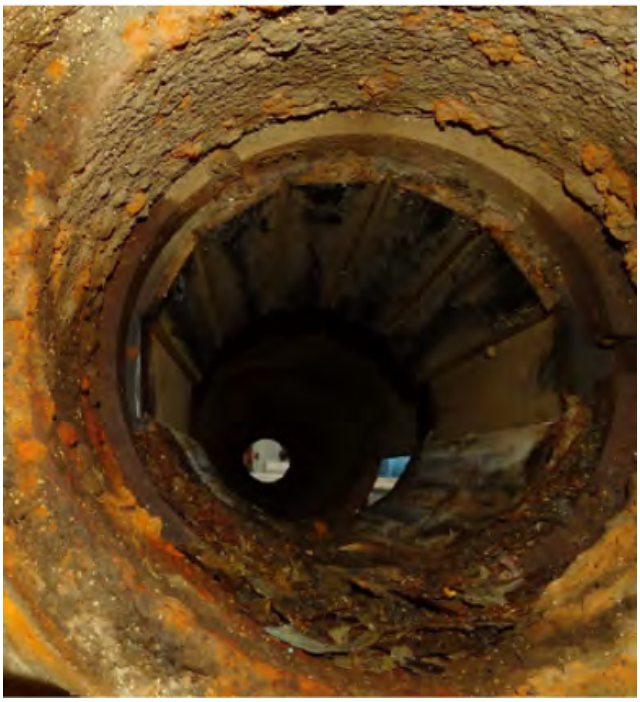

Figure 1-2: FRC Bearing Housing immediately after dry docking

After the initial inspection following a dry docking, the bearing housing is sand-blasted to better inspect the corroded area. In Figure 1-3 the deep pits are revealed. This degradation leaves the FRC with serious structural concerns. This corrosion appeared very different than typical corrosion experienced with carbon steel ships which lead to a number of unsubstantiated theories as to why the pits were forming [2]. In order to repair this area properly, the entire stern tub must be cut off of the cutter, and a new formed stern tube is welded on. Temporary repairs are possible by filling the holes with an epoxy-like substance (Belzona), however this is not a permanent fix, and the corrosion will quickly continue once the ship is back in the water. The corrosion was and will continue to get worse in this area, and with each dry dock, it was becoming increasingly clear that the shaft tubes would need to be continually cut out and replaced throughout the life cycle of the ship. These replacements would be an enormous cost for the US Coast Guard.

By design, the FRC has two systems providing cathodic protection to alleviate the corrosion of the hull steel in seawater. The first system is passive, meaning once it is installed, nothing changes, and it acts without a power source. This system

is accomplished through using zinc anodes which are installed throughout different areas of the hull [3]. The second system is active, meaning it responds to changes in voltage readings and is supplied via a power source. This system is an impressed current cathodic protection system (ICCP) designed by Cathelco [3]. These two systems are intended to work in tandum, however it is clear to the Coast Guard that something is going wrong. From here, a deeper dive into how each protection system works, the maintenance cycle, and a fleet field review is accomplished.

(a) Close-up view of sand blasted bearing housing.

(b) Wide view of sand blasted bearing housing.

Figure 1-3: FRC Bearing Housing following dry dock inspection and initial sand blast

1.2 The Importance of Zinc

As previously stated, the FRC has numerous zincs located throughout the hull. Figure 1-4 shows two zinc anodes installed on the stern gate of the FRC. Similar zinc anodes are installed on the propeller, in the shaft stern tube, and in the bow thruster tunnel. The zinc anodes act as a sacrificial metal in a cathodic protection scheme [4]. The zinc acts as an anode in the electrochemical cell between the carbon steel and the zinc. The zinc then deteriorates and is sacrificial as designed, rather than the carbon steel deteriorating which is the important part of the electrochemical cell [4].

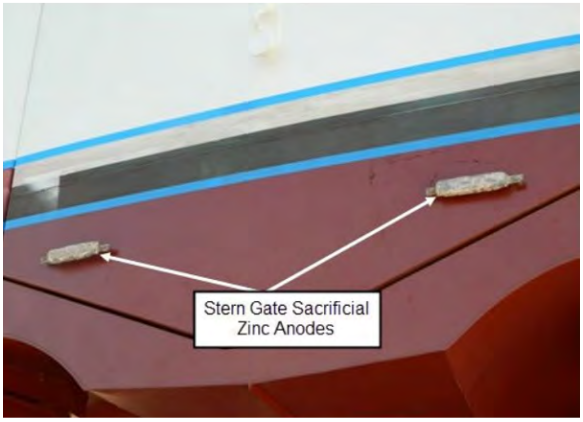

Figure 1-4: New Stern-gate Zinc Anodes

The presence of zinc anodes lowers the reference potential in the immediate area to a value closer to -1.0V based on a Ag/AgCl reference electrode, the type of electrode all reference potentials in this report are measured against. [3]. If there is no zinc in the area, the reference voltage will reach the steel's corrosion potential, E_{corr}, which is a value of around -0.65 V when it is just carbon steel submerged in salt water. Figure 1-5 shows zinc anodes retrieved from USCGC Margaret Norvell after one year of wear. It is clear that these zinc anodes are over-worn and provide very limited protection for the hull steel area they are closely connected to, allowing the hull steel to corrode since the zincs have already been wholly deteriorated [5].

(a) Forward Stern Tube Cover Zincs

(b) Middle Stern Tube Cover Zincs

Figure 1-5: Stern Tube Zinc Anodes removed after 1 year of wear

1.3 Zinc Maintenance Cycle

Due to the unique nature of the stern tube housing, zinc anodes needed to be installed along the inside of the hull tube through access covers seen in Figure 1-6. These stern tube covers are accessible in the water via a diver who will unbolt the cover, remove the old zinc anodes, install new zinc anodes, and reinstall the cover plate.

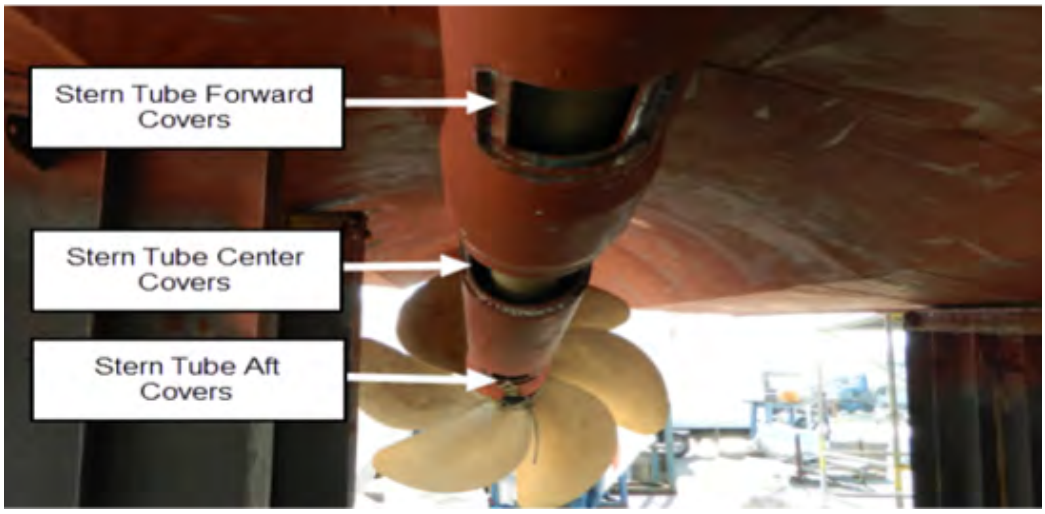

Figure 1-6: Stern Tube zinc replacement locations

The FRC was originally designed to have divers replace zinc anodes once every two years. The Coast Guard quickly noticed that there was no zinc remaining prior to replacement, so the maintenance cycle was increased to once every year [6].Despite this change, the zinc anodes were still severely deteriorated after one year in use,, demonstrating that this passive system was providing nearly zero protection in the stern tube housing by the end of the maintenance cycle. This is not the case in every area of the ship. Figure 1-7 shows the zinc anodes removed from the bow thruster tunnel and the propeller zincs after one year. These zinc anodes would still provide protection to the carbon steel hull and are in good condition.

Figure 1-7: Bow Thruster and Propeller Zinc Anodes removed 1 year after installation

Since these findings suggest that the zincs were no longer giving any cathodic protection to the hull steel in the stern tube, the second cathodic protection measure should be activated to provide protection. This prompted a fleet field investigation to gather information on how the ICCP system is assisting the cutter.

1.4 Fleet Investigation

A fleet investigation was conducted to determine how effectively the ICCP systems are working on the FRC. Specifically, the investigation considered CGC Lawrence Lawson, CGC Charles Sexton, CGC Nathan Bruckenthal, AND CGC William Chadwick. Each cutter located in a different home port so a variety of temperatures and salinity profiles were experienced. Figure 1-8 shows examples from the cutter logs. From each cutter, the logs indicated that the ICCP was providing nearly zero protection current.. Essentially, the ICCP system is inactive and not providing any active protection for the cutter.

Cathelco ICC

Vessel Name LAWRENCE LAWSON Hull Number 1120

Manufacturer Cathelco Serial Number

Aft System Capacity Amp Volts

Day	Area of Operation	Sea Temp/ C	Shaft Earthing Potential/ mV	Aft ICCP Syste Current /A	Voltage /V	Ref Cell S1/mV	Ref Cell S2/mV	Ref S3/
1	CAPE MAY	68		1	2.2	-850	-850	
2	CAPE MAY	72		1	2.2	-850	-850	
3	CAPE MAY	64		0	0.9	-865	-870	
4	ATLANTIC OCEAN	64		0	0.9	-880	-880	
5	ATLANTIC OCEAN	68		0	1.8	-845	-855	
6	ATLANTIC OCEAN	60		0	1.0	-900	-900	
7	ATLANTIC OCEAN	60		0	1.0	-910	-910	
8	CAPE MAY	69		1	2.1	-850	-850	
9								
10	ATLANTIC OCEAN	76		0	0.9	-875	-875	
11	ATLANTIC OCEAN	60		0	1.0	-930	-930	
12	ATLANTIC OCEAN	71		0	1.0	-910	-910	
13	Cape May	61		1	2.1	-855	-850	
14	CAPE MAY	66		1	2.1	-850	-850	
15	CAPE MAY	70		1	2.2	-850	-850	
16	CAPE MAY	59		1	2.2	-850	-845	
17								
18								

(a) USCGC Larence Lawson ICCP Log

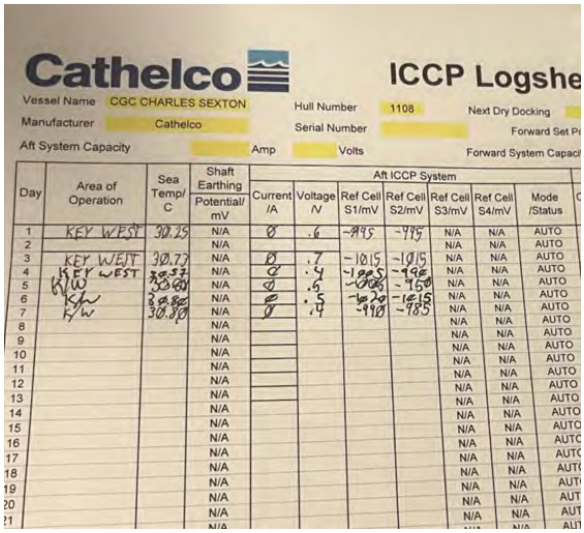

(b) USCGC Charles Sexton ICCP Log

Figure 1-8: Two Fast Response Cutter ICCP Amperage Logs

Since the ICCP is essentially providing zero protection for the cutter, further research into exactly how the ICCP system is supposed to operate was conducted.

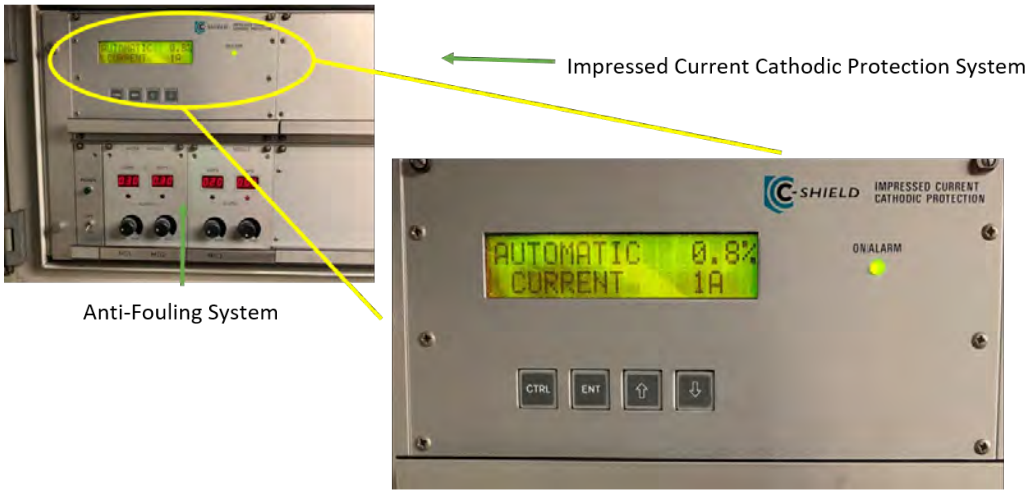

Figure 1-9: ICCP Screen on CGC Charles Sexton (WPC-1108)

Figure 1-9 shows the ICCP read-out screen onboard USCGC Charles Sexton. This picture is further evidence of nearly zero current output from the ICCP, which means it is not providing active protection for the cutter.

1.5 Impressed Current Cathodic Protection

The active method of protection on the FRC is an impressed current cathodic protection system. Figure 1-10 is a starboard profile view of the ship. The ICCP has a power supply unit located centrally in the Engine Room [6]. The reference electrodes, shown below and mirrored on the port side, are located forward near the ship's bow thruster tunnel in the bow. It is important to note that there is a significant number of zinc anodes inside the bow thruster tunnel. The reference electrode gathers a reference voltage signal and relays that back to the power supply unit. The power supply unit is programmed to have a set point of -0.85 V. If the reference electrode reads a value greater than -0.85 V, a variable amount of current will be impressed into the water through an anode located near the aft end of the ship [3]. The current impressed into the water will lower the value of the referencevoltage in the area to provide protection, reminiscent of how the zinc anodes protect carbon steel hull.

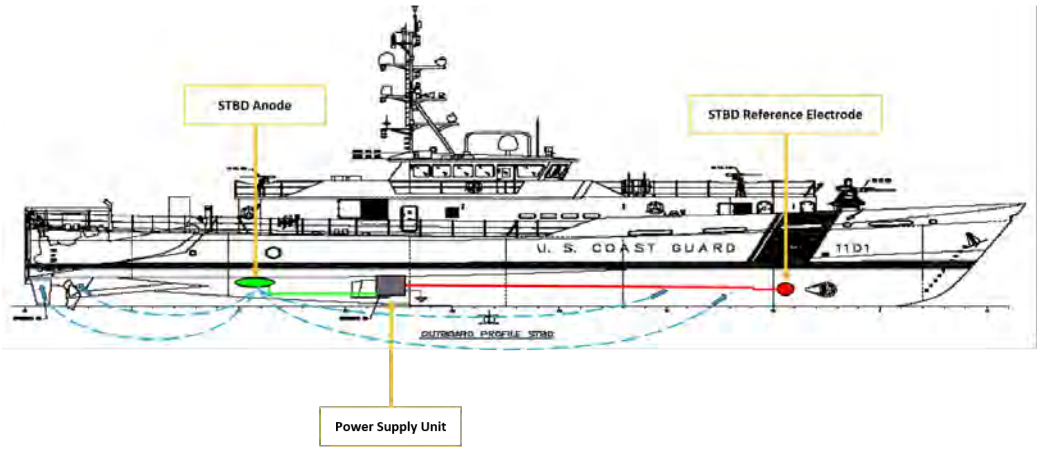

Figure 1-10: FRC ICCP Diagram

Having both a passive and active system inherently means they interact together. It would seem advantageous if the two systems worked together, but this does not appear to be the case. To better understand the implications of zinc anodes interacting with the ICCP system, laboratory experimentation is necessary. Figure 1-11 shows the experimental setup. In both images of Figure 1-11, there are four compo-

nents. The first is a silver chloride reference electrode. This is similar to the reference electrode located forward on the FRC. The next component is hull steel. The third component is a zinc-plated screw to mimic a zinc anode. In the experimental iteration of the left image of Figure 1-11, the zinc anode is electrically connected to the hull steel, but the circuit is not complete by putting the zinc screw in the water. Here, the potential reference voltage read is -0.555 V. This experiment is grounded differently so the respective voltage on the ship are negative rather than positive. If there were an ICCP connected to this system, this reading would indicate under protection and immediately begin impressing a current into the water via the aft-located anode.

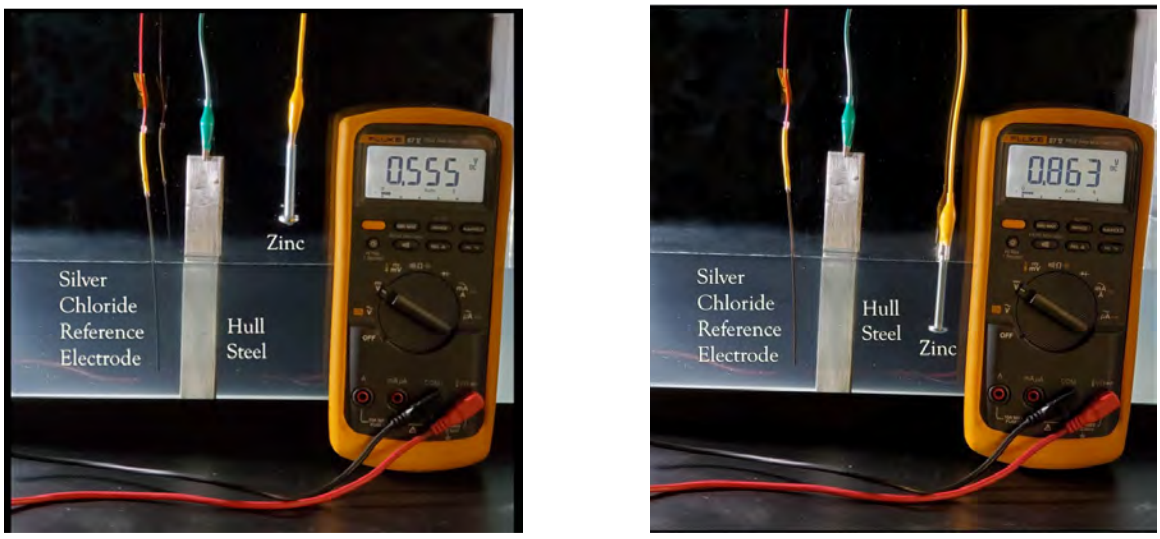

(a) Beaker Experiment with no zinc

(b) Beaker Experiment with zinc anode

Figure 1-11: Beaker Experiment With Zinc

In the second iteration of the experiment, which is the right image in Figure 1-11, the same components are used, however, this time the zinc-plated screw is inserted into the water thus providing protection to the hull steel and acts as a sacrificial anode. Here, the potential voltage reading is 0.863 V which is greaterin magnitude than the ICCP set point of -0.85 volts. If an ICCP wereconnected to this experiment, it would not impress any current into the water because the hull steel is properly protected [3].

This is the problem with the location of the FRC ICCP reference electrode. Be-

cause it is located so close to the bow thruster, which has many zincs attached, the ICCP system is "blinded" to the other areas of the ship and believes the ship is entirely protected even when it is not. The large number of zincs in the forward bow thruster tunnel overpowers the rest of the ship, ensuring the ICCP system does not turn on and ultimately does not push any current into the water to protect the rest of the ship, which is in need of additional cathodic protection.

To ensure that the ICCP still worked and could impress some level of current, an experiment was designed onboard the ship. Below in Figure 1-12 is an oscilloscope reading taken onboard USCGC Charles Sexton. Here, the ICCP reference voltage set point was effectively changed from -0.85 V to -1.1 V by using a circuit to shift the voltage measured by the reference electrodes.

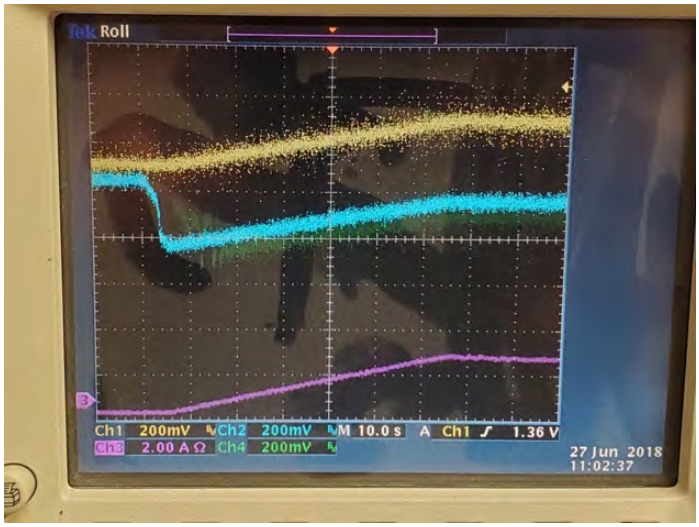

Figure 1-12: Reprogramming the ICCP Reference Potential Voltage on USCGC Charles Sexton (WPC-1108). (Yellow) starboard reference electrode voltage, (cyan) starboard reference electrode input to ICCP after shift circuit, (green) port reference electrode input to ICCP after shift circuit, (magenta) ICCP starboard anode current.

The ICCP has no knowledge of this circuit and will still try to maintain its -0.85 V set point. Immediately the ICCP recognized that the reference electrode was reading below the new set point and impressed a current into the water, meaning the ICCP system is fully functional. This can be seen in the incline in magenta waveform following the rapid, downward shift in the cyan and green curves in Figure 1-12. The ICCP was not being activated due to its reference electrode location and the vicinity

of the zinc anodes in the bow thruster tunnel.

Active protection systems like ICCP require unique safety considerations as well. This system has a set of silver graphite brushes to prevent electrical arcing between the shaft and the bearings. This is accomplished with a slip ring assembly around the stainless steel shaft. The brushes provide a low resistance path which allows for cathodic protection current to flow into the propeller blades and shaft and then to ground without creating electrical arcs [3]. Figure 1-13 is a rendering of the earth grounding brushes on the stainless steel shaft.

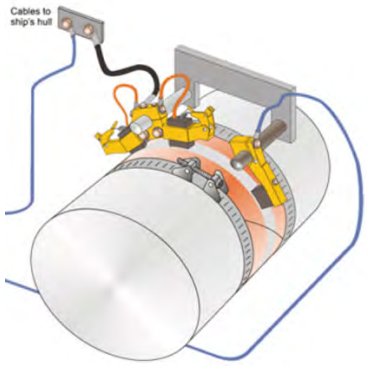

Figure 1-13: Stainless Steel Shaft with Carbon Brushes for grounding

Figure 1-14 is an additional diagram with a cross-sectional view of the stainless steel shaft, where the slip ring attaches, and how it is grounded to the hull structure. Although ships are not truly grounded to earth, the general consensus is that the ship hull is considered ground.

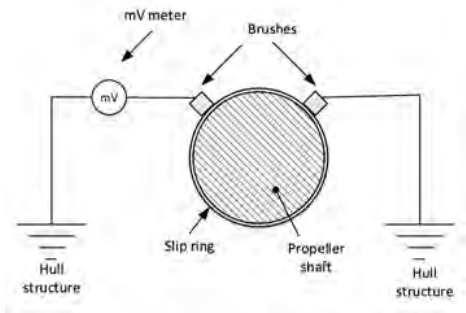

Figure 1-14: Line Diagram of the shaft grounding brushes

1.6 Excessive Protection

The ICCP current output levels are not without limit. Although increasing the number of electrons available to under-protected surfaces is the theory behind cathodic protection, there is a maximum amount of cathodic current before positive effects turn into negative ones. There are two main concerns when it comes to excessive current exposure. The first is paint failure. It is possible if the coating systems are exposed to too much current, they will degrade at an accelerated rate exposing the carbon steel. The second concern is hydrogen embrittlement. Although this is more commonly associated with high-yield strength steels, and the FRC is a medium strength steel, it is still an important concern. Figure 1-15 is a figure from the Cathelco manual [3] outlining under, ideal, and overprotection levels. The ICCP reference voltage should not be set beyond -1.15 V to avoid overprotection.

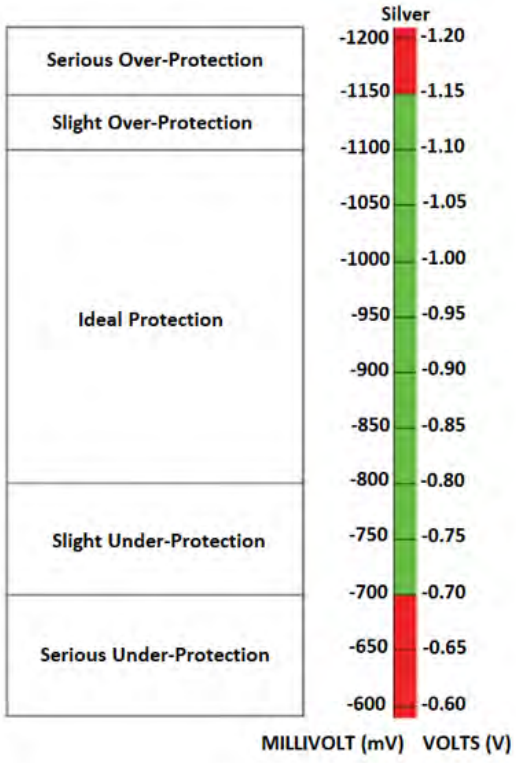

Figure 1-15: Cathelco Manufacturing Instruction for Ideal Protection Levels [3]

Although hydrogen embrittlement is primarily a concern with high-strength steels,

researchers have been able to hydrogen embrittle medium-strength steels. Figure 1-16 shows the stress strain curve of the same type of steel used for the FRC from *Hydrogen Uptake and Embrittlement Susceptibility of Ferrite-Pearlite Pipeline Steels* in 2018 and indicates the impact of hydrogen embrittlement. These researchers were able to impress enough hydrogen into the steel to eventually bring the steel outside of the American Bureau of Shipping (ABS) standards. ABS requires steel to withstand a 15% elongation [7]. The associated table is seen in Table 1.1.

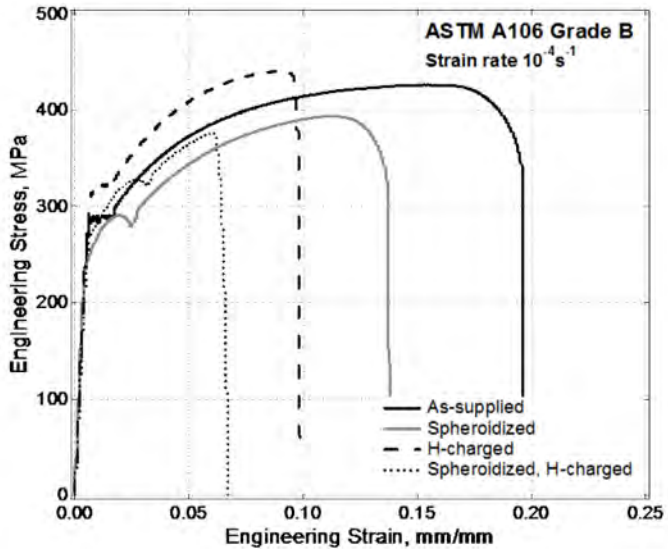

Figure 1-16: Strain Curve A360 steel [8]

Thickness in mm (in.)								
Exceeding	n/a	5(0.20)	10(0.40)	15(0.60)	20(0.80)	25(1.0)	30(1.2)	40(1.6)
Not Exceeding	5(0.2)	10(0.40)	15(0.60)	20(0.80)	25(1.0)	30(1.2)	40(1.6)	50(2.0)
Elongation %	14	16	17	18	19	20	21	22

Table 1.1: ABS Materials and Welding: Elongation Requirements for Alternative B Specimen (1995) [7]

Chapter 2

Stern Tube Corrosion Modeling and Laboratory Experimentation

As described in Chapter 1, severe corrosion is plaguing a rather complex area to protect. This work will discuss why a ship stern tube is a difficult area to protect and present tools and research for fast, accurate, and low-cost experimentation. Due to the stern tube size, trade-offs were necessary concerning scaling priorities. This chapter will discuss the reasons behind scaling, material selection, and results for various conditions. For all aspects of this work, conservative measurements and assumptions were chosen to present conservative results rather than uncertain ones. (This chapter is co-written with Michael Bishop.)

2.1 Scaling

Two main factors were considered when scaling the U.S. Coast Guard FRC stern tube for in-lab experimentation: relative surface areas and flow conditions. Relative surface area is important from a corrosion standpoint. First, the amount of cathodic current necessary for protecting area(s) depends on the area exposed to the electrolyte. The greater the surface area exposed to the electrolyte, the more current required. This can be explained through a simple equation shown below.

$$I_{i,max} = S_i \times f_{c,max} \times J_{bd} \tag{2.1}$$

Equation 2.1 is for calculating the required cathodic current for protection where S_i is the area being protected in m^2, $f_{c,max}$ is the maximum coating breakdown factor which is unitless, and J_{bd} is the current density for bare metal in dynamic conditions in A/m^2 [9]. The breakdown factor for a surface can be anywhere from 0.005 for a near perfectly coated surface to 1 for an uncoated surface [9]. This work will explore the importance of the breakdown factor within this equation later. Not only are the relative surface areas important from the standpoint of calculating the required cathodic current, but they are also important when an area is under-protected. If no protection is provided to the FRC stern tube, a galvanic cell remains between the dissimilar metals. How these metals corrode is partially dependent on the surface areas of the galvanic cell. General corrosion is expected if a very large anodic surface is electrically connected to a small cathodic surface. However, if the relationship is swapped where the anodic surface is much smaller than the cathodic one, we can expect corrosion that appears like pitting. Whether the corrosion can actually be considered pitting corrosion is dependent on whether the material can passivate. Materials that do not passivate, like carbon steel, generally are not associated with pitting [10]. Ship maintainers from a naval engineering background would still associate this type of corrosion with pitting.

Flow is the other factor considered for scaling the FRC stern tube to a more manageable experimental size. Flow plays a vital role in the corrosion of any metal. Increasing the flow increases the oxygen available at the surface, which can increase corrosion rates[11]. The FRC has a stainless steel shaft and carbon steel stern tube. The use of a stainless steel shaft for ship design has its advantages. Stainless steel can form a chromium oxide film which protects the surface from corrosion and decreases the required protection current [11]. However, flow can also disturb the formation of passive oxide films. Pitting of a stainless steel surface is generally the result of a partial or complete disturbance of the passive film of a metal that can passivate [10]. As a

result, stainless steel, although sometimes considered safe from corrosion, corrodes. In order to semi-accurately represent the situation inside an FRC stern tube, the flow was prioritized for a scaled-down experiment. Conducting an experiment where similar flow conditions exist assists in making accurate current density calculations.

2.1.1 Flow Characteristics

This work establishes that similar flow conditions for a scaled-down experiment are important, not only for measuring the corrosion rate of a carbon steel tube, but for ensuring a similar disturbance of stainless steel passivation occurs. A common issue concerning fluid flow is whether scaling with the Froude number or Reynolds Number is more appropriate for the given situation. Scaling the experiment to reflect the flow conditions of the stern tube was done by matching the Reynolds numbers of each [12]. The Reynolds equation is shown below.

$$Re = \frac{\rho v l}{\mu} \tag{2.2}$$

Reynolds matching involved assuming that dynamic viscosity and fluid density were the same in the lab experiment and FRC stern tube. Due to the diverse operating environments of the FRC, which involves most climates and times of the year, this assumption is safe. Canceling out dynamic viscosity and fluid density leaves both the experiment and ship Reynolds numbers a velocity component and length component, $vl_{exp} = vl_{ship}$. The FRC velocity component is variable, because of the different shaft speeds at which the ship operates. The slowest speed the ship can maintain is when the clutch first engages with the shaft, otherwise known as clutch ahead. Therefore clutch ahead, which is the most conservative speed from a corrosion standpoint, was chosen. The length component for the FRC is a known variable.

2.1.2 Material Selection

The FRC stern tube is made of carbon steel that would be considered on the lower end of medium carbon steel. Medium-strength steels are less brittle than high-strength

steels, vital for the dynamic loading conditions associated with ship design. The FRC shaft is made of stainless steel. The stainless steel used for the shaft has a considerable amount of chromium and molybdenum to prevent localized corrosion, which would be detrimental to the shaft's lifespan.

Steels with similar chemical properties were chosen for the in-lab experiment. The same materials we not available in the sizes that were considered. The experimental setup consists of a 1-foot, 1-inch diameter stainless steel shaft and an 8-inch, schedule 40, 4-inch NPS, medium carbon steel pipe. In addition to the two conductive metals, the FRC stern tube has two bearings supporting the shaft. The bearing staves are made from a rubber polymer with a low friction coefficient and, more importantly, are non-conductive. The electrical connection between the shaft and the rest of the ship was discussed in Chapter 1. The water film bearing system creates uncertainty about whether current can enter the stern tube through the tight clearance created by the bearing. To simulate this in the lab, two non-conductive delrin and plexiglass bearings were machined for each pipe end. The model for the FRC stern tube is shown in Figure 2-1.

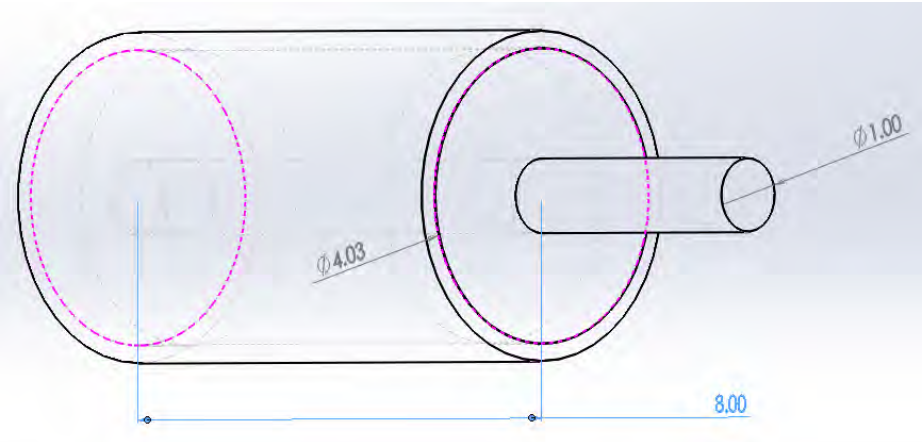

Figure 2-1: Experimental Setup: SolidWorks Model

2.1.3 Experimental Setup

The stern tube model in each experiment was submerged in a 3.5 percent NaCl solution. In addition to the three materials discussed in the previous subsection,

other equipment was incorporated into the experiment to model the FRC stern tube. Custom-made Ag/AgCl reference electrodes collected reference potentials inside and outside the stern tube model. The water temperature was collected with a thermometer. The carbon steel tubing and stainless steel shaft were electrically connected with a carbon brush. The shaft was spun at 500 RPM with a motor. In addition, a lab-made ICCP system injects current into the water through a platinum-coated anode. The external reference electrode voltage can be controlled by the ICCP system, which pumps current into the water to meet a pre-set potential. A computer-aided design (CAD) image of the experimental setup is shown in Figure 2-2. Figure 2-3 shows the actual experimental setup.

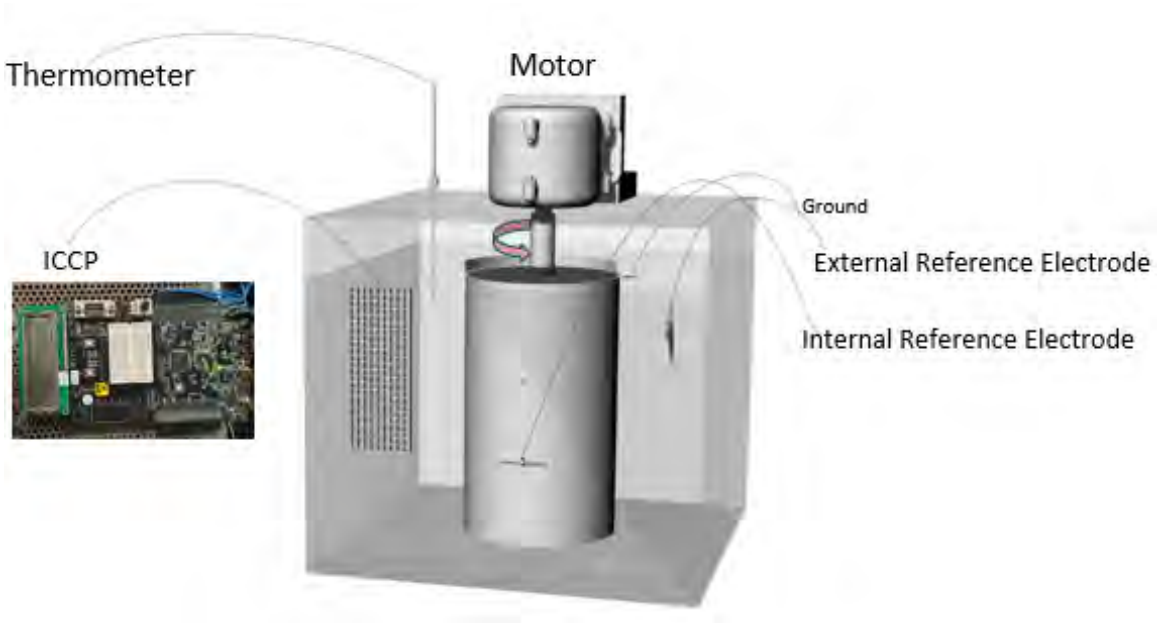

Figure 2-2: Experimental Setup: CAD Model

2.2 Results

These experiments will primarily provide only a qualitative picture of the FRC stern tube corrosion issue. Before exposing the experimental stern tube to any salt water, a picture was taken with a microscope. This shows each experiment's previous condition for the stern tube carbon steel. Additional pictures were taken at the end of each

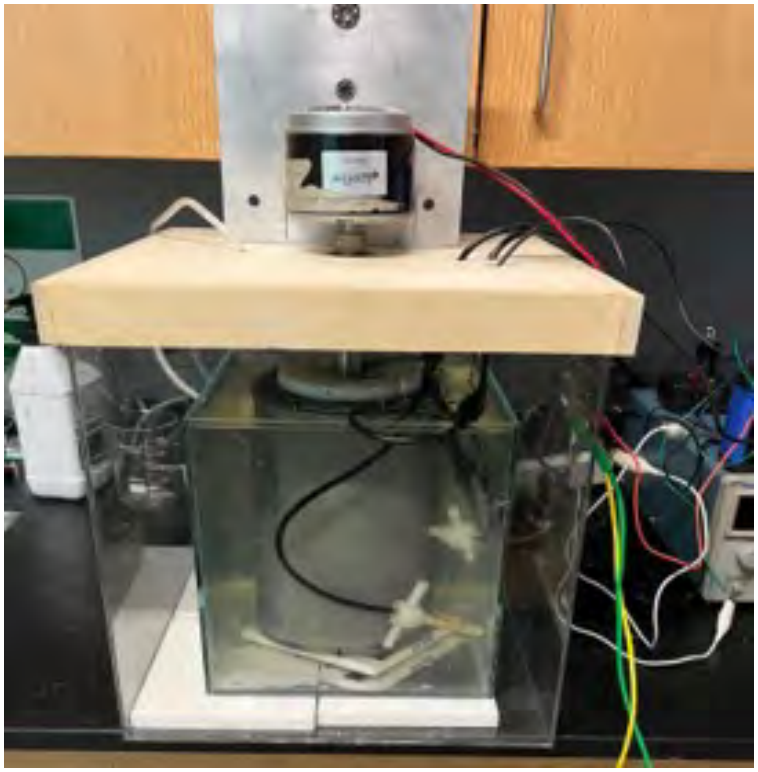

Figure 2-3: Experimental Setup: Actual Lab Model and Experimentation Tools

experiment. Each experiment measured interior potential, exterior potential, motor voltage, temperature, and ICCP current. The below subsections show the results obtained from each corrosion protection scheme. Experiments 1-5 are not shown in this report but gathered critical qualitative data for moving forward in the rotational experiments. Experiments 1-5 did not include any rotational periods, therefore, are not further detailed in this report. All qualitative findings from experiments 6-10 are further supported by experiments 1-5. The following subsections begin with experiment 6. Table 2.1 lists the FRC in-lab experiments by number.

2.2.1 In-lab Rotational Experiments

The operational tempo of a Coast Guard ship typically involves being underway for anywhere from one-half to one-third of a year. To account for underway and non-underway periods, the motor only spun the shaft for 8 of the 24 hours. Each experiment was consistent, with the 8 hours of rotation being the last 8 hours of the

Table 2.1: Comprehensive List of Experiments

1	Non-rotational. Uncoated hull and shaft with no zinc present.
2	Non-rotational. Uncoated hull and shaft with zinc present.
3	Non-rotational. Uncoated hull and shaft with no zinc present. ICCP addition.
4	Non-rotational. uncoated hull and shaft with zinc present. ICCP addition.
5b	Repeat exp. 2 with a coated shaft.
5d	Repeat exp. 4 with a coated shaft.
6	Rotational. Uncoated hull and shaft with no zinc present.
7	Rotational. Uncoated hull and shaft with zinc present.
8	Rotational. Uncoated hull and shaft with no zinc present. ICCP addition.
9	Rotational. uncoated hull and shaft with zinc present. ICCP addition.
10b	Repeat exp. 7 with a coated shaft.
10d	Repeat exp. 9 with a coated shaft.

experiment. The motor voltage for a rotational lab experiment is shown in Figure 2-4. A 4 V motor voltage turned the shaft at 500 RPM. The chosen motor speed of 500 RPM was below the goal of 800 RPM, which is the equivalent scaled value for clutch ahead on an FRC diesel engine. This is due to safety concerns with the experiment. The slower experiment shaft speed creates less severe flow conditions in the lab experiments than in an actual FRC stern tube, decreasing the overall corrosion compared to the FRC.

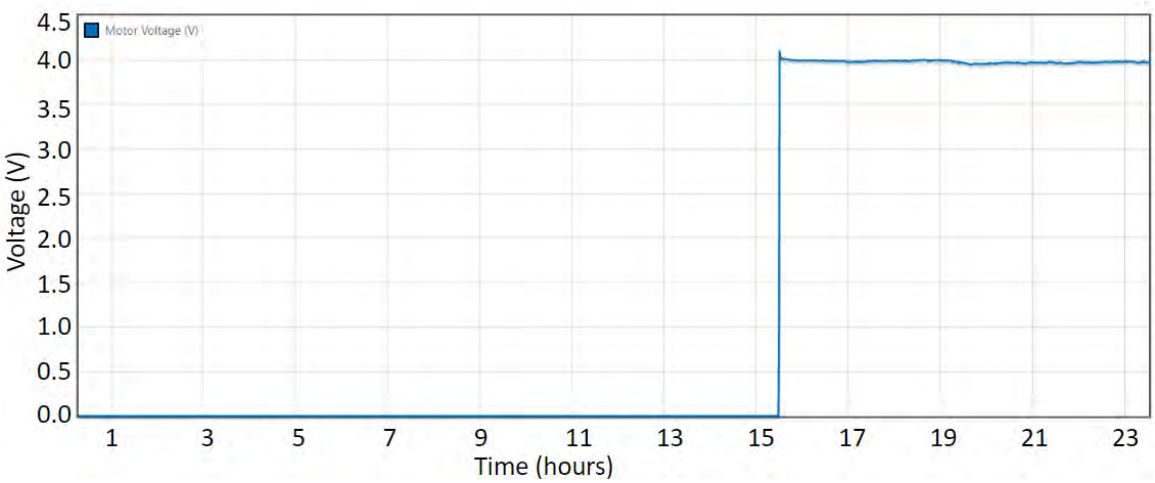

Figure 2-4: Experiment 6: Motor Voltage.

Once each experiment is concluded, the carbon steel pipe is sandblasted and cleaned to ensure consistency throughout all experiments.

2.2.2 Experiment 6: Baseline

The first experiment conducted with a rotating shaft provided a set of baseline voltages and a steel tube picture for the worst case. The worst case is that corrosion protection methods are not employed. Here, a completely unprotected steel tube is electrically connected to a dissimilar metal, a stainless steel shaft, and immersed in a saltwater solution. Experiment 6 is summarized by Table 2.2. A table summarizes the experimental setup for each experiment in this section.

Table 2.2: Experiment 6 Setup.

Shaft	Uncoated
Carbon Steel Tubing	Uncoated
ICCP	Off
ICCP Set Point	N/A
Zinc Anode Weight Before (grams)	N/A
Zinc Anode Weight After (grams)	N/A
Zinc Loss per day (grams/day)	N/A

The results follow expectations. The interior and exterior potential readings are well below what would be considered ideal protection, and are illustrated in Figure 2-5 and Figure 2-6. In this case, the interior potential of the stern tube model reaches a steady state, which is the corrosion potential for the given conditions, denoted E_{corr}. The potential settles at -0.70 V, which is not negative enough to prevent corrosion of the stern tube steel. As discussed in Chapter 1, -0.80 V is considered the beginning of the ideal protection zone for steel. The before and after pictures of the carbon steel stern tube in Figure 2-7 show that corrosion occurred during the 24-hour lab simulation. Furthermore, the interior and exterior potential suddenly change around 15 hours. The shaft begins rotating at 500 RPM, increasing the potential inside and outside the stern tube model. Any increase in potential, the voltage being less negative, will increase corrosion rates and corrosion current. The spinning shaft increasing the potential, even marginally, is a significant finding and supports the literature that suggests that increased flow requires increased cathodic current for protection [9, 10].

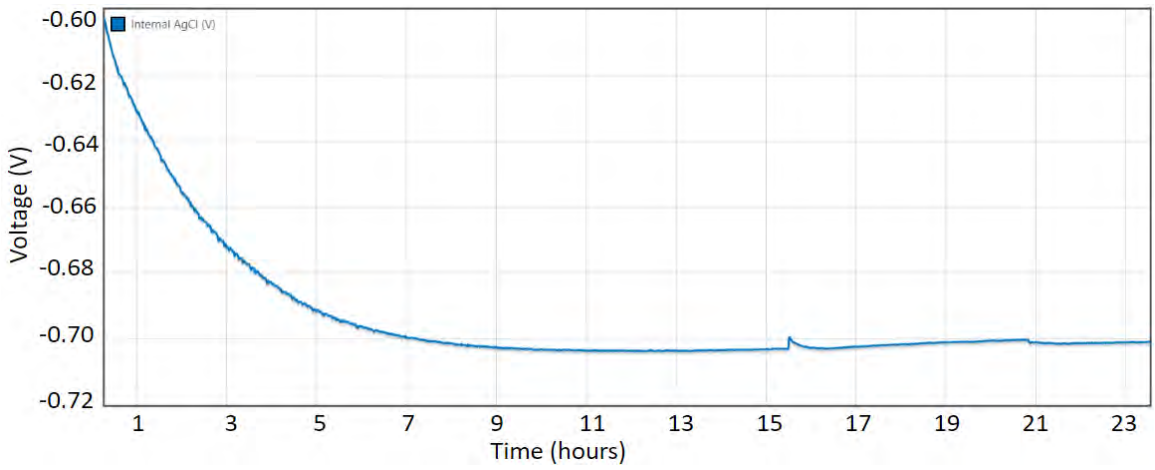

Figure 2-5: Experiment 6: Internal Reference Electrode Voltage.

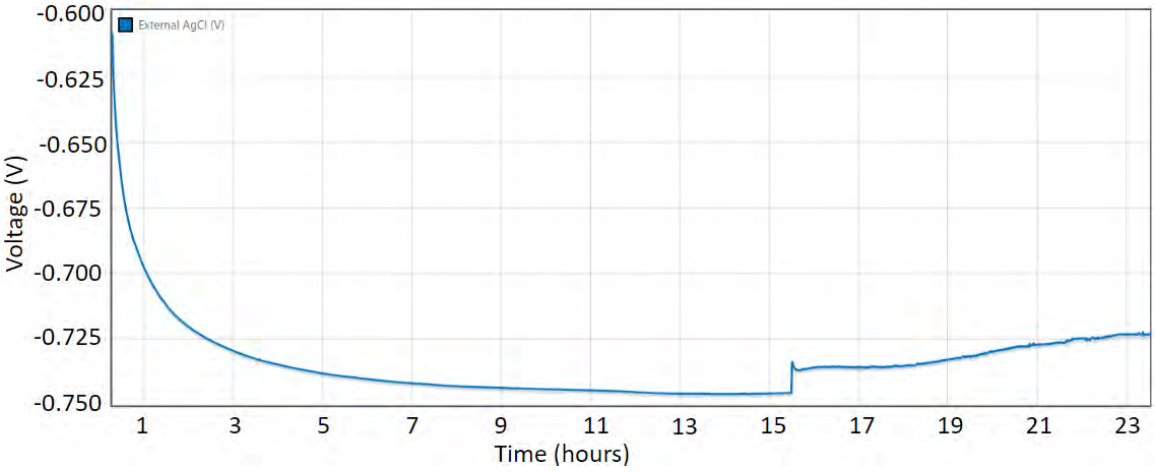

Figure 2-6: Experiment 6: External Reference Electrode Voltage.

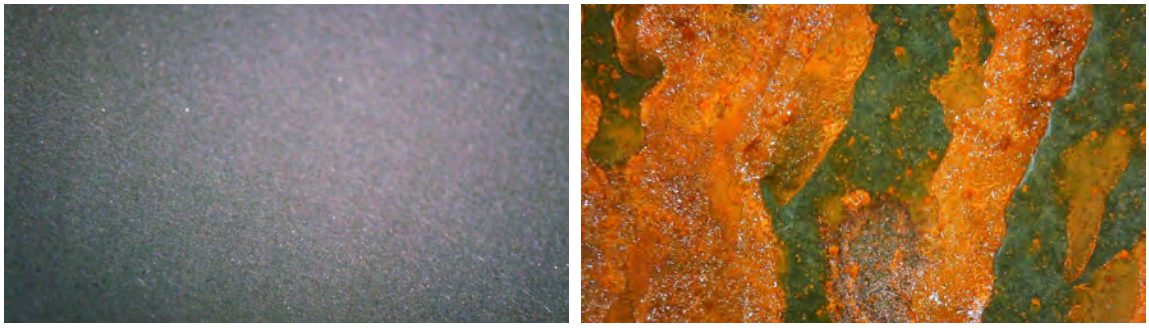

(a) Exp.6: Before Exposure (t=0 hours)

(b) Exp.6: After exposure (t=24 hours)

Figure 2-7: Experiment 6: Before and After Pictures for Tube Steel

2.2.3 Experiment 7: Passive Zinc Anode Protection

Experiment 7 adds passive anode protection to the stern tube. A passive zinc anode, machined to 1.795 in. x 0.475 in. x 0.185 in., with a drilled hole for a 6-32 screw, is secured to the stern tube's interior, shown in Figure 2-8. Each anode is precisely machined to keep each experiment's anode surface areas consistent. The anode surface area is important due to Equation (2.1). In experiment 7, the installed zinc anode will protect all exposed stainless steel and carbon steel inside the tube. Zinc is considered a sacrificial anode due to its reduction potential, which is lower than the more noble metals it is intended to protect, such as carbons steel and stainless steel [13]. The typical potential of zinc ranges from -0.98 to -1.03V relative to an Ag/AgCl electrode[13].

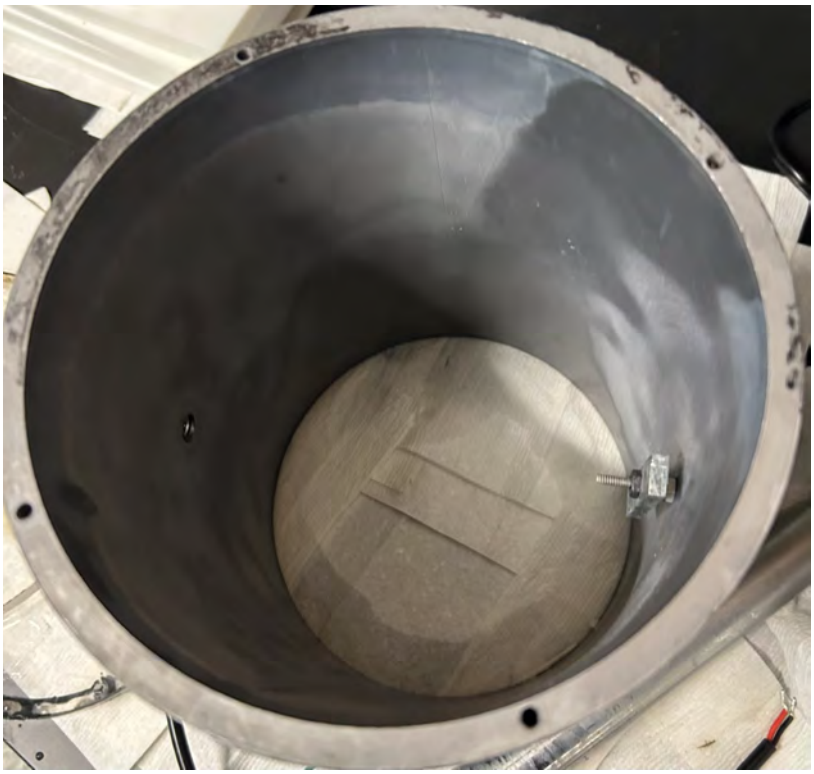

Figure 2-8: Passive Zinc Anode Secured to the Interior of the Model Stern Tube.

The interior and exterior potential measurements, illustrated in Figure 2-9 and Figure 2-10, show that the zinc anode provides adequate protection to the interior but not the exterior of the stern tube. The exterior potential is similar to exper-

Table 2.3: Experiment 7 Setup.

Shaft	Uncoated
Carbon Steel Tubing	Uncoated
ICCP	Off
ICCP Set Point	N/A
Zinc Anode Weight Before (grams)	17.039g
Zinc Anode Weight After (grams)	16.311g
Zinc Loss per day (grams/day)	0.724 g/day

iment 6, where no corrosion protection is incorporated. This experiment provides qualitative evidence that passive anodes installed in the FRC stern tube may only provide corrosion protection to the interior of the tube. The focus of this work is the interior of the stern tube which experiences corrosion. The FRC has additional zincs installed in other areas to protect areas that are not the focus of this work. Similar to experiment 6, rotating the stainless steel shaft increases the potential of the interior of the stern tube. For all experiments which include a zinc anode, the zinc mass is measured before and after the experiment. Table 2.3 includes the zinc mass before and after the experiment, as well as the mass lost per day. The zinc mass lost per day will be necessary for comparing protection schemes.

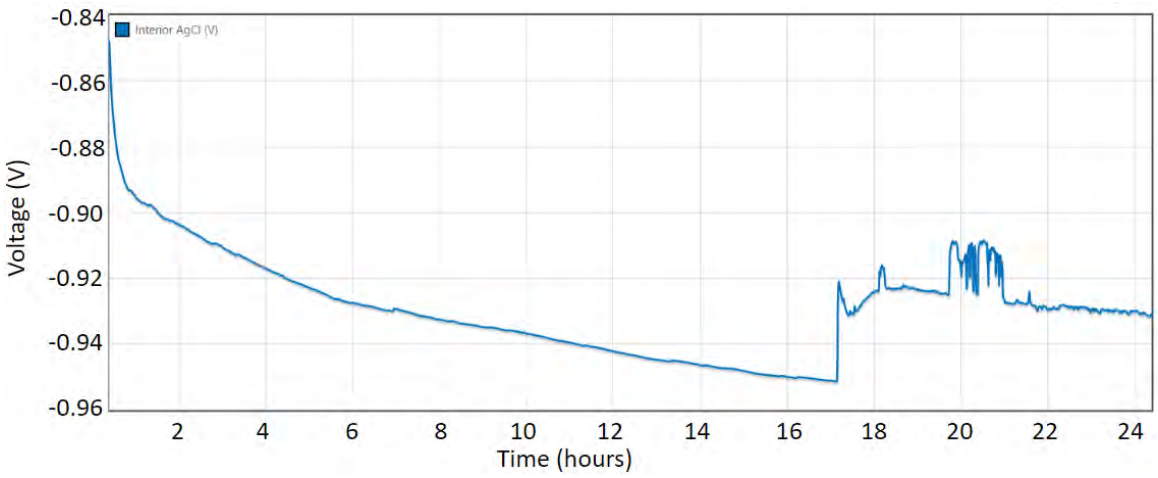

Figure 2-9: Experiment 7: Internal Reference Electrode Voltage.

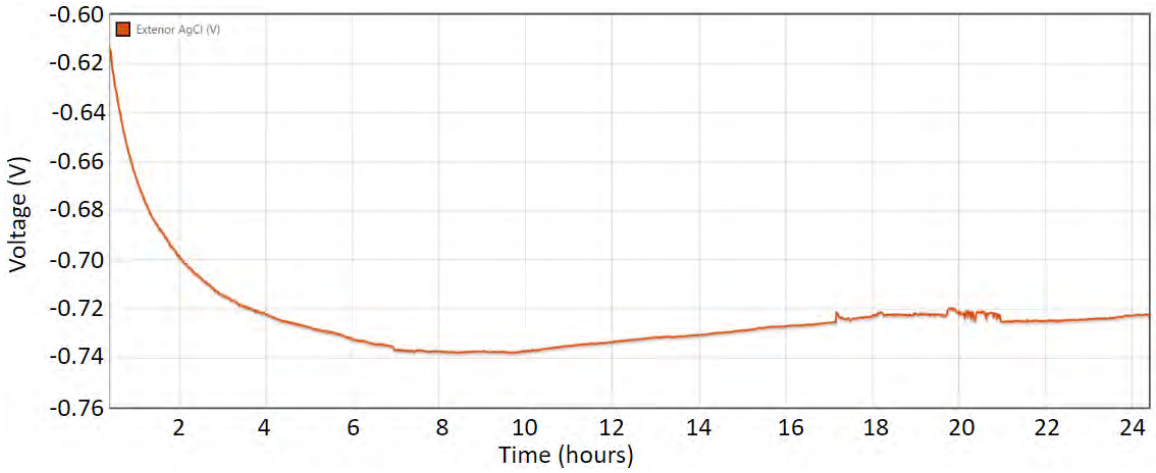

Figure 2-10: Experiment 7: External Reference Electrode Voltage.

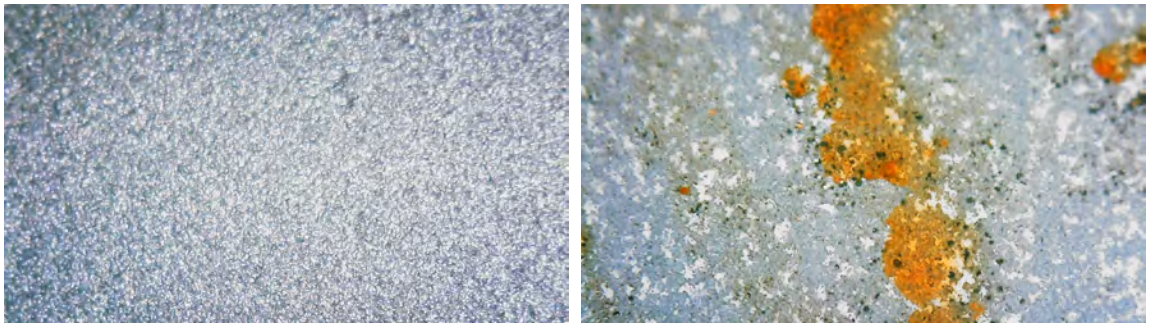

(a) Experiment 7: Before exposure (t=0 hours) (b) Experiment 7: After exposure (t=24 hours)

Figure 2-11: Experiment 7: Before and After Pictures for Tube Steel

2.2.4 Experiment 8: ICCP Protection

Experiment 8 does not include passive anode protection. Instead, the experiment attempts to protect the interior of the stern tube with an exterior ICCP system. This configuration is similar to that of the ship with fully degraded shaft tube zincs. Unlike the FRC, which has its ICCPs set to -0.85 V, the ICCP system in experiment 8 is set to maintain an exterior potential of -1.0 V. In this experiment, Figure 2-14 shows current being injected into the water through the platinum anode. In addition, Figure 2-12 shows interior potential approaching -0.80 V, which is 0.1 V more negative than the baseline experiment. This experiment provides evidence that current can enter through the water film bearings for the model stern tube, providing protection. In agreement with experiment 7, experiment 8 shows that rotating the

shaft increases the potential inside the tube. Significantly, for ICCP alone, rotating the shaft increases the potential for the model to be considered under-protected. The exterior ICCP shows some promise at providing protection to an enclosed space thanks to the various little gaps. However, the benefits are limited and may be insufficient with a spinning shaft. However, because the ship generally does not operate more than half the year, significant benefits can be had. Experiments on the effectiveness of exterior ICCP on a real ship will be explored in Chapter 4.

Table 2.4: Experiment 8 Setup.

Shaft	Uncoated
Carbon Steel Tubing	Uncoated
ICCP	On
ICCP Set Point	1.0 V
Zinc Anode Weight Before (grams)	N/A
Zinc Anode Weight After (grams)	N/A
Zinc Loss per day (grams/day)	N/A

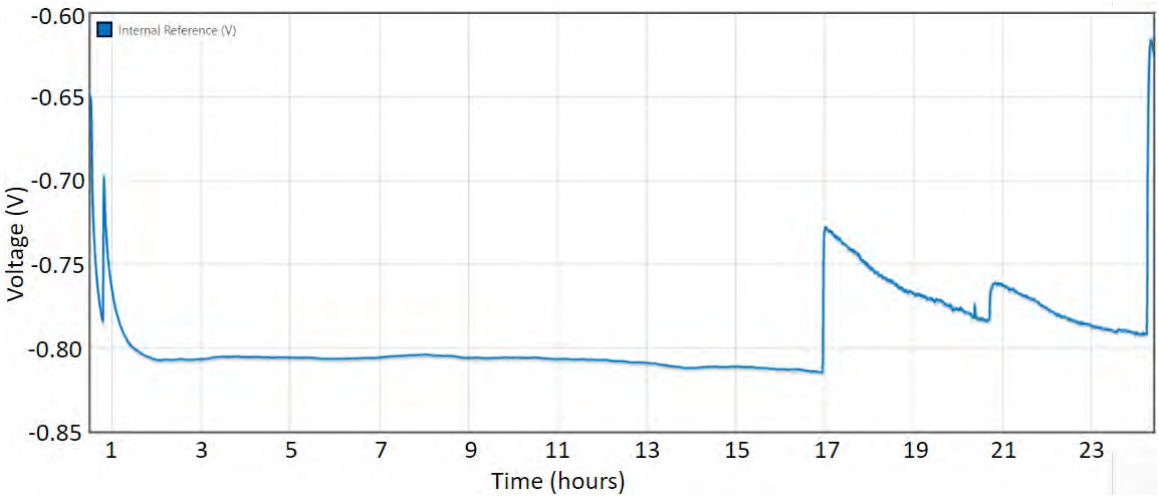

Figure 2-12: Experiment 8: Internal Reference Electrode Voltage.

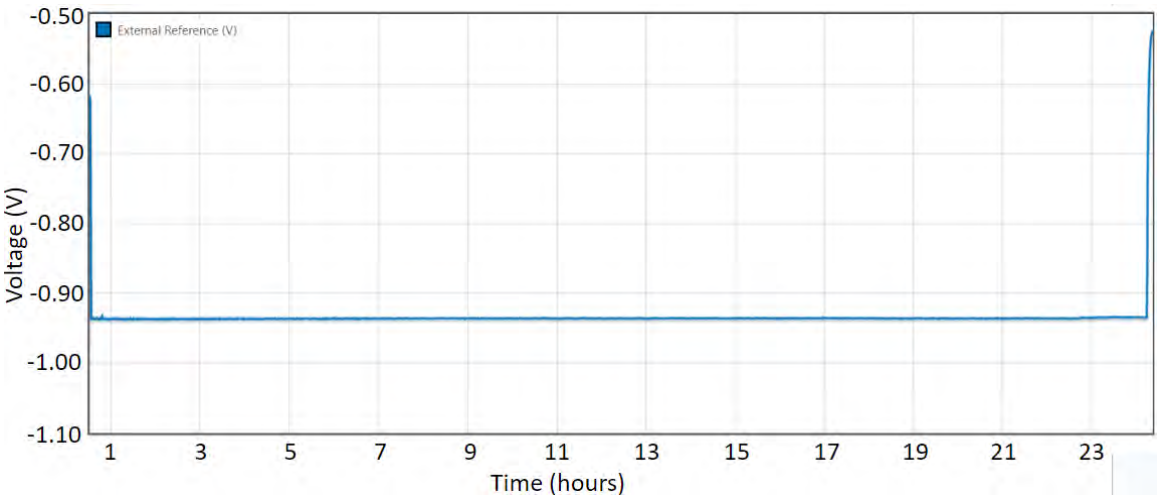

Figure 2-13: Experiment 8: External Reference Electrode Voltage.

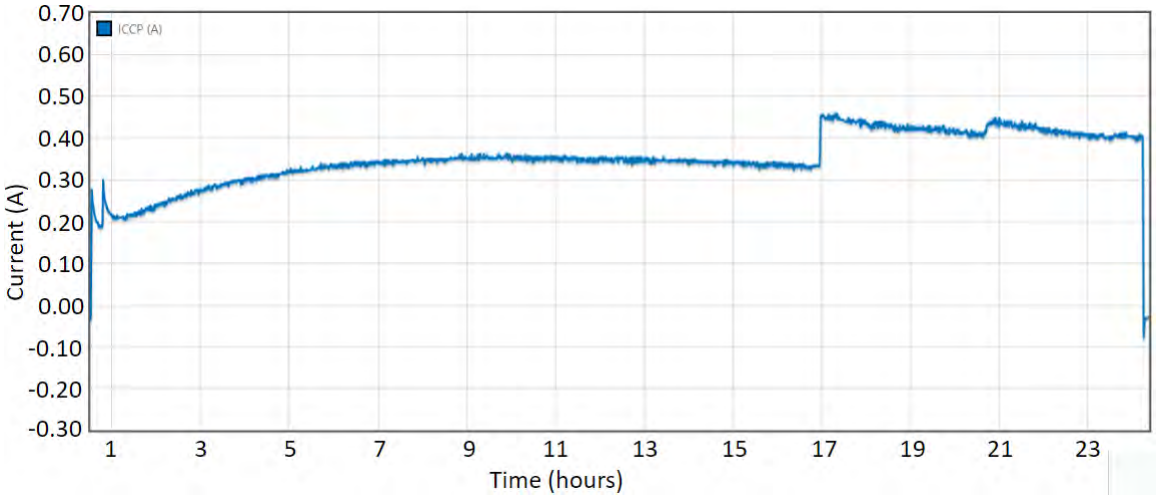

Figure 2-14: Experiment 8: ICCP Output Current (amps).

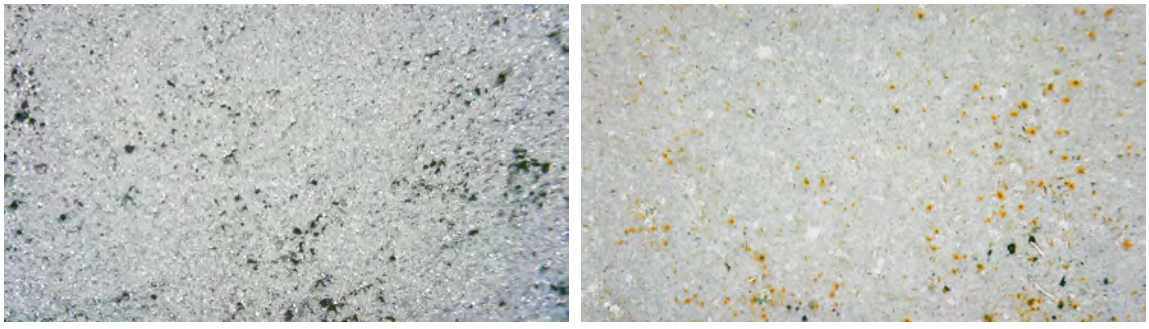

(a) Experiment 8: Before exposure (t=0 hours) (b) Experiment 8: After exposure (t=24 hours)

Figure 2-15: Experiment 8: Before and After Pictures for Tube Steel

2.2.5 Experiment 9: Passive Zinc Anode and ICCP Protection

Experiment 9, like the FRC, implements ICCP and zinc anode corrosion protection. Experiment 9 has an ICCP set point of -1.0 V. As previously discussed, the FRC ICCP system is not putting any current into the water. The goal of experiment 9 is to provide evidence, in the form of zinc loss measurements, for what ICCP current can do to benefit a stern tube outfitted with both zincs and an exterior ICCP.

Table 2.5: Experiment 9 Setup.

Shaft	Uncoated
Carbon Steel Tubing	Uncoated
ICCP	On
ICCP Set Point	1.0 V
Zinc Anode Weight Before (grams)	16.709g
Zinc Anode Weight After (grams)	16.179g
Zinc Loss per day (grams/day)	0.533 g/day

Figure 2-16 shows the interior potential for a dual cathodic protection scheme. An important finding of this experiment is that the interior potential is more negative than the previous two experiments, again demonstrating that ICCP current can enter the model stern tube. Chapter 3 will demonstrate that lower potentials will decrease the current density of the sacrificial zinc anode. By decreasing the current density of the sacrificial anode, the lifespan will be increased. The zinc loss per day further supports this finding. Experiment 9's zinc loss per day, shown in Table 2.5, was 0.533 grams/day. This is significantly lower than for Experiment 7, where the zinc lost 0.724 grams/day.

Lastly, Figure 2-14 and Figure 2-18 show that less ICCP current is injected into the water with the dual scheme. When using a dual protection scheme, neither the zinc nor the ICCP system needs to work as hard to provide adequate corrosion protection to the surrounding steels.

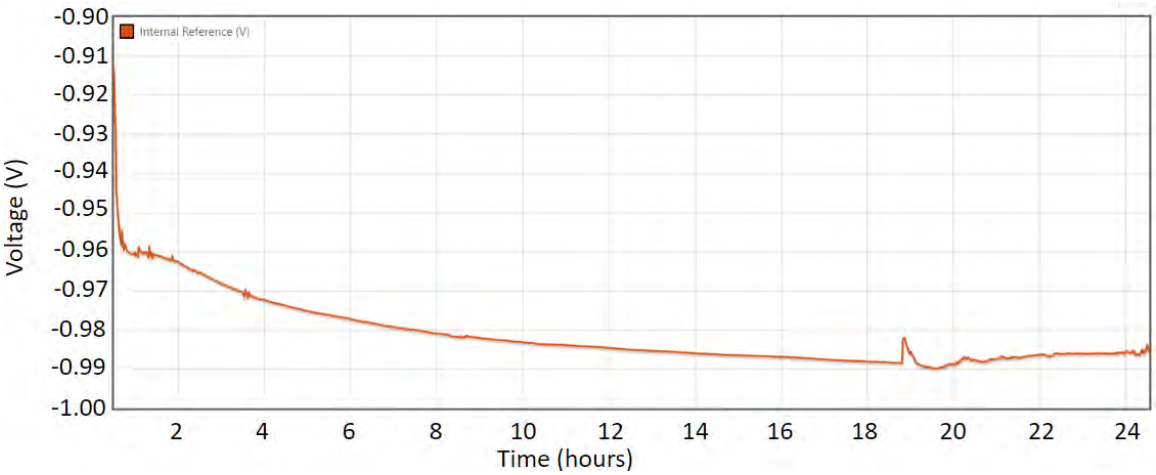

Figure 2-16: Experiment 9: Internal Reference Electrode Voltage.

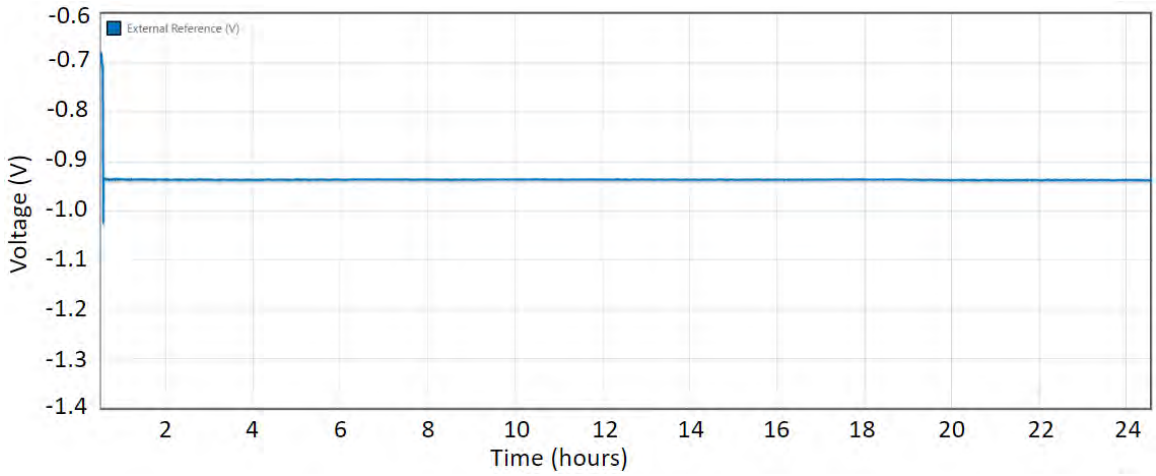

Figure 2-17: Experiment 9: External Reference Electrode Voltage.

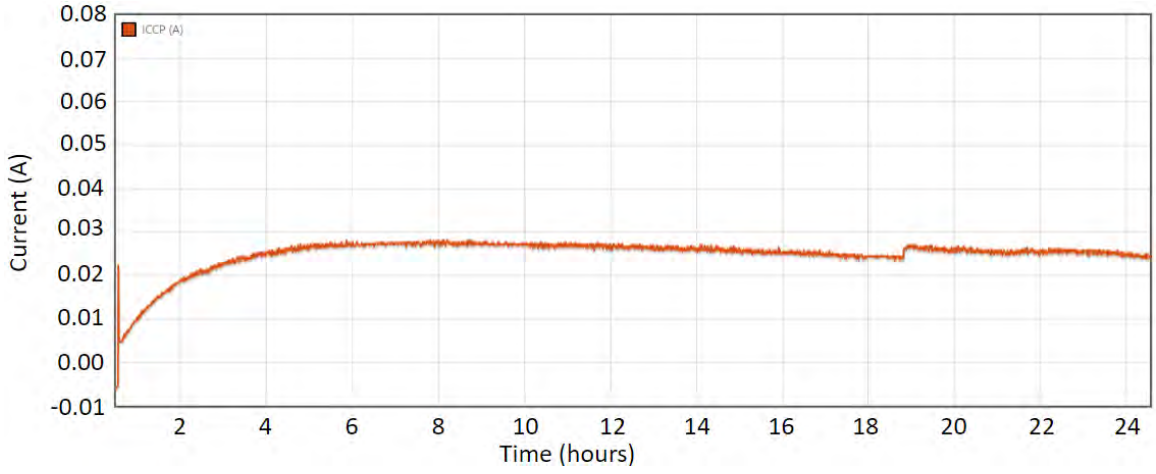

Figure 2-18: Experiment 9: ICCP Output Current (Amps).

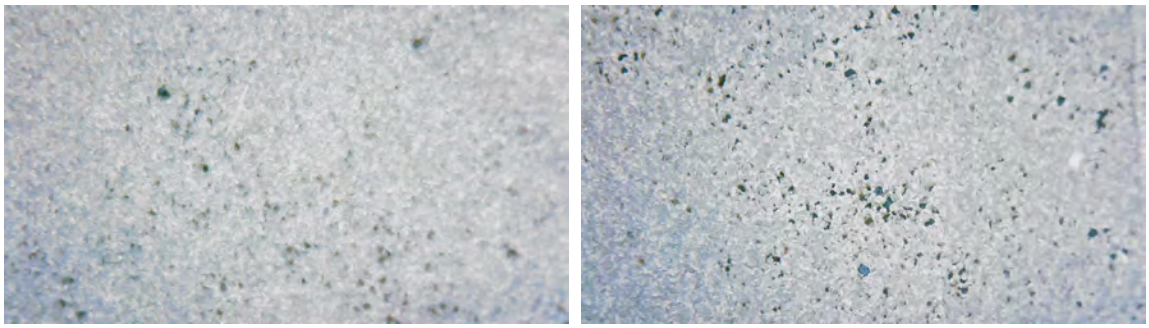

(a) Experiment 9: Before exposure (t=0 hours) (b) Experiment 9: After exposure (t=24 hours)

Figure 2-19: Experiment 9: Before and After Pictures for Tube Steel

2.2.6 Experiment 10b: Passive Zinc Anode Protection with Coated Shaft

The previous experiments have already established that rotating the shaft increases the potential, ICCP current can enter the model stern tube, and ICCP current can extend the longevity of the sacrificial zinc anode. An additional question these experiments aim to answer is whether coating the stainless steel shaft decreases the required cathodic protection. This question seems intuitive from eq. (2.1). The issue with answering the question, though, stems from the ability of stainless steel to form a passive film. If the stainless steel in the previous experiments can form and maintain a passive chromium oxide film throughout the experiment, then coating the shaft should not provide additional benefits as this film is not electrically conductive.

Table 2.6: Experiment 10b Setup.

Shaft	Epoxy Coating
Carbon Steel Tubing	Uncoated
ICCP	Off
ICCP Set Point	N/A
Zinc Anode Weight Before (grams)	16.828g
Zinc Anode Weight After (grams)	16.133g
Zinc Loss per day (grams/day)	0.685 g/day

In this experiment, the stainless steel shaft is coated with an epoxy coating. Passive zinc anode protection is the only form of corrosion protection, similar to exper-

iment 7. Neither the potentials presented in Figure 2-20 and Figure 2-21, nor the microscopic pictures in Figure 2-22, are different enough from experiment 7 to form a conclusion. However, the zinc loss per day decreases sufficiently to provide some evidence to support coating the stainless steel shaft. Table 2.6 shows that for experiment 10b, the zinc lost 0.685 grams/day, which is lower than the 0.724 grams/day from experiment 7. Less zinc loss per day when the stainless steel shaft is coated indicates that an uncoated stainless steel shaft is increasing the current demand on the zinc anodes.

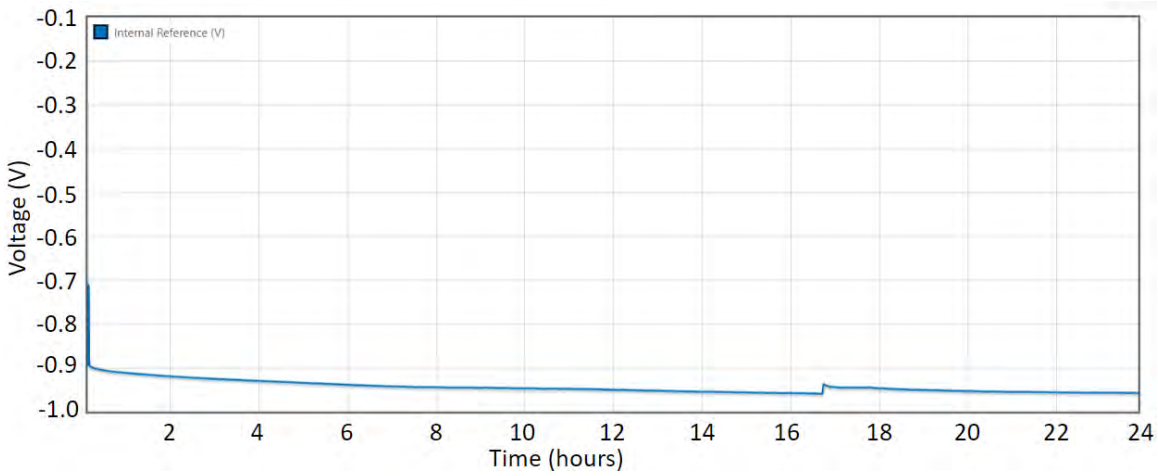

Figure 2-20: Experiment 10b: Internal Reference Electrode Voltage.

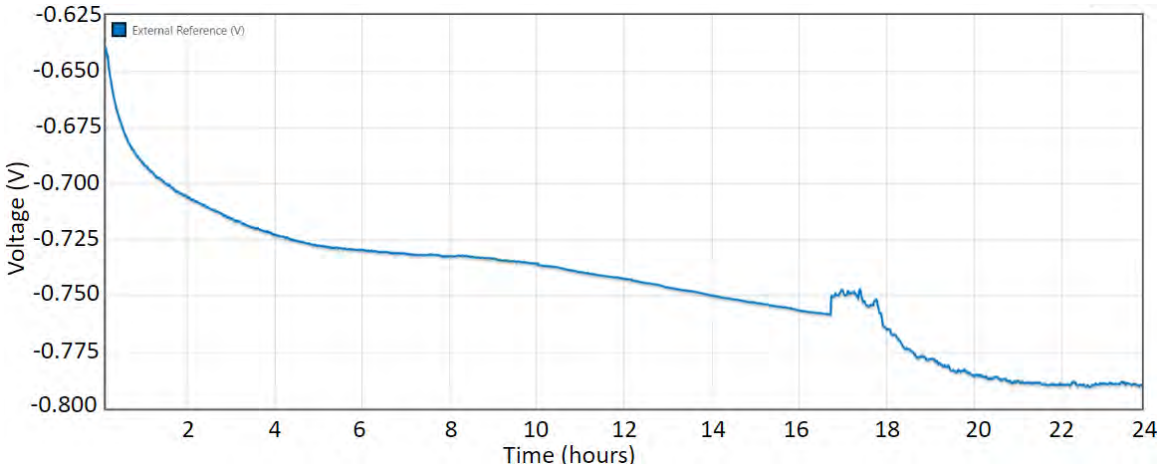

Figure 2-21: Experiment 10b: External Reference Electrode Voltage.

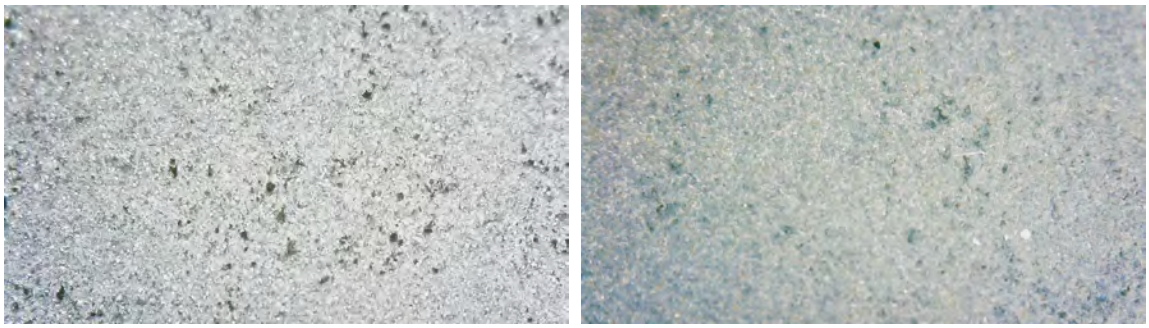

(a) Experiment 10d: Before exposure (t=0 hours) (b) Experiment 10d: After exposure (t=24 hours)

Figure 2-22: Experiment 10b: Before and After Pictures for Tube Steel

2.2.7 Experiment 10d: Passive Zinc Anode, ICCP, and Shaft Coating

The goal of experiment 10d is to build upon the evidence supporting stainless steel shaft coatings obtained in experiment 10b. The dual protection scheme is used for corrosion prevention in this experiment, similar to experiment 9.

Similar to experiment 10b, no noticeable distinctions can be made from the potentials or the microscopic pictures. Again, the zinc loss per day for the coated shaft experiment is lower. In this experiment, Table 2.7 shows that the zinc lost 0.346 grams/day. This compares to experiment 9, where the zinc lost 0.533 grams/day. Experiments 10b and 10d prove that, in the absence of a coating, the passive chromium oxide film is either disturbed or not forming.

Table 2.7: Experiment 10d Setup.

Shaft	Epoxy Coating
Carbon Steel Tubing	Uncoated
ICCP	On
ICCP Set Point	1.0 V
Zinc Anode Weight Before (grams)	16.950g
Zinc Anode Weight After (grams)	16.604g
Zinc Loss per day (grams/day)	0.346 g/day

The importance of experiments 10d and 10b's findings is that the current to protect all metals, including stainless steel, should be considered. Additional research will

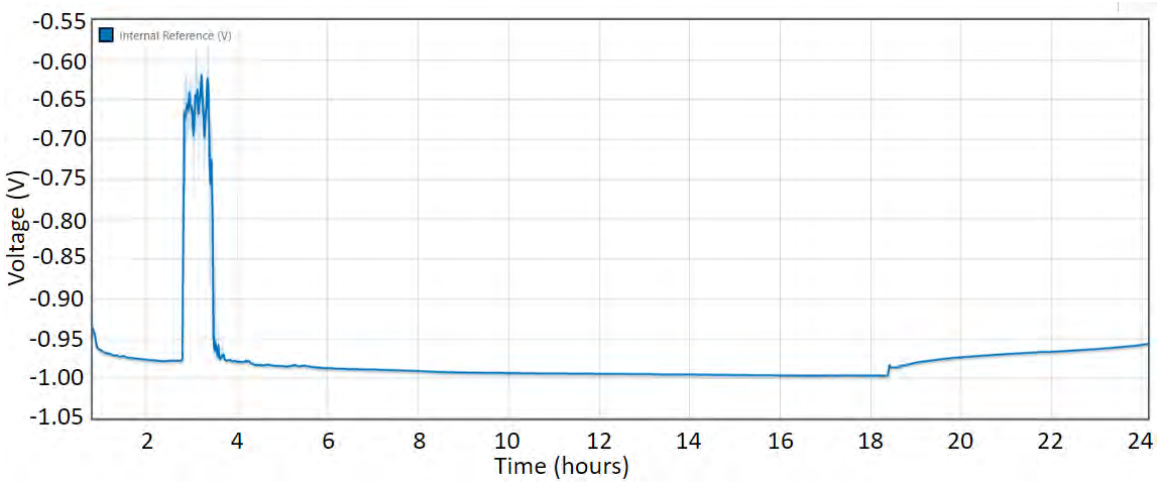

Figure 2-23: Experiment 10d: Internal Reference Electrode Voltage.

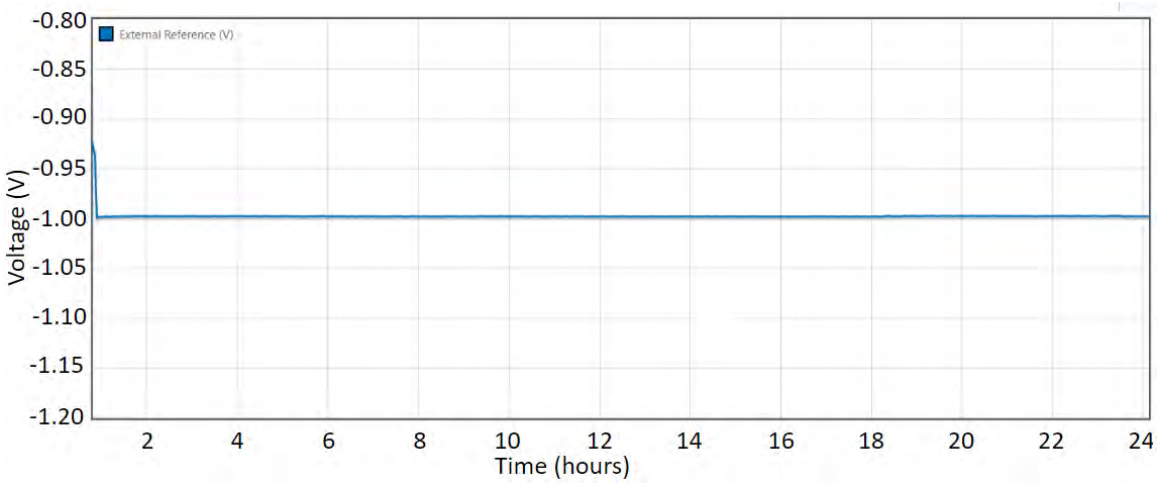

Figure 2-24: Experiment 10d: External Reference Electrode Voltage.

be presented in this work to support the idea that a developed passive film is not protecting the FRC stainless steel shaft and that a shaft coating will protect the stern tube from galvanic corrosion.

These experiments prove that all three protection methods, which are coatings, passive anodes, and ICCP, should be used when possible. Coatings will limit the amount of surface area requiring protection. An ICCP system used in addition to passive anodes will decrease the work required, in the form of current, of the sacrificial zinc anodes and extend their lifespan. Next, this work will present additional experiments to turn the qualitative insights into quantitative results.

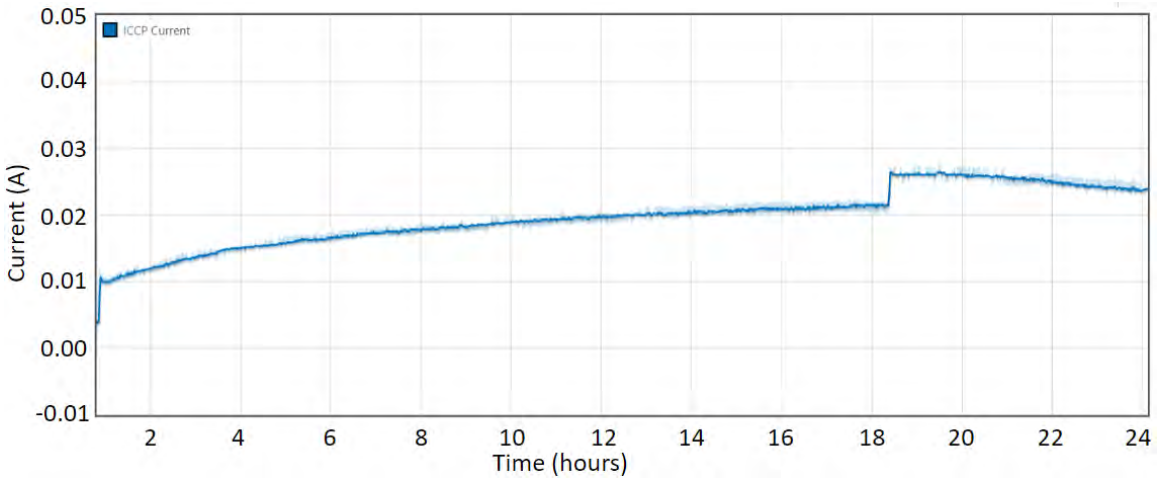

Figure 2-25: Experiment 10d: ICCP Output Current (amps).

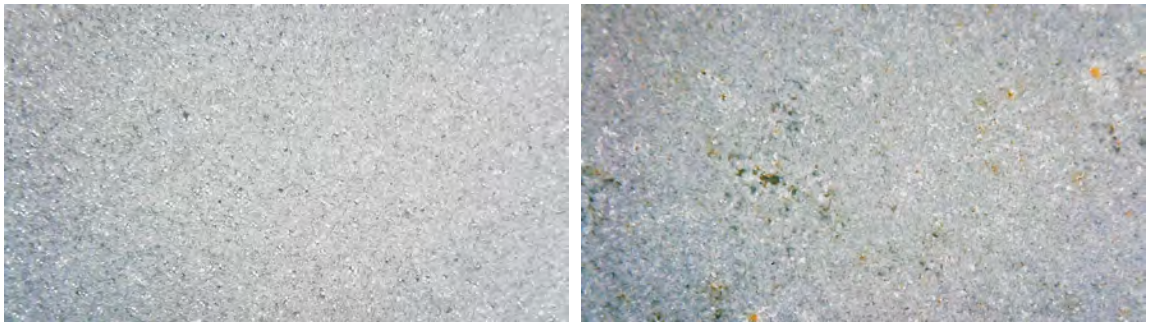

(a) Experiment 10d: Before exposure (t=0 hours) (b) Experiment 10d: After exposure (t=24 hours)

Figure 2-26: Experiment 10d: Before and After Pictures for Tube Steel

THIS PAGE INTENTIONALLY LEFT BLANK

Chapter 3

Field Experimentation - USCGC Margaret Norvell in Miami, FL

This chapter is a review of the field experiment conducted on USCGC Margaret Norvell in Miami, FL. In order to verify the the qualitative laboratory experiments, an experiment was devised and conducted on this FRC to ensure the ICCP can permeate the stern tube. Additionally, this experiment aimed to capture and verify if the reference electrode readings inside the stern tube are in fact different and the magnitude is lower than the value close to the reference electrode. USCGC Margaret Norvell was selected by collaborating with SFLC and determining that this cutter was the next to receive the zinc change out maintenance package. Additionally, the location of Miami, FL ensures that the salinity and water temperature levels are both high and would yield the most drastic results. This chapter was completed in collaboration with Michael Bishop and Jacob Skimmons.

3.1 Instrumentation and Measurements

The in-lab experiments presented in the previous chapter take advantage of a physical model designed to make easy measurements. Testing directly on the FRC requires taking advantage of existing features. When measuring the reference potential inside the shaft tube, it is necessary to preserve the geometry. Removing the shaft tube

inspection covers to insert a sensor will substantially manipulate the results when determining the effectiveness of the ICCP at protecting the interior of the tube. The proposed solution is a custom screw that can replace one the screws securing the inspection cover in place. These screws were hand machined to fit the same size bolt hole as the cover plates on the FRC. The screws are bored out and a strip of silver is epoxied inside. A short section of this strip is exposed at the end of the screw. To convert the silver strip in the tube into silver chloride, the electrode was left in a bath of ferric chloride, containing Iron(III) Chloride and hydrochloric acid, for at least 24 hours. These screws perform the same operation of any other reference electrode, producing a measurable voltage that indicates the level of protection in the area it is measuring. Figure 3-1 are pictures of the plastic reference electrodes in the lab and temporarily installed in a ship during a dry dock period. The T-handle is designed to assist the diver underwater in screwing the reference electrode into the stern tube.

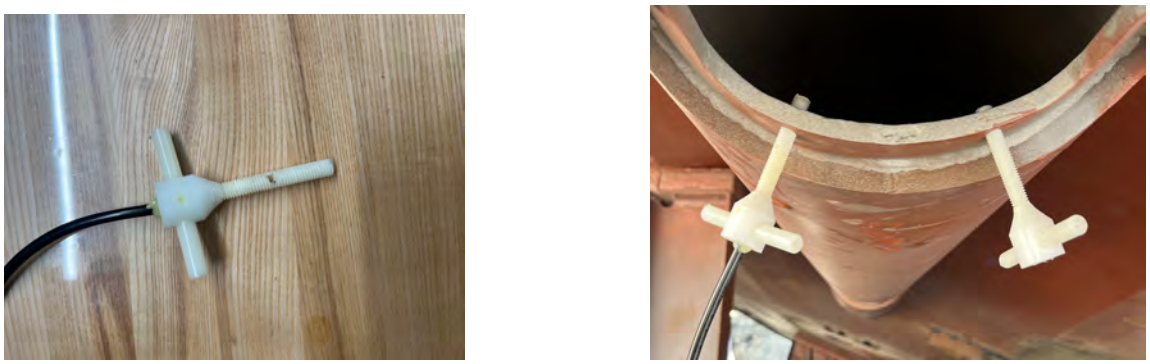

Figure 3-1: Temporary Custom Reference Electrodes

This experiment also involves taking reference electrode voltages in exterior areas where a bolt hole is not available. To accomplish this, another set of reference electrodes were designed with a magnet attached to the top to magnetically attach to the hull. Figure 3-2 is a picture of this design. These magnetic reference electrodes were placed on either side of the aft ICCP anode in the experiment. Because part of the experiment will cause large ICCP currents to be injected into the water, there is the potential for severe overprotection, and thus paint damage, in the immediate vicinity of the anode. These sensors measure this hot spot and will help determine safe limits for increased ICCP usage.

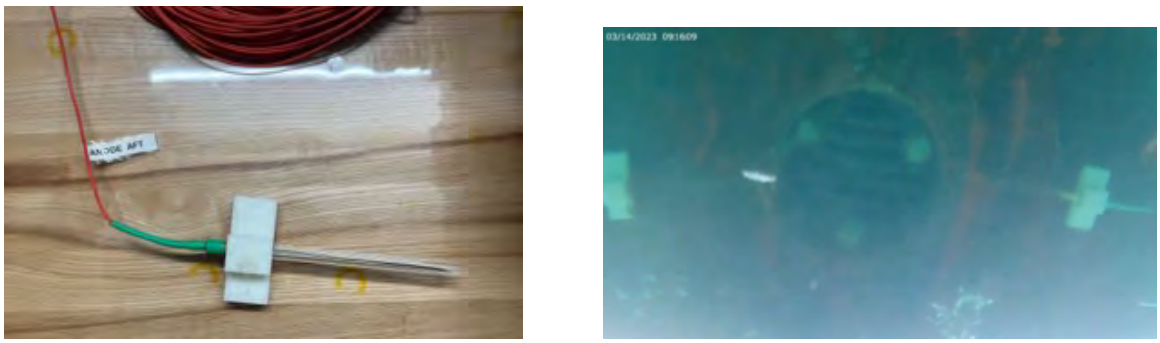

Figure 3-2: Magnetic Reference Electrodes in the Lab and in the Field

Figure 3-3 depicts how the screw electrode is connected to the long cables that reach from the stern tube to the engine room. There is 150 ft of cable and the waterproof underwater connection allows for the reference electrode to easily connect to the cable, preventing cable twisting while screwing in the electrode..

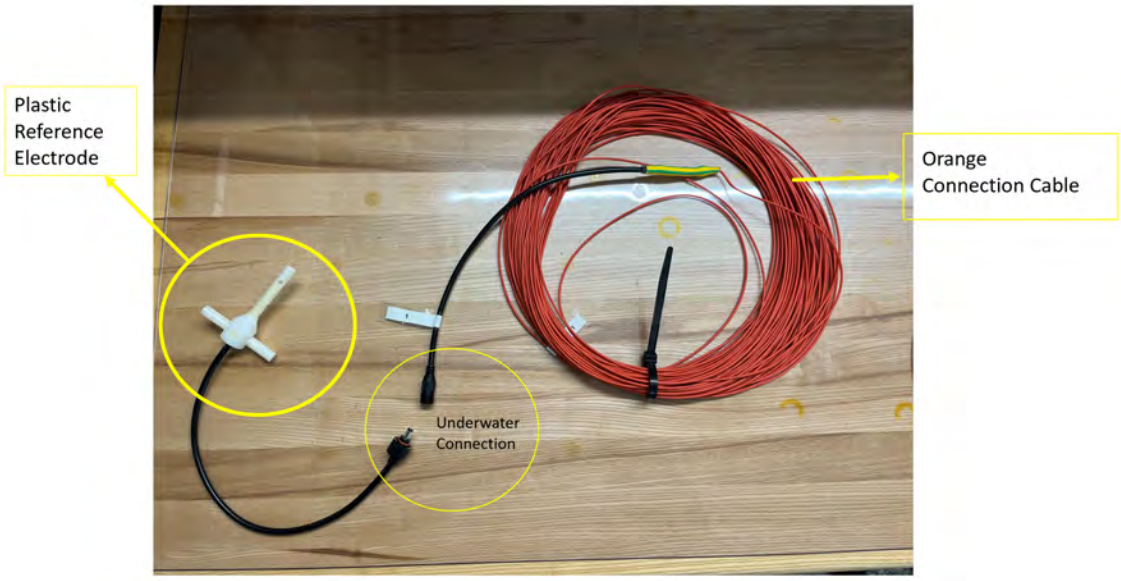

Figure 3-3: Custom Reference Electrodes with cable connections

Figure 3-4 shows the data logging setup brought to Miami, FL. Here are each of the 150ft long cables, the reference electrodes, and the a 10 channel Hioki data logger for measuring various voltages and currents. A strain relief was machined to clamp each cable inside the box to prevent cable disconnections or short circuits when moving cables in a cramped environment..

Figure 3-4: Hioki Data Logger with Cable Entries

3.2 Experimental Set Up

Performing an experiment on the shaft tube in lieu of the annual zinc replacement provided an excellent opportunity to determine tube protection over the lifetime of the internal zinc anodes. Specifically, this would allow instrumentation to be installed and voltages to be gathered while old zincs were on the ship, once they had been taken off and no zincs were installed, and lastly when new zincs had been installed. This is a lengthy process, but gathering data at each point will provide useful insight. The long form process guide to this experiment is listed in Appendix C.

Figure 3-5 provides a graphical depiction of the temporary screw electrode installation positions. In this figure, the three shaft covers are circled in red. The blue arrows point to an image of the inside shaft cover.

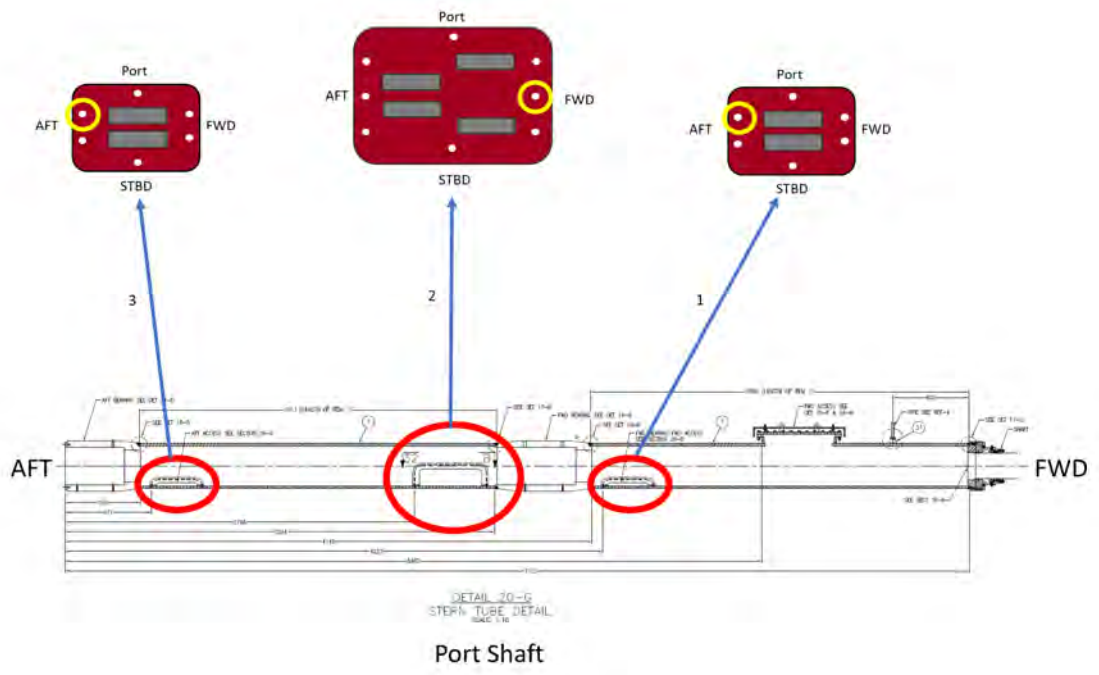

Figure 3-5: Reference Electrode Location along Stern Tube Cover Plates

Circled in yellow is the exact location the divers put the reference electrode screws. These locations were selected to get the closet readings both center line and to their respective bearings where the corrosion is most isolated. The location of the magnetic reference electrodes is shown in Figure 3-6. A magnetic reference electrode is placed forward and aft the anode to determine the worst case reference potential near the ICCP anode. This is particularly useful when the ICCP set point was changed to much higher values to see how the value provided by the ICCP's own reference electrodes related to that of the magnetic reference electrode readings. The divers and Coast Guard team were briefed on the timeline of events. First the divers would go under the water, remove a screw, and install the reference electrodes in the three cover plates along with the magnetic reference electrodes. The magnetic electrodes would not be moved for the remainder of the experiment. Values were taken from the data logger for this *old zinc state*.

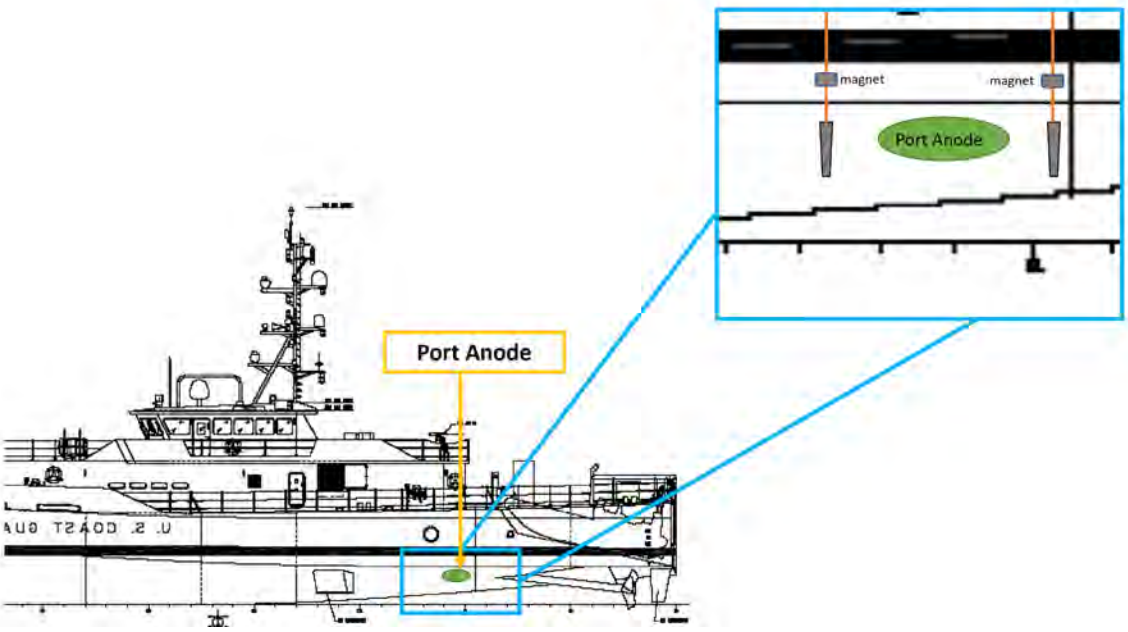

Figure 3-6: Magnetic Reference Electrode Location

Next, the divers removed the reference electrodes, removed the cover plates, and brought them above water. Here, they removed the old zinc anodes and did not attach new zinc anodes. The divers then took the empty cover plates back below the water and reinstalled them, leaving one screw missing for the reference electrodes. They then reinstalled the three reference electrodes and readings were taken for a *no zinc* state. Lastly, the reference electrodes were removed and the cover plates were brought back to the surface to have new zinc anodes installed. The divers again took the cover plates back underwater and installed leaving one screw empty for the reference electrodes and then electrodes were installed for *new zinc*. With each iteration of the experiment, the ICCP set point was changed using an adjuster circuit and the ICCP manually increased up to 30 A. Figure 3-7a is a picture of one of the divers in the experiment when he is about to install the reference electrode underneath the hull. The hioki data logger's 10 channels captured the three reference electrode screws, two magnetic reference electrodes, two ICCP reference electrodes, the total ICCP current, the shaft to ground curent, and the shaft voltage.

(a) Contracted Diver installing temporary reference electrodes in the water inside the stern tube covers.

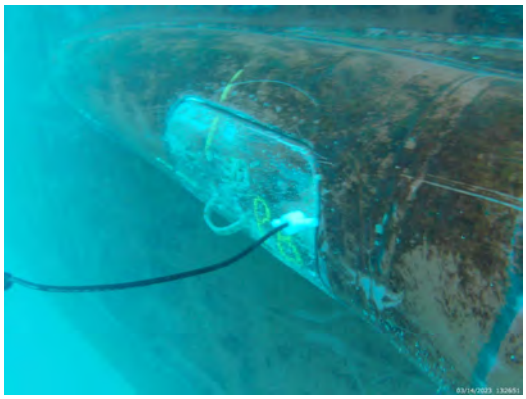

(b) Installed Reference Electrode

Figure 3-7: USCGC Margaret Norvell Experiment Pictures

3.3 Experimental Results

For each zinc configuration, a battery of tests was conducted to fully understand the effectiveness of the ICCP inside the shaft tube. Some tests enable system identification, potentially leading to the ability to determine remaining zinc life without opening the inspection covers. The following results focus on the former.

3.3.1 ICCP effectiveness under set point modification

To determine how changing the ICCP set point affects the reference potential inside the shaft tube, the adjuster circuit was employed to change the set point from -0.85 V to -1.1 V. This is done by setting the adjuster to offset the measured reference voltage by 350 mV and feeding the result into the ICCP measurement terminals. Figure 3-8 is a picture of the adjuster circuit used in this experiment.

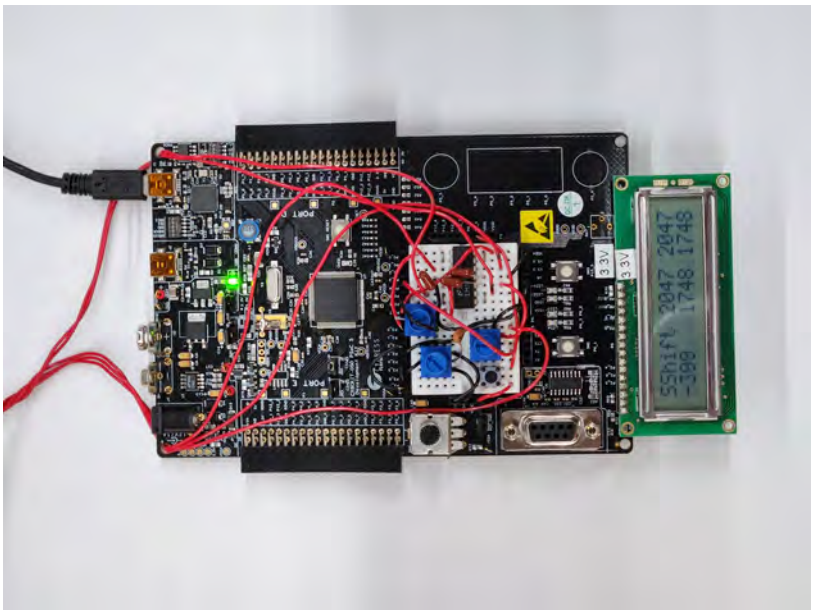

Figure 3-8: Adjuster circuit used to increase and decrease ICCP current

Figure 3-9 shows the first case with the old zincs still in place. The seven reference electrode values are shown along with the ICCP output current. Note that the anode electrodes are the magnetic electrodes placed close to the ICCP anode. The ICCP electrodes are the permanently installed electrodes mounted on the bow of the ship. This figure depicts a step change in the reference, and the thus the left side is not in equilibrium. The right side shows the new steady state, and the values are annotated. Some annotations include the initial value in parentheses when the ICCP is still configured for the -0.85 V set point. It is evident from this first experiment that ICCP can penetrate into the carbon steel stern tube and provide increased protection inside the shaft tunnel. This is because the values are more negative once the reference setpoint was raised. Ultimately, this means ICCP can help extend the life of the zincs inside the stern tube and help provide added protection to keep the hull steel from corroding longer. It is also evident that there is only a minor difference between the reference potential immediately neighboring the ICCP anode and at the bow of the ship. This 40 mV deviation means that localized overprotection is not an issue at this set point.

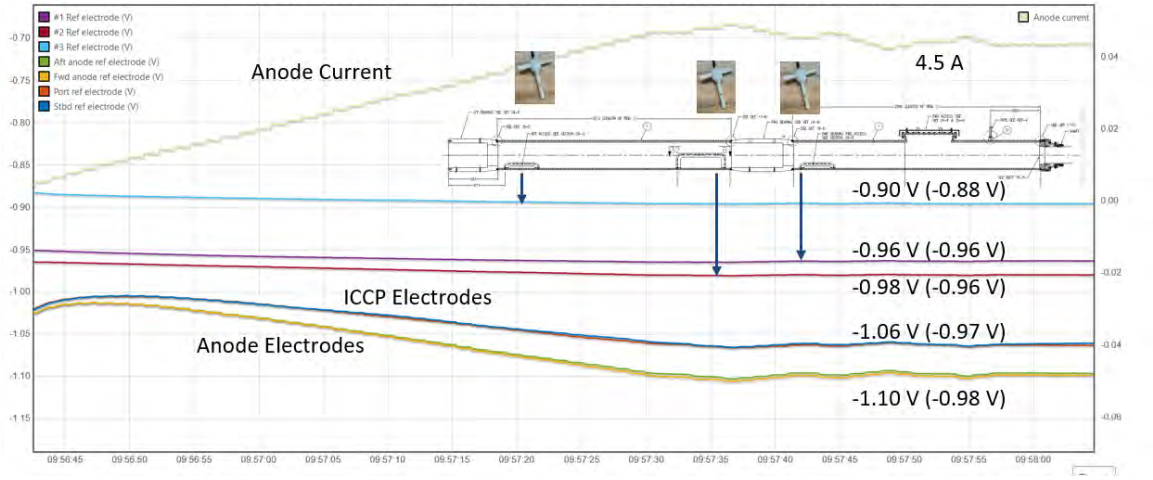

Figure 3-9: Old Zinc; -0.85 V to -1.1 V Reference Setpoint (Initial Value in Parentheses)

The following iteration of the experiment is with no zinc anodes installed at all. Figure 3-10 shows an important result as well. Again it shows that ICCP can permeate the stern tube and increase the absolute value of the reference potential. It also indicates that when the zinc has fully disintegrated, this area becomes susceptible corrosion due to the values being above -0.8 V. Since the ICCP is able to push down the potential inside the shaft tube, it is able to provide some protection to this area even in the absence of zinc anodes.

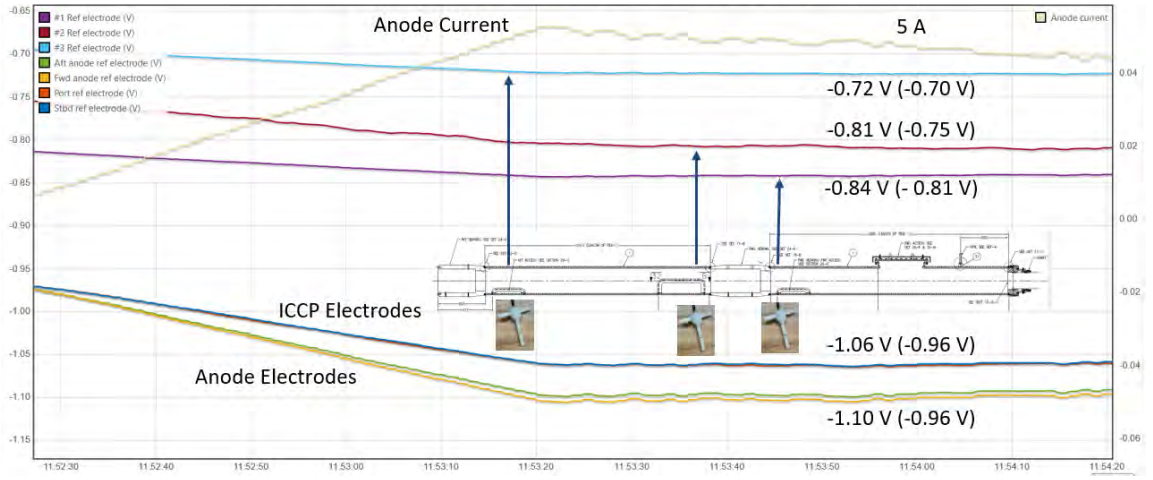

Figure 3-10: No Zinc; -0.85 V to -1.1 V Reference Setpoint (Initial Value in Parentheses)

The final iteration of the experiment is with the new zincs installed. These results

are detailed in Figure 3-11. Without the ICCP the area is fully protected indicating that new zincs are effective at preventing hull steel corrosion. In this case, the measured values are similar to the *no zinc* experiment. These results show minimal effectiveness of ICCP penetration into the stern tube with new zincs. However, the zinc anodes quickly form an oxide coating that decreases exposed surface area. It is likely that within a few days, the effectiveness of ICCP in the stern tube will be similar to that observed with the old zincs.

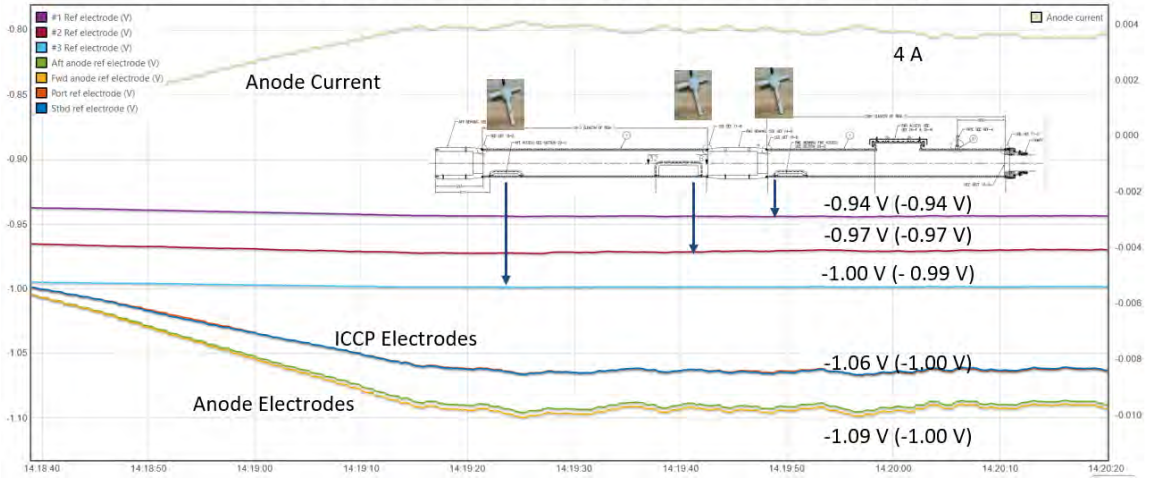

Figure 3-11: New Zinc; -0.85 V to -1.1 V Reference Setpoint (Initial Value in Parentheses)

3.3.2 ICCP Current vs. Reference Potential per Location

In another experiment, the ICCP was operated in manual mode to directly set ICCP current. This test will show the effectiveness of ICCP with stronger currents and for each zinc configuration. First, the behavior inside aft stern tube cover plate, shown in Figure 3-12, is considered.

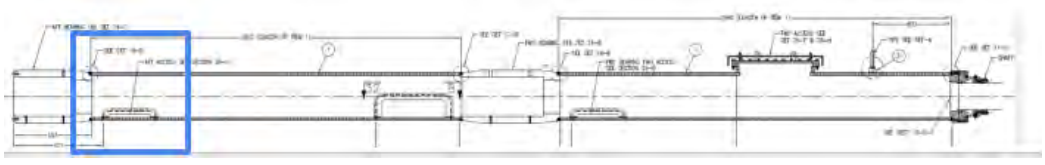

Figure 3-12: Aft Stern Tube Location

Figure 3-13 highlights areas of slight under-protection and ideal protection. With

increased current output, the protection absolute value increases. 5 A is circled as this value corresponds with a -1.1 V ICCP set point. With both new and old zincs, this area is safely protected. If no zinc is installed, the area is under protected even with 30 A of ICCP current. However, additional current always resulted in improved protection of this area.

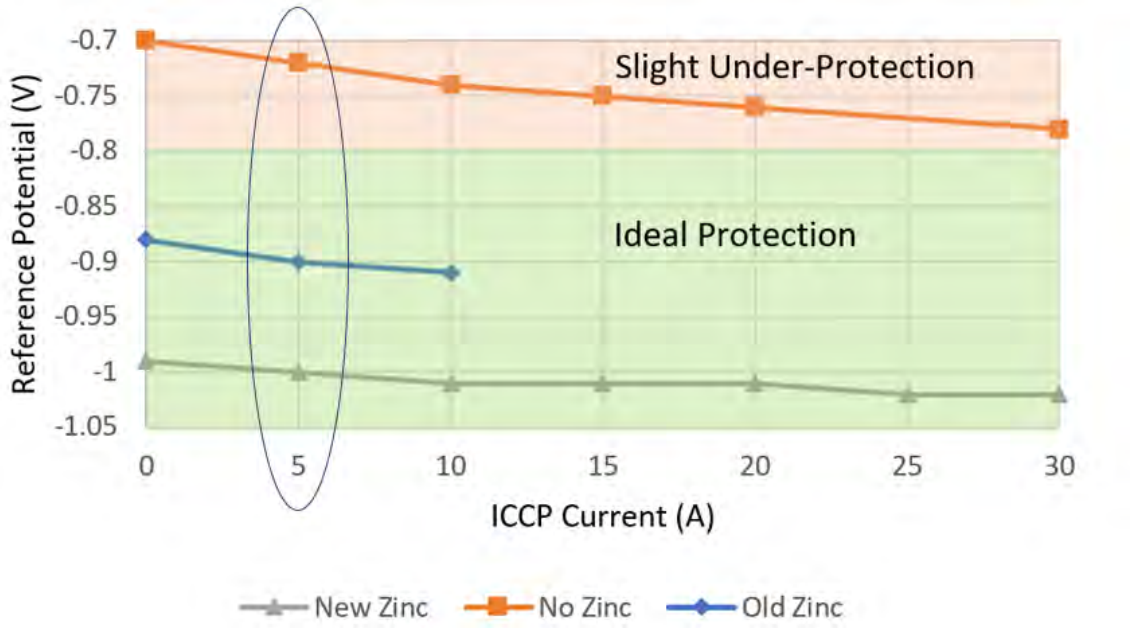

Figure 3-13: Aft Cover Plate- Reference Potential Vs. Current

The next cover plate location analyzed is the middle cover plate and is shown in Figure 3-14.

Figure 3-14: Middle Stern Tube Location

Figure 3-15 outlines the reference potential versus the ICCP anode current. Again, the circled section at 5 V corresponds with a set point of approximately -1.1 V. In this location, this amount of current is able to protect the shaft housing even with no zinc remaining. As with before, additional ICCP current always increased the level of protection in the tube.

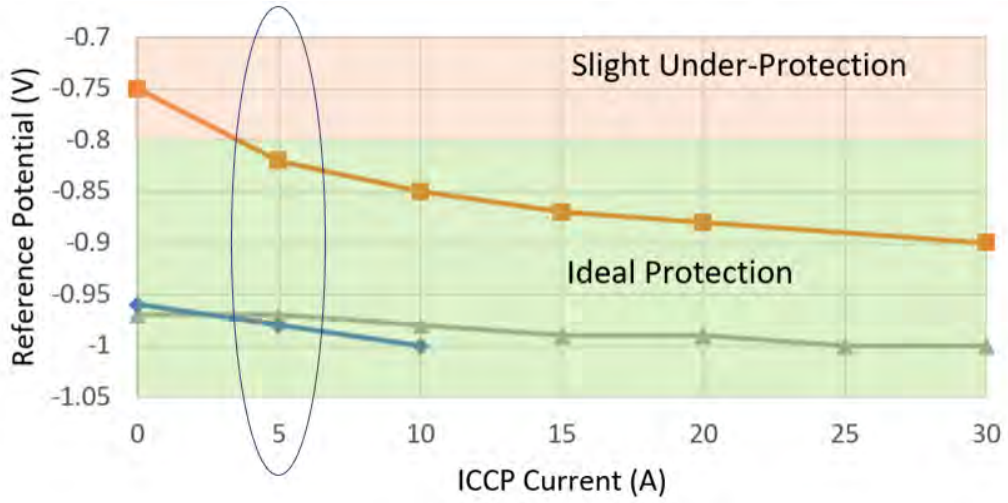

Figure 3-15: Middle Cover Plate- Reference Potential Vs. Current

Finally, the same considerations were analyzed for the most forward stern tube cover plate. Figure 3-16 is an image of the cover plate location. It is important to note that there is a very large, engine room zinc anode installed forward of this cover plate which which means there is no true *no zinc* case for this location.

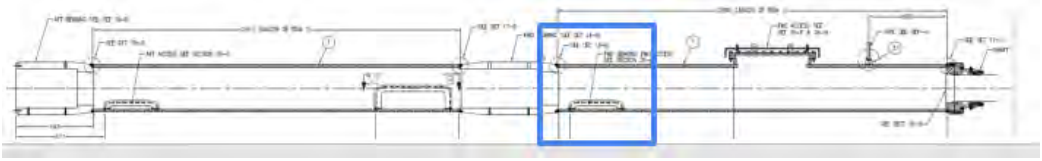

Figure 3-16: Forward Cover Plate- Stern Tube Location

Figure 3-17 shows the ICCP reference potential versus current for the forward-most cover plate. This is the most protected area due to the large zinc presence. With 5 A of current, the area is well protected. It is also important to note - that even with significantly higher levels of current, the area does not become over protected, but rather provides adequate protection and works to slow down zinc usage.

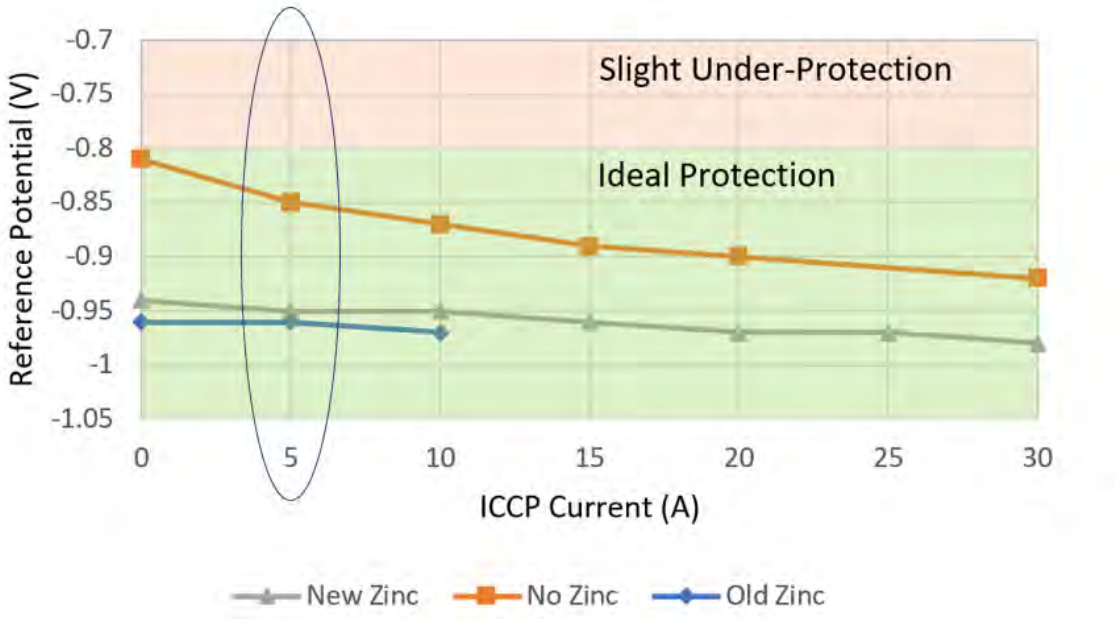

Figure 3-17: Forward Cover Plate- Reference Potential Vs. Current

3.4 Experimental Conclusion

The experiment on USCGC Margaret Norvell gave crucial insights into the operablity and efficacy of the ICCP system. The lower performance of the old zincs will be even more drastic when the shaft is moving and drops the potential as we have seen in chapter 2. The ICCP is able to be reprogrammed to a higher reference potential setting and it will impress current into the water that will permeate the stern tube housing, providing additional protection to the area and lengthening the life of the zinc anodes.

THIS PAGE INTENTIONALLY LEFT BLANK

Chapter 4

Results and Actionable Suggestions

The insights gained from the experiments in the previous chapters provide various techniques to improve the corrosion issue occurring in the FRC stern tube. This chapter proposes five actionable suggestions for the US Coast Guard based on laboratory and field experiments, and calculations on the data collected. These suggestions are not mutually exclusive and an combined approach is likely to achieve the best outcome. This chapter was completed in collaboration with Michael Bishop and Jacob Skimmons.

4.1 Additional Zinc Maintenance

The previous solution used by the Coast Guard for excessive stern tube corrosion was to add additional zinc anodes and shorten the maintenance interval for the stern tube. The first proposed suggestion echoes this approach. Zinc anodes are the only reliable protective measure in the stern tube, and adding more will increase both the lifespan and surface area, ensuring the zinc anodes are effective for longer. The additional surface area will be important in ensuring protection when the shaft is rotating. Figure 4-1 shows pictures comparing the state of the old zincs once removed after one year of wear versus newly installed zinc anodes. Additional zincs will increase the amount of protection in the area, but this space is very tight and many more may not fit. The ship is currently designed to have 16 lbs of zinc in the front half of the

stern tube and 16 lbs in the aft half. It is recommended to increase this zinc design weight to 20 lbs in each half.

(a) Old zinc anodes after one year of wear. (b) Newly Installed Zincs

Figure 4-1: Comparative example of zincs after 1 year vs newly installed zincs.

and adding more will increase both the lifespan and surface area, ensuring the zinc anodes are effective for longer. The additional surface area will be important in ensuring protection when the shaft is rotating.

4.2 Condition Based Maintenance

The second solution also focuses on ensuring the effectiveness of the zinc anodes. The zinc maintenance schedule should be updated and a shaft tube reference electrode should be permanently installed. By having a reference electrode reading in the stern tube, the crew gains a live indicator for protection status inside the stern tube, including during the worst case where the shaft is rotating. At this point, the crew could prompt a zinc change out to avoid the carbon steel deterioration from beginning due to the lack of cathodic protection.

A laboratory study was conducted to determine the zinc consumption rate in comparison to the potential voltage in the water. Figure 4-2 is the graphical result. The signs in this graph are reversed negative to positive. As the absolute value of reference potential rises, zinc current density decreases, directly resulting in slower

zinc consumption. As consumption slows, the lifespan of the zinc increases, providing protection for the carbon steel for longer. This inherently means, that when the absolute value voltage in the water surrounding the zincs is higher, the longer the zinc anodes will last. Ultimately, by extending the life of the zincs, that increases the time period the carbon steel is protected from corrosion. The zinc anodes do not need to "work as hard" providing protection when the reference potential absolute value is higher. When the voltage potential is low, the zinc anodes loose more mass at a higher rate. This means the zinc anodes will expend more quickly. Further calculations to determine this data can be found in Michael Bishop's report [14].

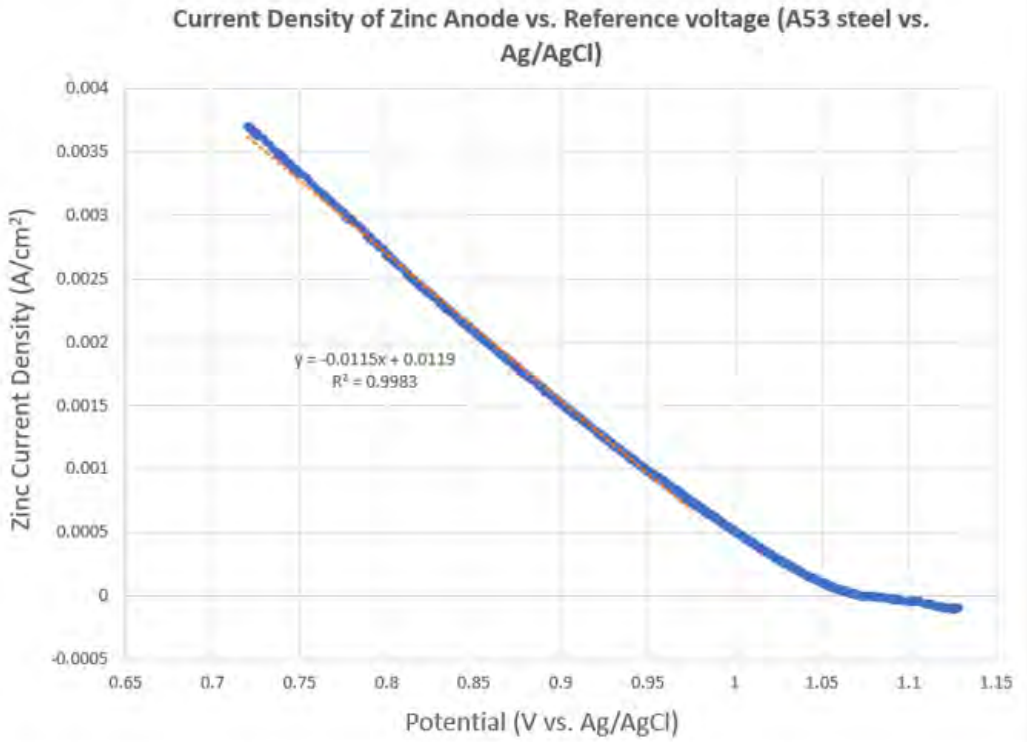

Figure 4-2: Current density of zinc anode vs. Reference Voltage

Using this information, an estimated timeline of zinc cathodic protection current was created. Figure 4-3 is a graphical representation of the decrease in zinc anode current provided versus time in days along with a threshold for the minimum current required to protect the stern tube based on ABS standards [5]. It was determined that after 231 days, or 7.6 months, the remaining zinc in the FRC stern tube will no longer provide adequate protection. This is consistent with the state in which the zinc

anodes were recovered from the divers. By visual inspection, the zincs pulled from the stern tube housing were no longer intact, whereas the zinc anodes pulled from the bow thruster still looked to be mostly whole. This suggestion entails combining this data and changing the maintenance based procedure card to be condition based rather than yearly. With the help of the newly installed reference electrode, once the crew recognizes that the reference potential is above -0.8 V, that will prompt a change out of zinc anodes. It also separates the maintenance card from the bow thruster and propeller zincs, which appear to be operating on a much longer maintenance schedule.

Figure 4-3: Calculations from experimentation of zinc expenditure

4.3 Update ICCP Voltage Set Point up to -1.1 V

The third suggestion is to update the ICCP reference potential voltage setting lower than -0.85 V, going as low as -1.10 V. As seen in Chapter 2 and 3, when significant ICCP current is being injected into the water, there is some penetration into the stern tube and protection of the carbon steel. This protection also decreases the

demand on the zinc anode , increasing the lifespan of the zinc. This is also evident from Figure 4-2 as ICCP penetration depresses the reference potential inside the stern tube, lowering the zinc current density.

This suggestion is advantageous because it a quick and cost effective solution for the Coast Guard. An electricians-mate can reprogram the power supply located in the Engine Room. Previously, this work showed how a circuit can effectively change the set point by modifying the voltage seen the the ICCP. This technique is useful for quick changes, but is not a permanent solution. The ICCP set point is user configurable. After this modification is made, the ICCP will inject current into the water until it measures -1.1 V at the bow of the ship, a potential beyond what zinc anodes are capable of producing. Thus, this change also works to avoid the problem of zincs "blinding" the ICCP.

Chapter 1 discussed the dangers of over protection, which is why it is not advised to push the reference potential setting beyond than the manufacturers cited ideal protection zone [3]. To ensure the area around the anode is protected from an excessive potential, a dielectric shield coating may be applied around the anode. A fusion bond epoxy coating system, comprised of a resin and hardener, can provided added protection to the surrounding area ensuring it does not experience over protection.

4.4 Coat the Stainless Steel Shaft

The fourth suggestion is to coat the stainless steel shaft. Through the laboratory experiments, it was demonstrated that the stainless steel increases current loading on the zinc, decreasing their lifespan. Coating the shaft electrically isolates it from the galvanic system, decreasing the load on the zincs and allowing the zincs to better protect the carbon steel. It is recommended to follow the Department of Defense Standard Practice MIL-STD-2199B as a guide for coating the stainless steel shaft [15].

Coating the shaft will increase the diameter of the shaft, preventing its usage with the current bearings. The maker of the current bearings, Duramax, confirms

that the bearing staves can decreased in size to allow for a thicker shaft. Figure 4-4 shows the clearances between the shaft tube and the bearing with the current design. Figure 4-5 is the proposed new shaft housing design. In blue is the new epoxy coating applied to the shaft in the areas where there is not a bearing. In yellow is a stainless steel sleeve adhered to the shaft in areas where there is a bearing to ensure a tight grip for the water lubricated bearing. This proposed design ensures that the shaft can be safely removed from the ship, coated, and reinstalled without damaging the coating system or the bearings. Additionally, it would be possible to complete this modification during every ship's next available dry dock cycle and the bearing staves are all replaced every 5 years.

Coating the shaft is common practices in most Navy and Coast Guard ships. Although this shaft is stainless steel, it does not alleviate the need to apply a coating system to the shaft. The Coast Guard already performs a similar process on the National Security Cutter, so it is a process familiar to the depot level managers.

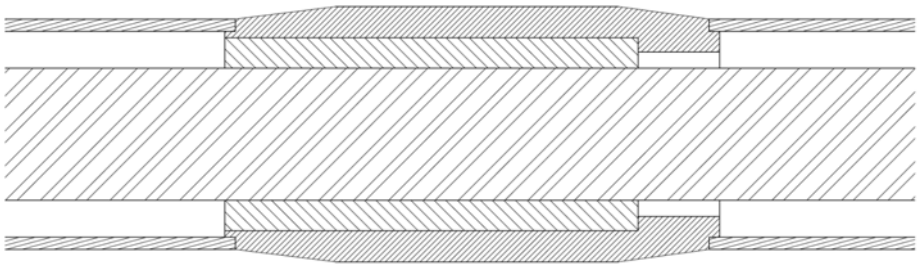

Figure 4-4: Current FRC Shaft Design

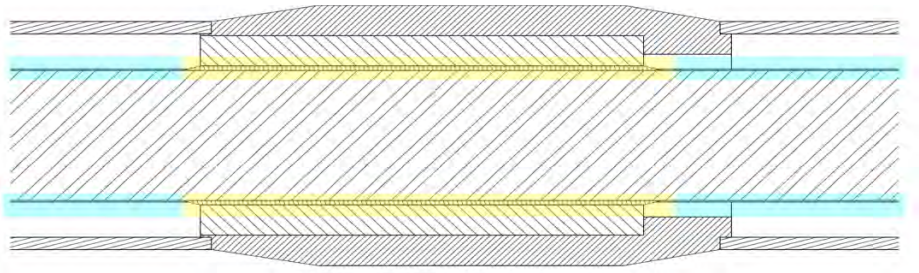

Figure 4-5: Proposed FRC Shaft Design

4.5 Coating Research

The final actionable suggestion is a different way to coat the stainless steel shaft. This idea proposes keeping the current bearing system and spraying a coating onto the shaft while slowly rotating in a dry dock. The spray-able apparatus will be connected through the three stern tube covers. This suggestion will require further laboratory testing to identify the most appropriate coating that meets the ASTM B117 coating standards. A corrosion salt spray test chamber will be employed to test new spray-able coating systems along with future graduate students building and testing the spray mechanism.

THIS PAGE INTENTIONALLY LEFT BLANK

Chapter 5

Shipboard Microgrids and Automation

This chapter diverts from corrosion prevention and focuses on shipboard microgrids. With nonintrusive load monitoring we are able to gleam key insights into the integrity of a ship's power stream data. We specifically gathered crucial insights into the FRC's ICCP Calthelco system in order to help diagnosis the root causes of the stern tube corrosion. Using similar techniques in the ICCP investigation, nonintrustive load monitoring can be applied broadly acrros the US Coast Guard fleet. Electric power systems for marine vessels provide the beating heart for survivability, serviceability, movement, and mission. Fleet modernization for USN and USCG vessels, both existing and planned, builds critically on electric power systems. Unfortunately, automation and feedback control, hallmarks of many modernization efforts, can actually increase the challenge of maintaining mission readiness by masking developing or impending fault conditions in critical systems. This chapter begins with a survey of electrical power system configurations common on ships. Opportunities for power monitoring are identified. In particular, nonintrusive power monitoring can augment or provide automatic watchstanding, logging and usage tracking, energy score keeping, and indicators that prognosticate impending faults. Nonintrusive power data is naturally collated in an easily accessed and securable monitoring system. This data can support ship design by providing up-to-date electric plant load analysis (EPLA)

load factors. This chapter demonstrates techniques across several types of marine power systems and demonstrates support for automated or semi-automated ship operation. This chapter was completed in collaboration with Michael Bishop and Aaron Langham.

5.1 USCGC William Chadwick Install

To verify that the ICCP system was working and not broken, a portable nonintrusive load monitor (NILM) was brought to USCGC William Chadwick in Boston, MA. Here the NILM analyzed the current output from the ICCP onboard. Figure 5-1 shows when the set point on the ICCP was changed from -0.85 V to -1.0 V. Where the graph steps up is the change in set point indicating that the ICCP is working as designed. This gave further evidence that the ICCP reference electrode is being blinded by the forward zincs in the bow thruster tunnel, not giving the ICCP a clear picture of the entirety of the ships reference potential voltage reading.

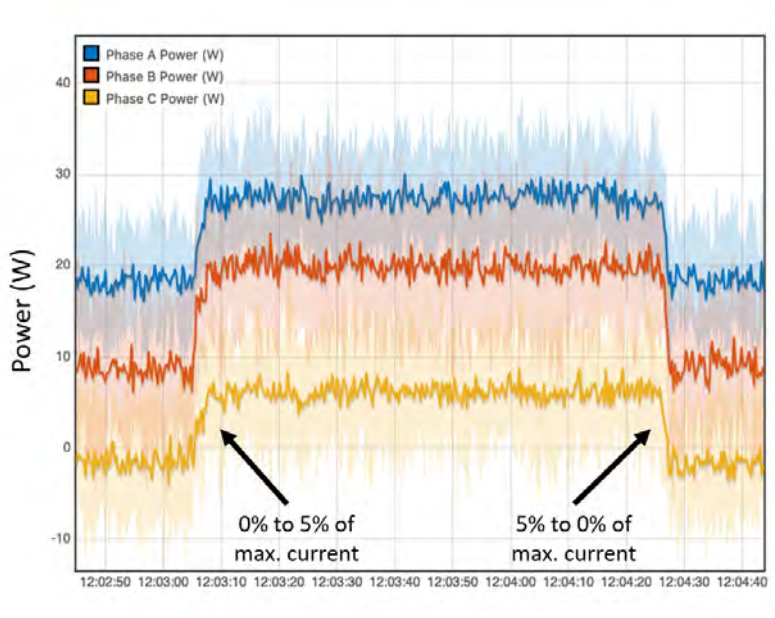

Figure 5-1: Nonintrusive measurements using a portable AIO box onboard USCGC William Chadwick in Boston, MA.

5.2 Historical Background

In 1880, the SS Columbia became the first ship to implement electric lighting [16]. Since then, electric power has become vital to shipboard operation. Designers have continuously experimented with a variety of electrical systems and controls. The United States Coast Guard (USCG) and United States Navy (USN) operate and maintain a diverse ship and cutter fleet. There are significant differences between how each ship or cutter generates, distributes, and regulates electrical power. Ships moored to a pier typically rely on ac "shore" power. Ships underway rely on their onboard or "ship" microgrid. Generally, shipboard power systems are designed closer to the requirements of shipboard loads in comparison to conventional land-based utilities and facilities. Therefore, the ac power quality aboard a ship, especially the ability to maintain a constant voltage amplitude and frequency, tends to be poorer than that of the terrestrial, shore-based electrical grid. For example, Figure 5-2 shows the instantaneous supply frequency onboard a USCG cutter for an example day at sea on generator power versus an example day on land-based shore power. The shipboard generation struggles to maintain operating conditions in comparison to the land-based power feed.

Although nearly all US military ships supply electrical power with marine diesel generators or gas turbines, their microgrids have several varying design characteristics. Maintaining electrical continuity in the event of a failure is vital. Unlike USN counterparts, whose generators are commonly each installed in separate spaces, USCG cutters' ship-service marine diesel generators (SSDGs) are often all located in a single space known as the generator or engine room. In the interest of marine survivability, some of these cutters have an emergency diesel generator (EDG) located in a separate space. The EDG is commonly smaller and only designed to maintain vital loads and must be located above the damage control deck level. Operation of the ship microgrid depends on the availability of controls and user display interfaces. Both the age and the size of a ship contribute to the variety of electrical controls, configurations, and watchstander procedures. Generators aboard older military ships

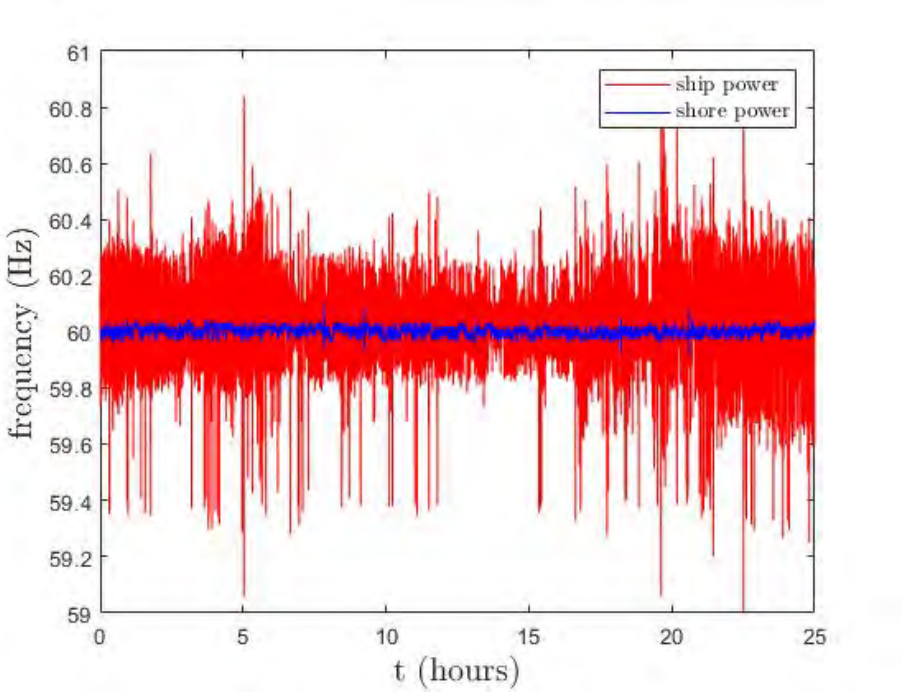

Figure 5-2: USCGC MARLIN supply frequency for a typical day at sea on generator power and in port on land-based utility power.

must be paralleled manually using an installed synchroscope, which shows the phase angle and frequency difference between the two generators. Newer ships and power systems can automatically parallel generators to meet load power demand. Ship size and mission affects the choice of power system topology and bus configuration.

Power systems are the vital arteries for energy flow on ships. It is no surprise, therefore, that power monitoring has a proven, but still not fully exploited, record of assisting with ship operation and maintenance. One approach for power monitoring, nonintrusive power monitoring, uses a single or small set of voltage and current sensors to monitor a collection of loads, disaggregating individual load behavior from measurements on an aggregate power stream, e.g., at a feeder to a panel [17]. A nonintrusive load monitor (NILM) samples the voltage and current (in this work at 8 kHz) at the utility point, and then computes real and reactive power, harmonic content, and system operating frequency [18]. A "NILM Dashboard" can present vital information to ship operators, providing a summary of equipment status and metrics about historical load operation and impending soft faults [19]. Feedback loop controls

often mask "soft faults" which are failures in system performance that do not result in a complete shutdown of the system[20]. Examples of soft faults include slipping belts, vacuum leaks, and low refrigerant charge. In these cases, the system will continue to operate within predetermined set points such as temperature and pressure, giving no obvious indication of failure. If a soft fault is left unresolved, it will eventually become a "hard fault," i.e. a completely broken system coupled with feedback loop controls that indicate as such. These soft faults are difficult to detect, but they cannot hide their power consumption. A NILM is thus a valuable tool in identifying soft faults that can be applied to all types of shipboard microgrids [20]. Common shipboard microgrids deployed by the USCG and USN include systems with single, sectionalized, zonal, and ring bus distribution. With appropriate configuration, nonintrusive power monitoring can be extended to all of these types of microgrids. Nonintrusive power data can provide a unique window to actionable monitoring information for recording ship operations and for performing condition-based maintenance. This chapter reviews common shipboard ac power systems and discusses applications of nonintrusive power monitoring for these various microgrids.

5.3 Shipboard Microgrid Configurations

Typically, ships require redundancy to ensure the availability of vital loads under a range of conditions [21]. In some cases, having multiple generators in one space is satisfactory. However, some ships require further redundancy, for example, by spreading generators and switchboards over several compartments and requiring multiple power routes for certain equipment. In such cases, more complex electrical distribution systems may be desirable [22]. The configuration and operation of any particular electrical plant determines the necessary configuration of power monitoring equipment for ship-wide diagnostics, load monitoring, and life-cycle planning. This section explores a representative set of ac power grid configurations with examples from the USCG including the 87' Marine Protector Class Patrol Boat (WPB), 140' Large Ice Breaking Tug (WTGB), 154' Fast Response Cutter (FRC), 270' Medium

Endurance Cutter (WMEC), and the 418' National Security Cutter (NSC). Additional review is made of the ring bus power system employed on the DDG-51 Arleigh Burke destroyers.

Modern electrical microgrids implement controls that attempt to increase safety and overall power availability, with the ultimate hope of a decreased dependence on user input. Grid architectures used on USCG and USN ac microgrids are outlined in this section. Approaches for control, including paralleling generators, vary with ship type, size, and mission. Protection methods also vary in sophistication to accommodate different microgrid configurations and mission demands.

5.3.1 Electrical Distribution

The centerpiece of a shipboard power system is an electrical generator (or a set of multiple generators). Typically, this is a diesel or gas turbine generator. However, alternative fuels such as liquefied natural gas or hydrogen, and the use of fuel cell technology, are continually being assessed [23, 11]. Once electricity is generated, a distribution system must reliably bring power to loads. Electrical distribution systems on ships, particularly those with hybrid or electric propulsion, face a unique set of challenges that distinguish them from terrestrial power systems. These issues include but are not limited to the variable frequency associated with shipboard microgrids, load sharing, load dynamics, and ungrounded or high impedance grounded systems [24].

Power systems deliver power through a conductor or set of conductors referred to as a "bus" or "bus bar." Several bus bar configurations exist, and the configuration depends on the size, age, and design requirements of the ship. A bus bar may be considered part of a switchboard, which consists of a frame that houses protective devices and controls. Load centers (LCs) are circuit breaker panels connected to the bus bar; connections from LCs energize smaller breaker panels. Breaker panels and individual loads may also be connected directly to the bus bar without an LC. We consider five example ships that illustrate typical arrangements of these distribution components. The 87' WPB, 154' FRC, 270' WMEC, 418' NSC, and USN DDG-51,

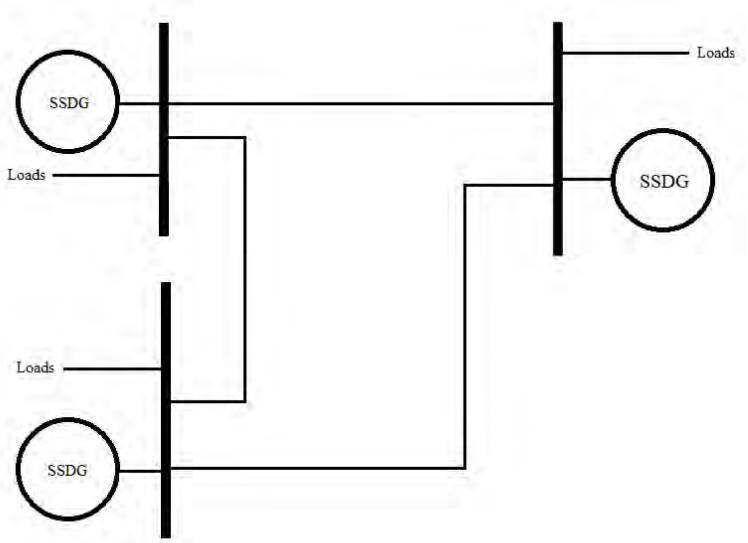

Figure 5-3: Single bus with two SSDGs and two load centers.

presented in increasing size, demonstrate that the distribution complexity generally increases as ship length increases, in addition to other constraints. Additionally, we will discuss ship designs that do not quite fit more conventional arrangements.

The 87' WPB uses a single bus configuration, as illustrated in Figure 5-3. Here, the main switchboard feeds power directly to several loads, as well as to two load centers, which distribute power to subpanels throughout the ship. The single bus configuration is relatively simple, but a failure of the main bus leads to an outage throughout the entire ship. The 87' WPB incorporates two SSDG sets, both connected to the main switchboard where the main bus is located.

The 154' FRC and 270' WMEC use a modified form of a sectionalized bus configuration with two main switchboards and one emergency switchboard, illustrated in Figure 5-4. The two main switchboards are often identified as the 1S/2S switchboards or starboard/port switchboards, and are connected with a circuit breaker known as a "bus tie." The bus tie breaker prevents damage on one side of the bus from disrupting the other side. This setup also allows for maintenance on individual electrical panels without de-energizing the entire ship. In addition to having a bus tie to sectionalize the main switchboard, both the 154' FRC and 270' WMEC have an EDG (located above the waterline in a separate space), emergency switchboard, and automatic bus

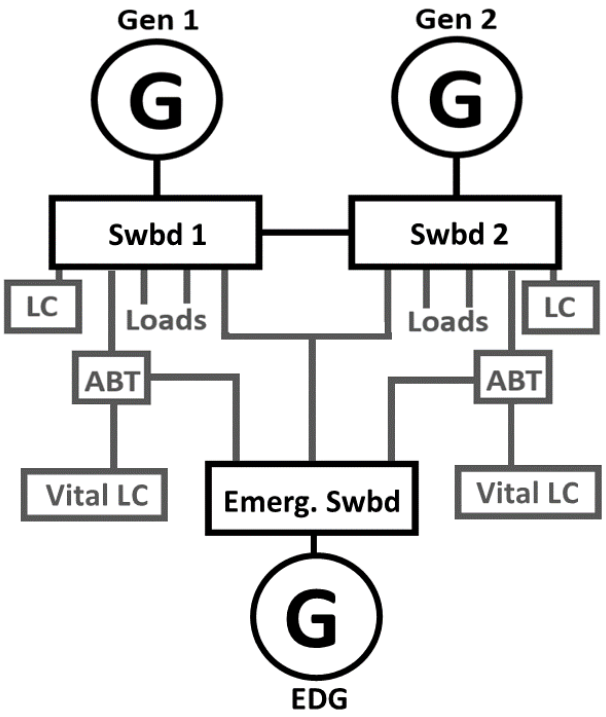

Figure 5-4: Sectionalized radial bus with two SSDGs, two main switchboards and an emergency switchboard.

transfers (ABTs), which protect the overall grid and vital loads such as navigation controls, emergency lighting, and fire pumps. In the event of a power loss, these vessels use the EDG to supply 100 percent of the vital load for at least 30 minutes.

Larger ships generally incorporate more complex power distribution networks. Unlike the "radial" distribution systems discussed so far, the 418' NSC uses a "ring bus" configuration, in which switchboards are connected in a ring. Figure 5-5 illustrates a ring bus schematic with three SSDGs, similar to that found on an NSC. A load can receive power through more than one path, increasing possibilities for power flow continuity. Also, unlike the previous USCG examples, the generators onboard the NSC are all located in separate spaces, and there is no installed EDG.

Newer USN ships have a Zonal Electric Distribution System (ZEDS), which is a ring bus design with added redundancy [22]. Figure 5-6 illustrates an example ZEDS configuration, such as that found on the DDG-51 Arleigh Burke class destroyers, hull number 79 and above [22]. This flexible configuration allows a user to conduct

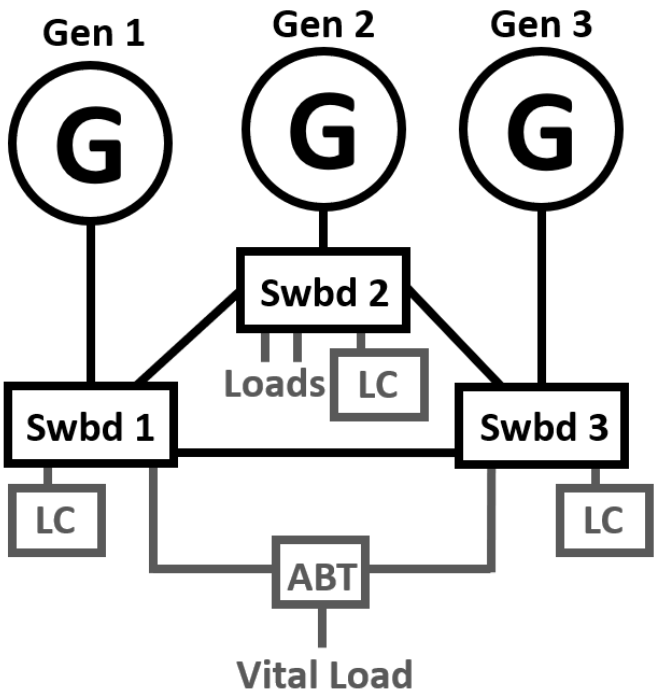

Figure 5-5: Ring bus with automatic bus transfer for vital loads [22].

maintenance or lose one section of the bus without impacting the other sections [26]. Zonal systems also allow the electrical buses to be separated into port and starboard bus rails. This is important aboard USN ships, where continuing to operate in spite of battle damage is vital. However, significant concerns with ZEDS and multi-ring bus configurations are complexity and protection schemes. For this reason, multi-ring architectures are less practical for many USCG ships with smaller hull sizes.

The 140' WTGB, a Coast Guard icebreaking vessel, is an example of a rather unique electrical power distribution system. The WTGB incorporates a single bus configuration for its electrical plant. The WTGB also employs electric propulsion, still a relatively rare feature on USCG and USN vessels. In addition to the two installed SSDGs, there are two main propulsion diesel generator (MPG) sets for electric propulsion. The SSDG electrical plant provides excitation for the MPGs and the main electric propulsion motor via the main switchboard. The throttle position on the bridge commands the MPG and main motor armature voltage, main motor field current, and diesel speed. These relationships translate to the output shaft and propeller speed. Regardless of the specific type of electric propulsion, e.g., from a dc bus

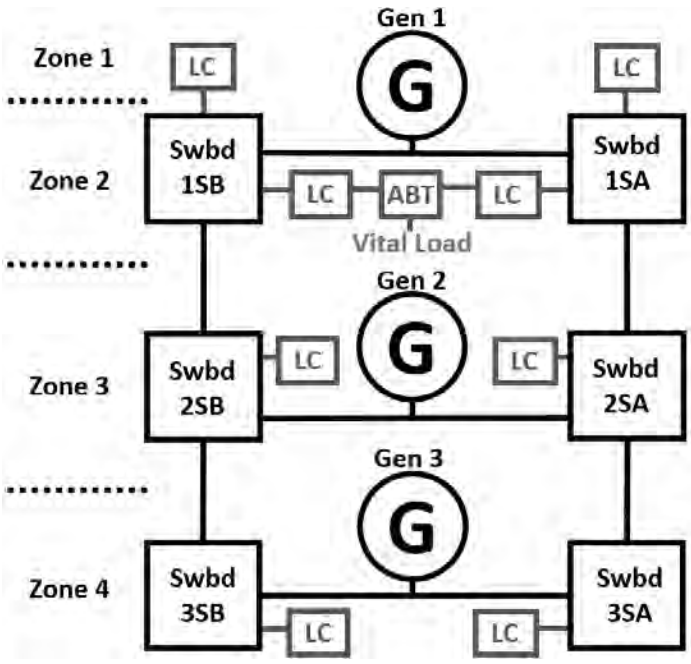

Figure 5-6: Zonal Electric Distribution System (ZEDS) [25].

with power electronics on a DDG-1000, or on the more classical multi-machine drive on the WTGB, electric propulsion brings important changes to a ship's microgrid and, therefore, new electrical monitoring opportunities.

5.3.2 Control Methods

Ship microgrids generally provide enough electrical power generation to meet all of their normal and emergency needs. For certain missions, ships may supply needed power with multiple generators using a process known as "paralleling." The architecture of a shipboard microgrid includes generator controls and control methods to reliably distribute power for different plant setups, such as varying number of paralleled generators. These controls generally consist of two primary components: governors and automatic voltage regulators (AVRs). Load sharing governors use a feedback loop to control their generator's respective prime mover [27]. The load sharing is dependent on the installed generators' horsepower or kilowatt (kW) rating [27]. If similarly sized generators are installed – typically the case onboard military ships, except for EDGs – the load control will nearly equally balance the load between the

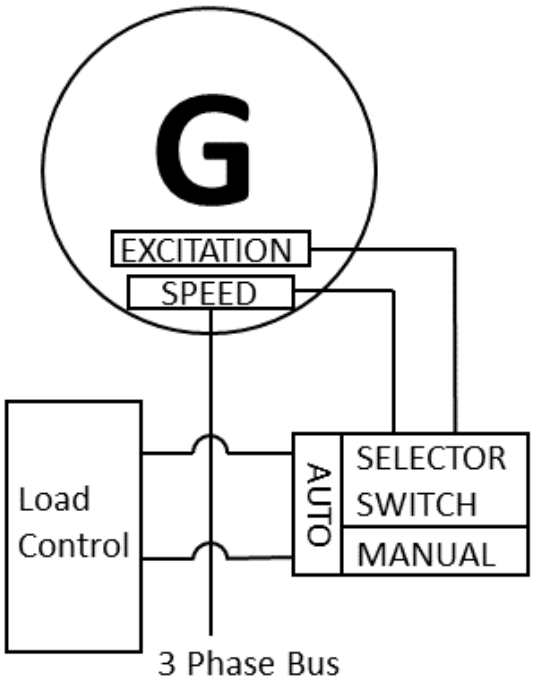

Figure 5-7: Closed-loop generator control example.

generators [27]. However, when ships parallel both a SSDG and EDG, which often have different ratings, the load will be shared unevenly. AVRs control the excitation of a generator in order to maintain constant terminal voltage [27]. Figure 5-7 shows a schematic of closed-loop generator load control that can be found on a USCG ship. The load control is capable of automatic paralleling of generators and balancing the load for parallel operation.

With droop control, the load is balanced between two paralleled generators based on the generators' rating and their "droop" characteristics [28, 29, 30]. Droop is defined as the percent difference of generator frequency between no-load and full-load conditions [27]. As more load is drawn from a generator, the system frequency will decrease slightly based on the droop. Automatic governors can account for the generators' droop characteristics in order to balance the load [27]. Similarly, AVRs are equipped with droop compensation to share the reactive component of the load [27]. If two paralleled generators have the same droop, the load will be split in proportion to their power ratings. Figure 5-8 shows an example of a 100 kW load being

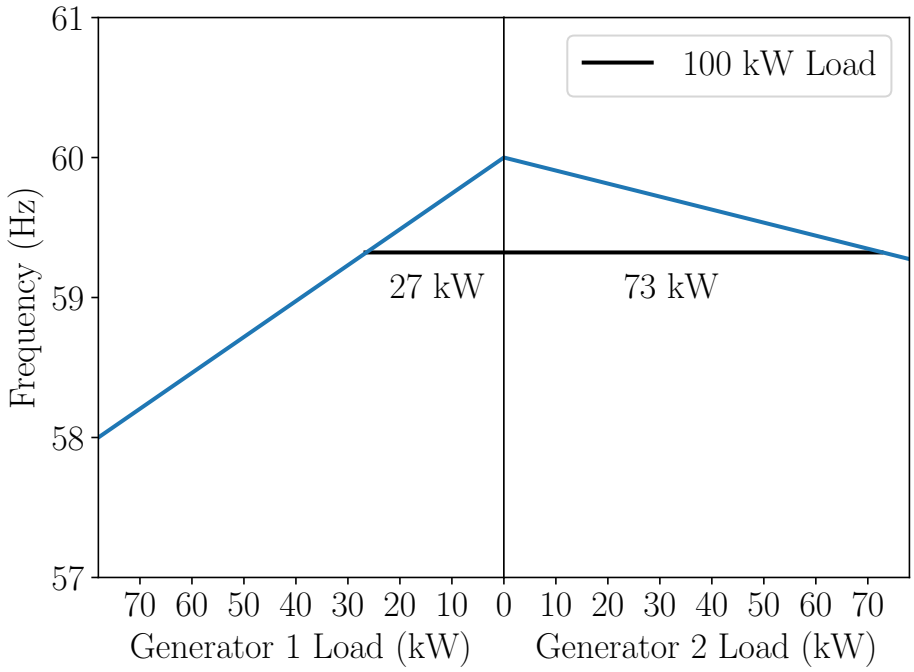

Figure 5-8: Graphical representation of load sharing between two similar sized generators with differing droop characteristics.

split between two 78 kW generators with different droop settings. Figure 5-8 demonstrates that the load is split in proportion to the generators' droops. Isochronous control, in contrast to droop control, maintains a constant frequency of the electrical grid regardless of load on the generator. This is typically only employed for single generator operation due to the added complexities associated with isochronous load sharing [31]. Older USCG cutters such as the 270' WMEC allow the watchstander to switch between automatic and manual modes of synchronization in order to parallel generators. In manual mode, additional switches allow the engineering watchstander to choose between droop and isochronous control. Automatic control refers, for example, to a load sharing control method which uses droop control. Other cutters such as the 87' WPB and 154' FRC have both automatic and manual control of the generators and do not allow watchstanders to switch between isochronous and droop controls.

Additional controls that allow watchstanders to manually adjust a generator's speed and voltage can be adjusted with reference to dials on the switchboard. De-

pending on platform-specific guidelines, crew members may be relied on to continually balance the paralleled generators while on engineering rounds of the ship.

5.3.3 Synchronization and Paralleling of Generators

Generators need to be paralleled for a variety of reasons, most often to prevent the overloading of a single generator when operating high-power loads. This could occur while operating advanced weapon systems or maneuvering thrusters. High-risk evolutions, such as transiting close to shallow water, may also motivate the paralleling of generators for redundancy. For any of these scenarios, generators are paralleled to decrease the likelihood of a total power loss. To parallel generators, the generator being brought online must have voltage amplitude, frequency, and phase angle synchronized to that of the online generator. This process can be performed automatically or manually, but in both cases requires input from the shipboard watchstander. As an example, automatic paralleling is performed on the 154' FRC using the installed load control. The process begins by selecting "e-Power Plant." The watchstander uses the control panel and ensures the offline and online generators are both available. From here the watchstander follows a series of steps on the control panel to start the paralleling process. The oncoming SSDG is selected and started. Once the SSDG is verified to be on and both generators have the same frequency, voltage, and phase angle, the oncoming generator breaker will close, paralleling it to the bus. The FRC also has the ability to parallel an online generator with the EDG.

Manual, or "permissive," paralleling of the generators involves a synchroscope, an instrument that measures the phase angle and frequency between two ac systems. The synchroscope onboard a USCGC is shown in Figure 5-9. The initial equipment verification is the same as the automatic process, where the oncoming generator must reach 450 V ac and 60 Hz. From here, the operator ensures that the synchroscope indicator has moved to the 12 o'clock position. At this point, the operator may attempt to close the generator circuit breaker. If closing the breaker is successful, the associated switchboard indication lamp indicates that the two generators are in parallel.

Figure 5-9: US Coast Guard cutter switchboard and synchroscope.

These same basic concepts are true for both radial and zonal electrical networks. Ring bus or ZEDS microgrids require that generators synchronize prior to closing interconnect bus tie breakers.

5.3.4 Paralelling Generators

Paralleling on the 154' FRC is performed automatically using the Woodward Easy-Gen 3200. The process begins by selecting "e-Power Plant." The watchstander places the generators in programmable logic controller mode, or "PLC Manual" mode, via the panel and ensures the offline and online generators are both available. From here the watchstander ensures the designated SSDG Local/Auto operating panel is in Machinery Control Monitoring System (MCMS) mode. MCMS is the central engineering user interface where users can monitor and control several systems. The alignment is verified via the control panel and the oncoming SSDG is selected and started. Once the SSDG is verified to be on and both generators have the same frequency, voltage, and phase angle, the oncoming generator breaker will close, paralleling it to the bus. The FRC has the ability to parallel an online generator to the EDG as well. For

automatic or manual paralleling of generators, the 87' WPB and the 270' WMEC rely on a synchroscope. Figure 5-9 is a picture of an 87' WPB switchboard with the synchroscope labeled. In the following description, to start it is assumed that the No. 1 generator is online and the No. 2 generator is the oncoming generator. For automatic paralleling, the first step is to verify equipment status and have both generators running. Before this can be accomplished, the No. 1 generator must be running and delivering power to the bus. The No. 2 generator must then be started, and the voltage on generator No. 2 should become stable at 450 V ac. The frequency should become stable at 60 Hz. The following steps are performed on the main switchboard. The paralleling switch is switched from off to the 2S position. The synchronizing switch is placed in the check position, voltage select switch in the main bus position, and the No. 2 circuit breaker is closed. At the moment of synchronism, the No. 2 generator breaker control switch must be momentarily closed. If the breaker does not close, the 1S switch must be placed in the reset position. If the closure was successful, a light indicates that the generators are sharing the load. Once the generators are synchronized, the isochronous switch can be placed back into the normal position with generators both supplying power to the main bus equally and operating using isochronous control. Paralleling the generators manually with a synchroscope is referred to as permissive paralleling. The initial equipment verification is the same as the automatic process, where the oncoming generator must reach 450 V ac and 60 Hz. From here, the paralleling switch is placed in the 2S position and the synchronizing switch in manual 1 or manual 2. At this point, the watchstander can manually adjust the voltage sharing. If the 2S voltmeter is greater than 5 percent higher than the reference, the voltage regulating switch (VRS) on the 2S generator must be placed into the auto position and the 2S VRS to the right is used to adjust the voltage. The oncoming generator is the one adjusted, not the online generator. To adjust the No. 2 generator's frequency, the 2S speed adjust rheostat (SAR) can be turned clockwise to increase frequency, and counterclockwise to decrease frequency. From here, the voltage selector switch to the main bus position and the voltage monitoring/frequency monitoring (VM/FM) switch is placed in its active position. The synchronizing indi-

cation lamps should be extinguished. When the synchroscope indicator is moved to the 12 o'clock position, the operator may attempt to close the 2S generator circuit breaker. At this point, the No. 2 control switch generator circuit breaker is momentarily closed. If the breaker closer is successful, the associated switchboard indication lamp will indicate the two generators are in parallel. Next, the isochronous switch is placed in the normal position allowing both generators to supply power to the main bus equally.

The same basic concepts are true for both radial and zonal electrical networks. Ring bus or ZEDS require the bus tie breakers, similar to the FRC and WMEC, to be synchronized prior to closing the bus tie breaker.

5.3.5 Microgrid Protection

Several methods exist to ensure the overall protection of the grid including automatic bus transfers (ABTs), panel networks, overspeed trips, overpower protection, and multi-function monitors (MFMs). In addition, real-time electrical plant properties such as oil temperatures, jacket water temperatures, voltage, and frequency can warn watchstanders of abnormal conditions. On many Coast Guard cutters, limits for the aforementioned properties are set through the Machinery Control Monitoring System (MCMS) or a similar system.

The complex nature of ring buses and Zonal Electric Distribution Systems (ZEDS) may complicate the detection and isolation of faults. Currently, the Navy has installed multi-function monitors (MFMs) on many Navy ZEDS to minimize the number of unavailable sections of a ring bus during a fault [32]. The MFM can control a contactor or breaker which can interrupt power flow to a specific section of the switchboard. MFMs are placed throughout the zonal distribution system and compare the voltage magnitude and angle as well as power to recognize a fault condition. If a fault is detected by the MFMs, they will collectively determine the location of the fault by examining the change in power flow. This is a challenge because power can flow in either direction around a ring or section.

Emergency switchboards can be a component for survivability on smaller ships

that do not have space for a ring bus or ZEDS. The EDGs installed aboard USCG ships have switch inputs that process auto start and auto stop commands. In case of a generator failure, the emergency generator system senses a fault and automatically starts the emergency generator. On the emergency switchboard the generator and bus tie have motor-operated breakers. The switchboard only allows for the remote closure of the motor-operated circuit breakers if one side of the circuit breaker does not have power (indicating a power loss) or if both sides are synchronized, indicating that the EDG is ready to be paralleled. The ABTs ensure the continued operation of all emergency systems onboard. The ABTs will power the systems on the vital power panels when the main bus is supplying power to the ship. If power from the main bus is interrupted, the ABTs will switch to the emergency switchboard. Ideally, this process is nearly immediate, ensuring the availability of vital loads.

5.4 Power as Predictor

MCMS systems installed on Coast Guard ships allow watchstanders to identify certain faults. For example, sensors such as temperature sensors can inform a watchstander that a system is not cooling or heating a space or machinery system properly if the temperature falls out of set limits. However, soft faults – faults that degrade but do not disable operation – often go unnoticed, as feedback control works to maintain commanded output levels by altering net energy consumption and run times. Power monitoring can identify soft faults that would otherwise go unnoticed, potentially preventing "hard faults" that lead to equipment failure. A NILM can not only provide an easily installed platform for fault detection and diagnostics, but can also provide data to supplement design processes such as electric plant load analysis (EPLA) conducted for ship designs.

Fascinatingly, power monitoring, including nonintrusive power monitoring, can be implemented on all of the microgrids described in the previous section, including ring bus and dc distribution systems [25]. Power monitoring can augment existing monitoring and control systems and watchstanders, flag soft faults that feedback systems

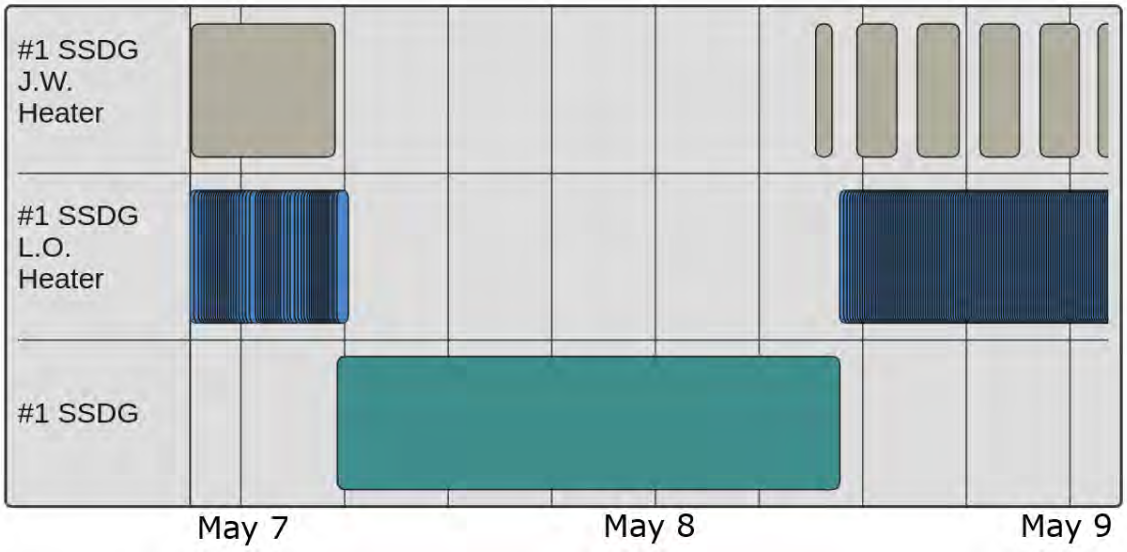

Figure 5-10: NILM Dashboard timeline view showing SSDG operation based on load status. Colored blocks represent periods equipment is online.

and MCMS may miss, and provide sustained data that informs ship operations, alterations, and future designs. We have installed nonintrusive load monitors on five US Coast Guard Cutters (USCGC): ESCANABA (WMEC-907), SPENCER (WMEC-905), THUNDER BAY (WTGB-108), MARLIN (WPB-87304), and STURGEON (WPB-87336) [33, 34]. Among many other applications, field results demonstrate that a NILM can track plant lineup using only the plant frequency. A NILM can also identify signatures that prognosticate faults and provide basic data for energy scorekeeping and automatic watchstanding.

5.4.1 Automatic Watchstanding

Crew members aboard US military ships perform multiple assigned roles. In many cases, watchstanders are tasked with typing or writing up changes in shipboard operation in either paper or electronic logs while simultaneously physically performing the watch requirements. These logs include plant status, liquid transfers, on-loads or off-loads, failure reporting, casualty control steps, and any other pertinent engineering needs. Safety requirements and operational tempo may interrupt the exact timing and recording of events, which may be estimated at later times by watchstanders.

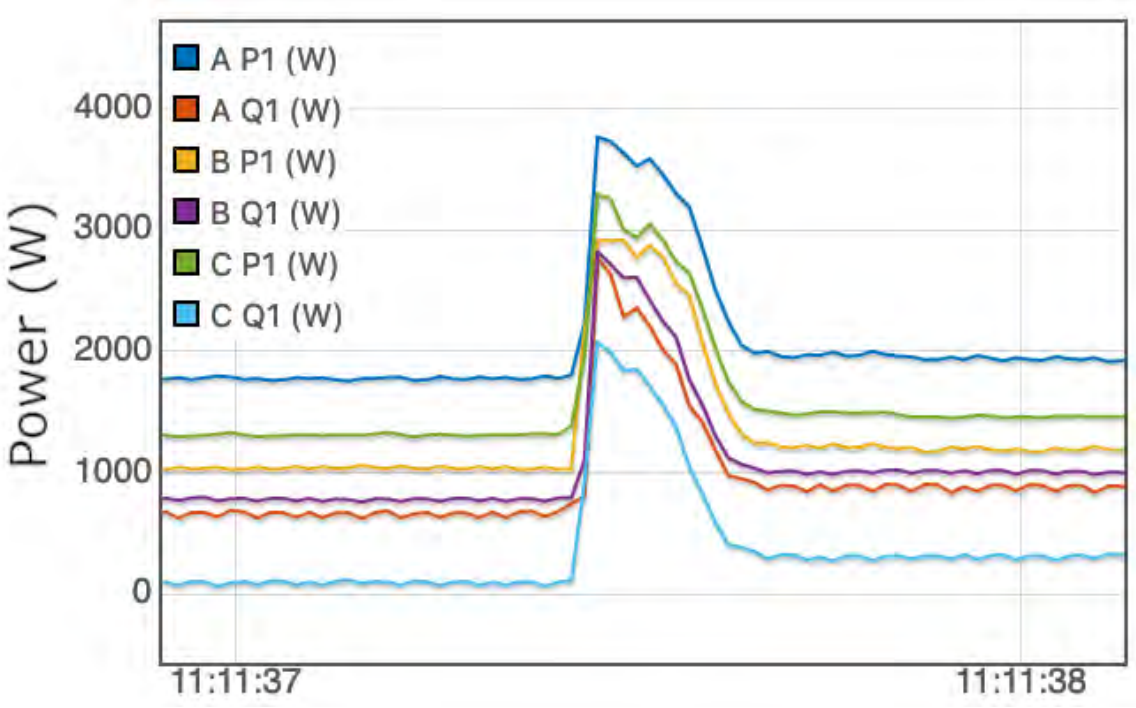

Figure 5-11: USCGC MARLIN fuel oil transfer pump turn-on power transient.

High-bandwidth data coupled with automatic transient recognition in a power monitor like a NILM enables a machine learning system to generate an automatic log of shipboard load operation. This automatic log can supplement or corroborate the accuracy of the manually generated log, which can shift some or all responsibility from the watchstander to the NILM, allowing a heightened vigilance from human operators and more accurate records from power monitoring throughout a watch. Strictly considering cost within the US Coast Guard, the hourly cost to employ an E-5 for watchstanding is $70 [35]. In some instances, three engineering watchstanders are billeted at a time. Automatic watchstanding, enabled by a NILM, could decrease this to one or two watchstanders, which would amount to significant cost savings over the ship's life cycle.

As an example of automatic watchstanding possibilities through power monitoring, consider the main diesel engine (MDE) lube oil (LO) heater on a 270' WMEC. The operation of this heater is a tell-tale that reveals the operating schedule of the engine itself. The MDE lube oil heater cycles actively when engine temperature falls below a setpoint, and secures when the active engine's temperature rises above the setpoint

[19]. By observing the power consumption of the lube oil heater, a NILM can infer and extract the operating times of the engine (a non-electrical device in and of itself). NILM Dashboard can display both the observed operating characteristics of the lube oil heater and also the extracted or inferred operating schedule of the engine, all for quick review by the crew on a "timeline view." Similarly the SSDG operating schedule on a 270' WMEC can also be captured from the associated jacket water (JW) heater and lube oil heater [36]. Figure 5-10 shows the operation status of a 270' WMEC's SSDG and SSDG JW and LO heaters. We have found that, on an 87' WPB, the MDE jacket water heater can provide similar operating data. In addition, the operation of a fuel oil transfer pump can provide information about the ship's MDE operation. Figure 5-11 shows the turn-on power transient of the MARLIN transfer pump. Relatively constant fuel transfer indicates increased fuel consumption of the engines and a higher ship speed. With analysis considering the transfer pump's electrical consumption in light of the transfer pump's fuel flow rate, a ship's patrol fuel consumption can be estimated and broken down into shorter periods of operation. This type of analysis provides redundant or backup estimates even on ships that track fuel consumption in other ways. The electrical loads on different ship microgrids provide a variety of both direct and inferred monitoring opportunities that can document ship operation directly or as a backup monitor.

In addition to turn-on and turn-off events, dynamic or continuous changes in power demand during active operation can expose details of physical tasking. For example, some loads draw power under operating demands that are reasonably modeled as stochastic. In such cases, even when deterministic events may ultimately govern operation, analysis of the statistical properties of power consumption can provide valuable summary insights into load operation and ship operation. For example, power surges seen in a hydraulic pump connected to a controllable pitch propeller (CPP) can indicate increased demand for pump actuation while maneuvering the ship, as shown from the WMEC data presented in Figure 5-12. Analogously, on electrically-propelled ships, the power demand of generator exciters monitored by a NILM can provide a direct history of driving patterns, as shown in Figure 5-13.

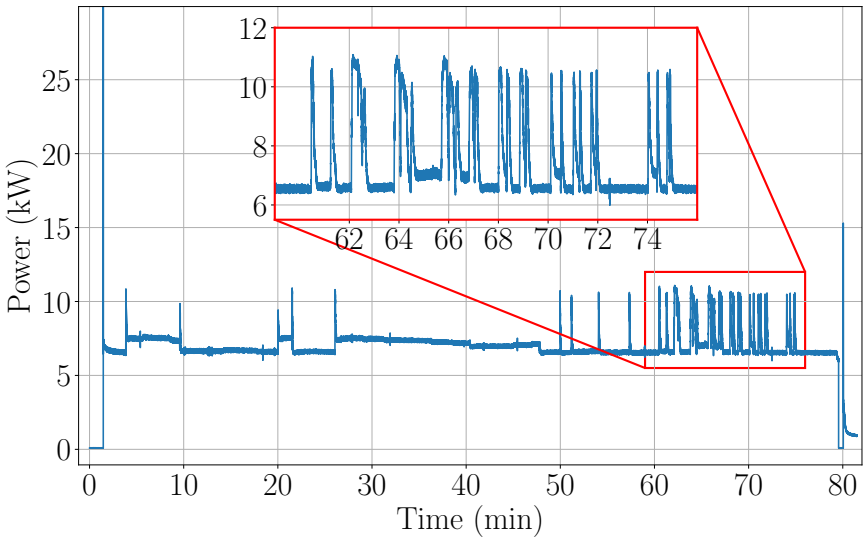

Figure 5-12: Power consumption of a controllable pitch propeller pump with a zoom-in on power "surging."

Analysis of seemingly random power variations, appropriately tailored for particular loads like CPP or drive propulsion, can provide an automatic logbook of ship handling to complement manual logs.

Shareholders in a data-driven world seek tools to analyze project efficiency and manage costs. For crew watchstanding and energy consumption analysis, crucial cost-saving potentials are at stake. An example within the US Coast Guard is the "operational availability metric" that tracks the amount of time per year a cutter is fully operational [35]. Hourly rates of ship operation are closely tracked for cost-cutting and accounting considerations. For example, the 87' WPB's hourly operational cost is estimated to be $4,410 [35]. A significantly larger vessel with different operational capabilities, the 418' WMSL, has an hourly operational rate of $30,859 [35]. Power monitoring coupled with machine learning can allow engineers to more easily see operating profiles and opportunities for increased efficiency and economization. With fuel costs second only to personnel costs, this could result in remarkable savings across an entire fleet or hull type. Also, the ability of power monitoring to decrease repair costs and shift maintenance and repair to planned maintenance periods instead of operational periods can provide unique opportunities for cost saving.

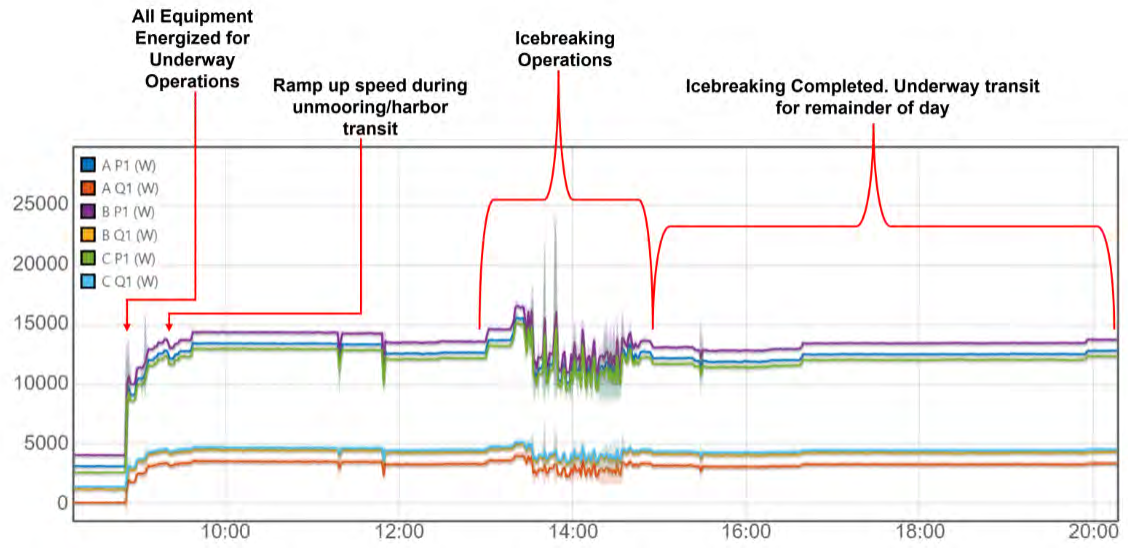

Figure 5-13: Power consumption reflecting driving data of an electrically propelled icebreaking ship.

5.4.2 Frequency as a Generation Metric

Variations found in a ship's microgrid frequency data provide various automatic diagnostic and logging opportunities. Additionally, as computing power has become abundant and cheap, onboard monitoring systems can run scientific computing software for real-time analysis of data streams. To illustrate this, a NILM installed on the USCGC MARLIN captured over three months of frequency data, including ten underway periods where the ship relied on its marine diesel generators for electrical power. Analysis revealed correlations between the ship logs and observed phenomena in the captured frequency data. If exploited, these correlations suggest that ship plant status can be automatically logged from power data.

Sharp transitions in operating frequency were correlated with changes in the MARLIN plant lineup. An example is shown in Figure 5-14, in which the plant status changes from one to two generators at minute 4. We concluded that an increase in steady-state frequency of between 0.04 and 0.08 Hz indicates a transition from single to dual generator operation. The physical explanation for this increase lies in the droop characteristics of generators, shown in Figure 5-8. With a constant total load, adding generators in parallel reduces the individual load on each generator, increasing

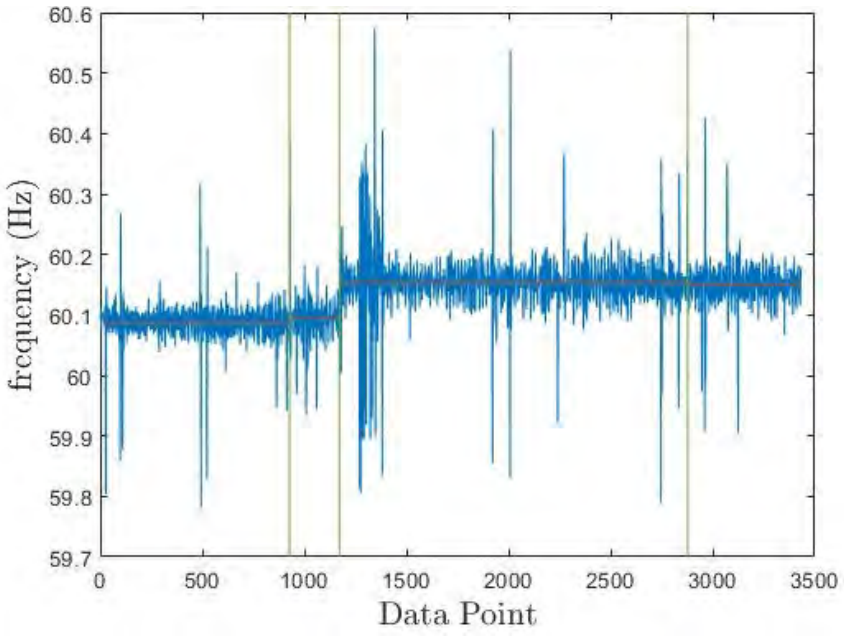

Figure 5-14: Frequency data on USCGC MARLIN showing generators paralleling at minute 4.

the operating frequency.

Furthermore, periods of shore power exhibited much smaller variance in system frequency compared to the periods of onboard ship power, as shown in Figure 5-2. To explore the use of frequency variance as a metric for ship plant status, we calculated the standard deviation (i.e. the square root of the variance) of ship frequency for 10 periods of shore power and ship power. The average frequency standard deviation across the periods of shore power was 3.44 mHz; the same metric for the periods of ship power with one generator was 24.3 mHz. This difference in frequency is explained by the poorer ac power quality associated with ship generation when compared with terrestrial grid power.

Combining these techniques allows an automatic logbook of ship plant status to be generated in real time. A NILM can observe large changes in frequency variance to identify changes between shore and ship power. A NILM can also identify discrete steps in steady-state frequency to track number of generators online. It is worth noting that these techniques may not generalize across the variety of plant equipment and controllers. Careful analysis of electrical data can facilitate similar metrics for

individual power systems.

Compared to terrestrial systems, shipboard microgrids present unique issues for nonintrusive load monitoring. Whereas grid frequency is typically near-constant, microgrid generator frequency is subject to dramatic fluctuations. Many of these fluctuations are due to the limited generation capacity and finite inertia of generators. Accordingly, more sophisticated power computation is required to adaptively track system frequency. The Sinefit algorithm uses successive 4-parameter sine wave fitting to fit an observed voltage to the functional form:

$$v[n] = A \cdot \sin\left(2\pi n \frac{f_0}{f_s} + \phi_0\right) + C, \tag{5.1}$$

where A is the amplitude, f_0 is the line frequency, f_s is the sampling frequency, ϕ_0 is the phase angle, and C is the offset [18]. Frequency is computed for every line cycle and used for power spectral envelope computation, and is also recorded in the database.

However, adaptive frequency computation is not only useful for correcting for microgrid frequency fluctuations. System frequency provides interesting system operation information that would otherwise go undetected if a fixed 60 Hz frequency was assumed. For example, the amount of frequency variation can depend on the number of generators paralleled. In contrast, when connected to utility shore power the voltage waveform and frequency is much more "stiff." Thus, the instantaneous line frequency calculated by Sinefit provides valuable information about ship status. The section presents methods for using system frequency to improve NILM Dashboard's ability to predict ship or specific load statuses.

5.4.3 Equipment Diagnostics and Condition Based Maintenance

Changes in load power demand provide valuable indicators to augment frequency analysis and also provide unique diagnostic and prognostic indicators on their own. For instance, the WMEC includes several three-phase jacket water (JW) heaters. The

fleet has observed nagging failures on these from corrosion. This is a difficult fault to detect because the heaters are concealed in the engine manifold. Such a fault is extremely concerning because it is an electrical interaction around water that in certain instances has almost resulted in a fire [37]. This particular fault is a perfect example that illustrates how power can be used for shipboard diagnostics. Although the heater suffered physical degradation, it was still able to maintain the temperature commanded by the automatic controller by increasing the duty cycle. This soft fault was therefore able to hide from watchstanders through feedback control. A NILM, however, clearly observed the heater degradation by detecting a decrease in steady-state power consumption once corrosion caused a heating element to open circuit [37].

Furthermore, power monitoring can also identify soft faults from characteristics of observed on and off events. A drift in run time of systems may also indicate a fault. With these types of diagnostic insights, maintenance and repair can be shifted towards a condition-based, rather than scheduled, strategy. It is rare for US Coast Guard platforms to have a 100 percent operational availability, and these methods can help close the gap, having positive effects on the Coast Guard missions.

5.4.4 Updating Design Data

In addition to improving shipboard microgrid understanding and safety, power monitoring can be used to improve ship alterations and future designs. Electric plant load analysis (EPLA) is the method for calculating the ship loads over standard operating conditions and ambient environment as described in Design Data Sheet (DDS) 310-1 [38]. EPLA is used for calculating fuel requirements in DDS 200-1 [39]. In conducting EPLA, the US Navy sets standards for the estimated electrical plant deterioration and modernization. EPLA is done in the design phase and then will typically be adjusted during one or two sea trials prior to delivering the vessel to the US Navy [38]. A NILM can augment the EPLA process in multiple ways. First, EPLA requires each load to be individually monitored [40]. In some cases specified by DDS 310-1, multiple loads can be monitored at once [38]. A NILM can replace individual sensors

and instead incorporate a single set of sensors at each panel, disaggregating the individual loads from the power stream of the panel. Additionally, running one or two sea trials may also be costly. The NILM can serve as a semi-permanent component of an electrical grid, continually updating the EPLA of a ship or class of ship. This continuity can provide industry data that can be used to create models for future deterioration and modernization of ships and their systems. Finally, EPLA requires load factor information for its calculations [38]. A NILM can provide the industry with accurate load factors during real-time operations, resulting in more timely ship alterations if needed.

5.5 Automating the Future

Although automation alleviates the need for constant human oversight, applying automation to machinery plants cannot be approached simplistically and without nuance [41]. Automation can introduce feedback loops that hide faulty behavior. Although "soft faults" can hide in feedback loops, they cannot hide from their power consumption. Power monitoring goes deeper into the plant's health and gives credence to whether or not machinery is operating optimally.

Ship design requires an accurate picture of individual load energy consumption. In addition to equipment diagnostics, nonintrusive load monitoring provides long-term power data for new ship modeling, regardless of plant configuration. Ship power consumption evolves over the life-cycle of each ship as newer, more advanced weapon systems and navigation packages become available. The record of energy consumption provided by a NILM gives designers in the seagoing services a continuously evolving picture of present and future power requirements.

We also observe that quick access to power information provided by a NILM may present a unique training opportunity. Electric power systems are frequently the "mysterious" parts of a ship to maintainers and watchstanders. Power monitoring creates a clear window into the electromechanical systems of a microgrid. The power profile provided by a NILM and its relation to the ship's missions provides valuable

training opportunities for new users and operators.

THIS PAGE INTENTIONALLY LEFT BLANK

Chapter 6

Conclusions and Future Work

The Fast Response Cutter is an enormous investment for the US Coast Guard, Department of Homeland Security, and the United States of America. This investment supports the Coast Guard's missions of search and rescue, drug and migrant interdiction, maritime law enforcement, maritime response, and defense readiness. Ensuring this cutter can operate properly and for its entire life cycle is critical. Solving the corrosion problem prevents catastrophic corrosion that takes cutters out of operation for repair, immediately impacting operational availability and capability.

As indicated in Chapter 4, future work will focus on determining the optimal shaft coating system to extend zinc life. This work must be completed in coordination with Bollinger Shipyard and Cathelco to ensure feasibility.

Additional future work for this project includes the installation of the upgraded AIO box on USCGC William Chadwick and to analyze the ICCP system and other shipboard systems. Nonintrusive load monitoring has proven useful to numerous Coast Guard cutters, and this will be the first deployment on an FRC. Although the electrical loads on the FRC are different, the diagnostics that can be performed with the NILM help to detect faults before mechanical failures occur.

Overall, the FRC is a fascinating and complex research platform. Providing actionable suggestions and solutions to the Coast Guard is the pinnacle of graduate research. As solutions are implemented, further research will be continued on the FRC through NILM and other graduate student research ensuring the Coast Guard

is given the best possible means to curb corrosion and continue the safe operation of such a crucial military asset.

Appendix A

USCGC William Chadwick NILM Documentation

This Appendix includes modified documentation created for use by the US Coast Guard Surface Forces Logistics Center (SFLC) Patrol Boat Product Line. The documents were submitted in order to receive appropriate authorization to install all of the aforementioned NILM equipment on USCGC William Chadwick (WPC 1150). This documentation was initially provided to the US Coast Guard in September of 2022 and the installation of all equipment was completed in June of 2023. Certain approval documentation was not classified for public release and could not be included in this Appendix.

A.1 MIT NILM Research Proposal for USCGC WILLIAM CHADWICK (WPC 1150)

A.1.1 Introduction

The purpose of this proposal is to provide detailed information regarding the request for authorization for the Massachusetts Institute of Technology's (MIT) Research Laboratory of Electronics (RLE) to conduct research onboard United States Coast Guard Cutter (USCGC) WILLIAM CHADWICK (WPC 1150). This proposal comes from the above US Coast Guard Officers in the Electromechanical Systems Group (ESG) under the supervision of Professor Steven Leeb in the MIT Research Laboratory for Electronics (RLE).

Since 2004, a strong relationship has existed between United States Coast Guard (USCG) officers pursuing DCMS sponsored graduate level education and USCG assets located in the Boston area including USCGC ESCANABA (WMEC 907), USCGC SENECA (WMEC 906), USCGC SPENCER (WMEC 905), USCGC THUNDER BAY (WTGB 108), USCGC MARLIN (WPB 87304), and USCGC STURGEON (WPB 87336) . Students have researched vibration and electrical monitoring to improve fault detection, determine machinery health, extrapolate human activity, and provide energy scorekeeping to improve automation and machinery-monitoring technology. These research opportunities allow active duty officers to remain engaged with the fleet while pursuing higher education, simultaneously posing an opportunity for the USCG to remain at the forefront of maritime automation and monitoring research.

A.1.1.1 Research Focus

Current research is focused on Non-Intrusive Load Monitoring. A Non-Intrusive Load Monitor (NILM) takes electrical power readings from a centralized monitoring point,

making it a low-cost, durable, and sustainable method of equipment monitoring. Applications of these readings include energy savings, load factor management, platform energy use optimization, activity monitoring, log generation, and machinery health monitoring. The NILM systems are low-cost and easier to install compared to equivalent systems comprised of individual sensors on each piece of equipment.

MIT RLE requests authorization to install two NILM boxes onboard USCGC WILLIAM CHADWICK (WPC 1150) in accordance with the Memorandum of Agreement between MIT-RLE and USCG Surface Forces Logistics Center (SFLC) Engineering Services Division (ESD). Details of the proposed installations will be provided in this document. Installation specifics will be outlined in a separate Installation Plan.

The proposed installation will last for one year, beginning on the installation date. At the end of that year, the MIT RLE will communicate with SFLC ESD to determine if the project will continue or not.

A.1.1.2 Background

Power system microgrids serve mission critical systems for naval platforms. System component degradation can often be observed as changes in demand on the power system. As the performance of a critical component in a system degrades, automatic controllers often compensate to maintain commanded output levels. By design, feedback control works to mask the effect of "soft faults," variations and vagaries in internal component performance in a larger system that do not fully stop the system. Low refrigerant charge, slipping belts, fouled fans, vacuum leaks, and degraded hydraulic fluid are all examples of mechanical insults to a system with insidious effect: the system will continue to operate and provide apparently acceptable service and performance while an automatic controller forces more energy consumption and induced wear. Soft faults may elude even vigilant watchstanders. These situations can persist for expensively long periods before a "hard fault" finally stops the system, alerting

operators but also creating a "casualty" that may cripple mission readiness.

The vast implementation of automatic controllers often masks soft faults by automatically altering run times and drawing excess power to maintain system operability. Enhanced vigilance in watchstanding can lead to soft fault detection, but it is at the expense of the watchstander. Further, such enhanced inspection leads to increased monitoring efforts and a greater watchstanding demand, as well as a dependence on a multitude of sensors which could introduce additional fault points in an already complex system. While this introduction of new sensors to a system can provide a more detailed view of individual component operation, it does not simplify system operation or watchstanding practices. Instead, it commonly adds to the burden of system maintenance by producing a raft of raw data that is often not presented in a useful way. The ability to parse useful data and present it in an easily-extractable manner is necessary to successfully identify soft faults and allow operators to address them prior to system failure.

A.1.1.3 NILM Technology

Non-intrusive electrical power monitoring has been applied for condition-based maintenance, energy scorekeeping, and activity tracking in marine environments for several decades. The nonintrusive load monitor can determine the operating schedule of individual loads and components by observing electrical transients in an aggregate electrical power stream. Figure A-1 illustrates a NILM installation at the feeder to an electrical panel that serves a collection of loads. Strictly from measurements made at this aggregate point, a NILM determines the operating schedule of the downstream loads through association of observed waveforms with specific loads. This technology can then develop a physics-based load model and determine the health of the loads. Then, by effectively detecting transient events, a NILM can automatically log operation of system components, producing a computer-generated log that rivals or exceeds human-made logs for accuracy and vastly reduces watchstander effort in documenting equipment operation. A NILM's ability to record the operation time and

power consumption for individual loads creates a convenient, one-stop access point for energy scorekeeping.

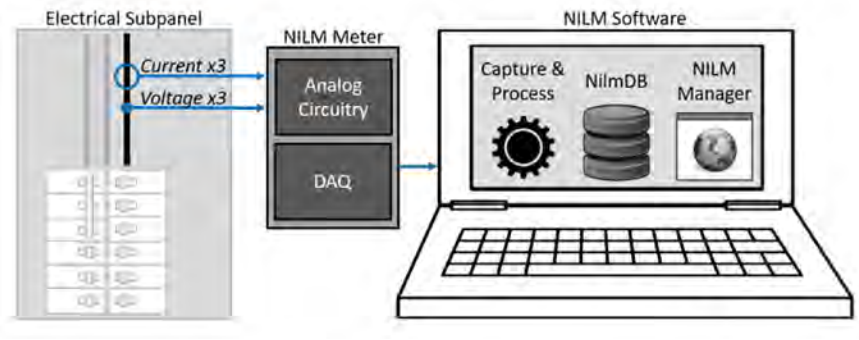

Figure A-1: Schematic overview of a typical installation of a NILM at the feeder to a power panel on a ship. The NILM Meter provides sensing for waveform measurement. The NILM Software runs on a Linux-based personal computer, laptop, or similar platform.

Within a NILM, sensors record current and voltage from the electrical panel and analyze waveforms to compute real power, reactive power, apparent power, and higher harmonic content. This information directly corresponds to the physics that governs load behavior, producing distinct signatures in power data, to which the NILM is "trained" to recognize. Such load transients can be identified by developing fingerprint exemplars in the laboratory through testing of example loads, from previous shipboard equipment observation, or from on-site observations of loads during a training period following installation. The monitor can also observe load behavior for a period of time and classify the loads using guided machine learning and clustering to produce a data set that is likely most useful after a facilities operator has reviewed and corrected the automatic load identifications as needed.

A.1.1.4 Past NILM Installations

Various configurations of nonintrusive monitoring equipment have been installed onboard USS Michael Murphy (DDG-112), USS Independence (LCS-2), USS Champion (MCM-4), the USNA YP (Yard Patrol) Fleet, USS Indianapolis (LCS-17), USCGC

THUNDER BAY (WTGB 108), USCGC MARLIN (WPB-87304), USCGC STURGEON (WPB-87336), and the Famous-class US Coast Guard Cutters in Boston. The longest installations have provided observations from the three Famous-class Medium Endurance Cutters (MECs) SENECA, ESCANABA and SPENCER for over 10 years with various hardware setups. These 270 ft. (82 m) length overall vessels have a 440 V electrical power distribution system run by diesel power generation and distribution equipment required to support missions and sustain operations at sea.

On SPENCER, a readout for the crew displayed the NILM Dashboard. Figure A-2 shows front and side views of a touch screen installed that displayed graphical results from NILM Dashboard. The front view on the left shows the NILM Dashboard displaying a timeline of operation for three different service loads in the main engineering space, extracted from the power monitoring of the electrical panel feeding these loads. The side view on the right shows the screen displaying “meter"-style displays with green (normal), yellow (worrisome), and red (poor) operating zones for the different statistics concerning the monitored load of interest. This display allows the crew to quickly select and interpret visual indicators that draw awareness to unusual or unacceptable operating parameters, including too frequent or infrequent operation, excessive power demand, excessive or inadequate duration of operation, and other unacceptable operating states. With such a tool available to the crew, watchstanders have the ability to identify soft faults in their engineering systems prior to their failure as highlighted by the NILM.

A.1.2 Installation Requirements

This section will denote the details regarding the proposed NILM installation for USCGC William Chadwick. It will begin outlining the equipment required for the installation, then detail the proposed locations for installation onboard the WPB. Each proposed NILM installation will include the following components:

- All-in-One (AIO) NILM Box (1)

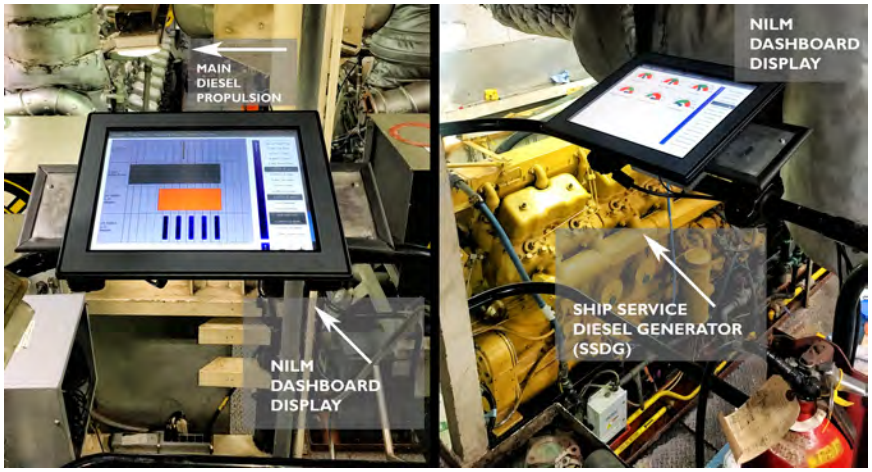

Figure A-2: The NILM Dashboard display on USCGC SPENCER (WMEC 905).

- Current transducers (3, one per phase)
- Conxall cables (3, one per phase)
- Voltage leads (encased in single conduit)
- IEC power cord (1)
- Mechanical mounting hardware

A.1.2.1 All-in-One (AIO) NILM Box

The All-in-One (AIO) NILM Box combines several aspects of NILM technology into a single, robust, easily-installed box designed for shipboard installation. This configuration minimizes space requirements by combining the sensor hardware, computer, and backup power supply necessary to collect data and display it in a useful manner into a single enclosure that is reasonably-sized with respect to the limited space within shipboard engineering spaces. Figure A-3 shows an example of an AIO NILM Box install. As shown, this single box includes a touch-screen computer display on the outside, while also encasing the majority of the NILM sensor hardware. Figure A-3 also showcases much of the additional hardware required for installation, including the IEC power cord, voltage leads encased in conduit, and Conxall cables. The box dimensions are 16 in x 7 in x 13.5 in.

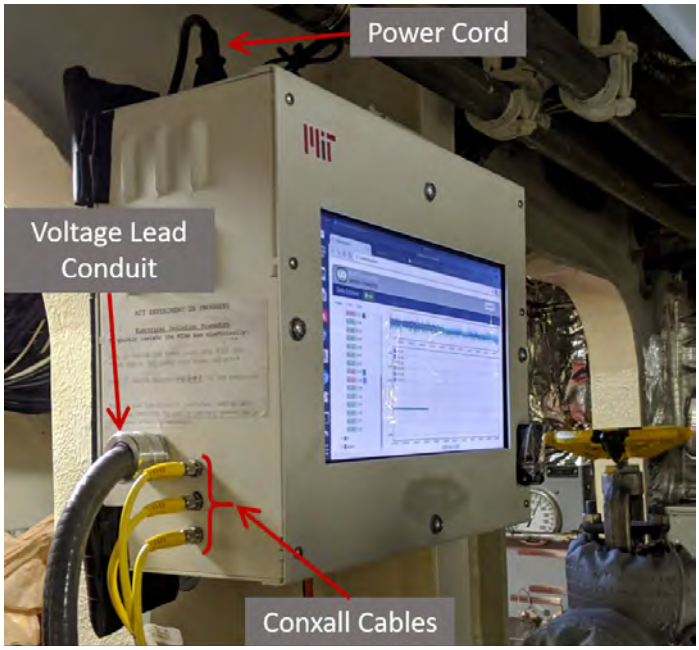

Figure A-3: AIO NILM Box install.

A.1.2.2 Other Installation Hardware

The current transducers, shown in Figures A-4a and A-4b (blue), are installed onto each phase of the power cables feeding the panel. These sensors connect to the yellow Conxall cables, (also depicted in Figure A-4a), which then feed current readings to the All-in-One Box as shown in Figure A-3. Figure A-4b also shows the voltage lead installation onto the spare breaker within the power panel. Once these wires exit the power panel, they are encased in conduit that runs to the AIO box, which is shown in Figure A-3. The final piece of hardware to install is a IEC Power Cord that connects the AIO Box to a 120V power supply. This IEC cord will plug into the nearest power outlet and run through neighboring cable runs to provide power to the AIO Box. All mounting hardware is specific to each ship and each install, and will be addressed in greater detail in the Installation Plan.

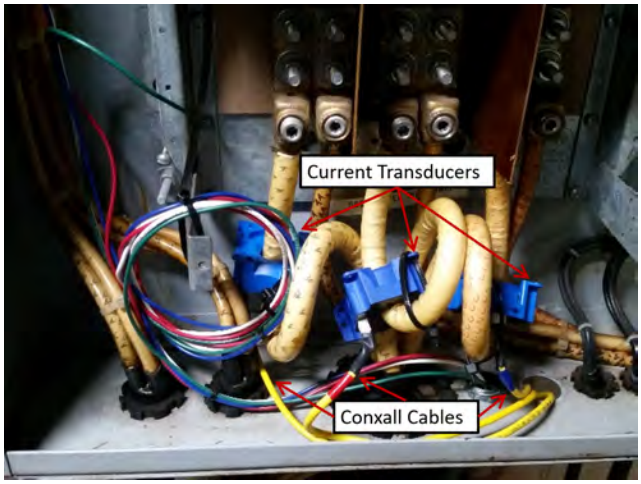

(a) Close-up view of installed current transducers (blue). Conxall cables connect to each current transducer.

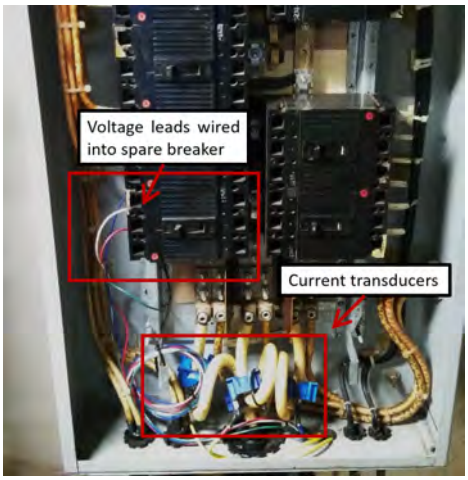

(b) Open power panel with NILM hardware installed. Current transducers are shown at the bottom installed on the 3-Phase power cables leading into the panel. Voltage leads are shown wired into a spare breaker on the panel (red, white, & blue wires leading into breaker.)

Figure A-4: Current and voltage sensor installation on USCGC SPENCER (WMEC 905).

A.1.3 Proposed Installation & Mounting

The MIT NILM team proposes that NILM devices be installed on the starboard and port machinery power panels. Each device will include all the items listed previously (AIO Box, current transducers, Conxall cables, etc.). Each AIO box would monitor one of the designated panels. Figure A-5 shows a modified schematic of the electrical generation and distribution plant onboard USCGC WILLIAM CHADWICK (WPC 1150), highlighting the power panels that will be monitored using NILM sensors.

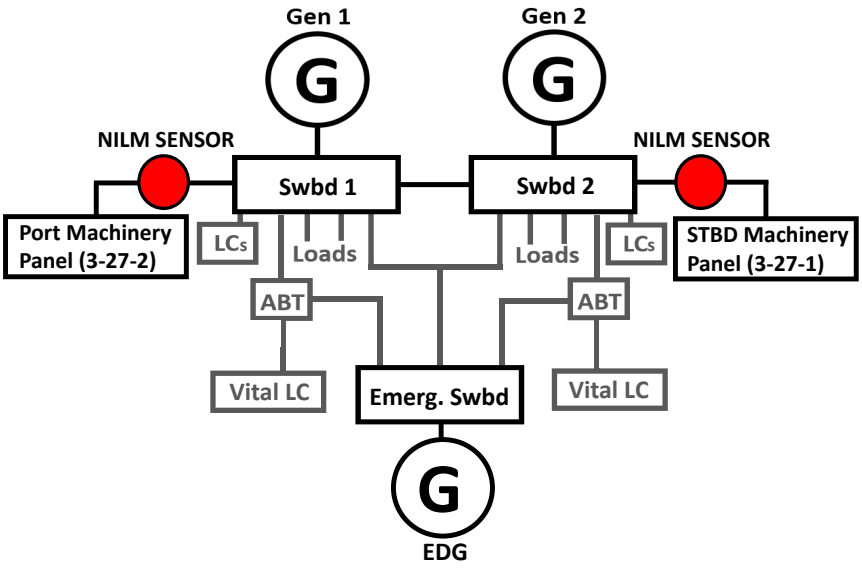

Figure A-5: USCGC WILLIAM CHADWICK (WPB 1150) electrical diagram with NILM sensor installation points identified (red circles).

A.1.3.1 Hardware Mounting Location

The proposed installation locations for the boxes can be found in Figures A-6 and A-6. The AIO boxes for panels 3-27-1 and 3-27-2 will be mounted on the center catwalk located above and in between the two MDEs. The NILM boxes will be attached to the railings using additional framing and this location provides ample space for the AIO boxes to be mounted on temporary brackets, to be installed by the MIT-RLE team. Further, because of the close proximity to the Power Panels, the length required for the Conxall Cables and Voltage Leads will be minimized.

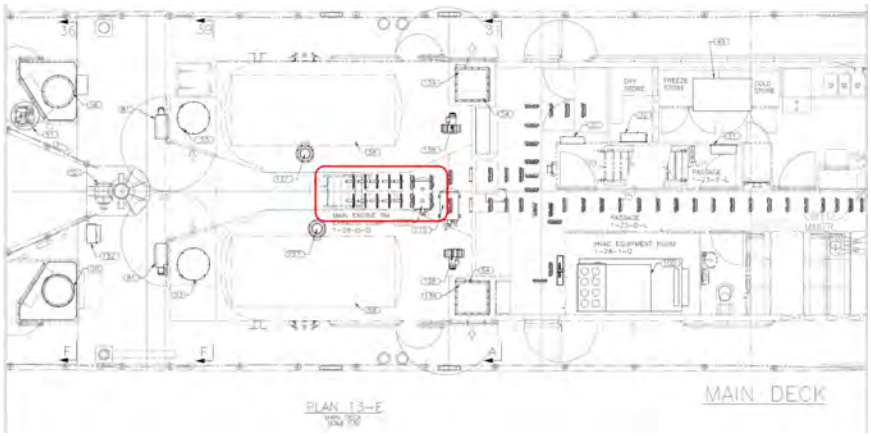

Figure A-6: Proposed installation location for AIO box on Power Panel 1S-4P-(1-66-2) located in the Engineering Control Center (1-58-0-C).

Figure A-7: Proposed installation location for AIO box on Engine Room 'Catwalk'

A.1.4 Conclusion

Further information regarding the nature of this project can be found by contacting the US Coast Guard graduate students at MIT (listed below). The details of the exact

installation regarding hardware, bracketry, and procedures for install will be outlined in the Installation Plan. Further details regarding MIT and the Coast Guard's roles with regard to this situation can be found in the Memorandum of Agreement between MIT-RLE and SFLC-ESD.

All questions should be directed to LT Isabelle Patnode (ipatnode@mit.edu), LTJG Michael bishop (mjbishop@mit.edu), and LTJG Jacob Skimmons (jskim10@mit.edu).

A.2 MIT NILM Installation Plan for USCGC WILLIAM CHADWICK (WPC 1150)

A.2.1 Proposed Mounting

A.2.1.1 Mounting Hardware Details

The proposed installation and mounting will be set up to be temporary. That is, no permanent modifications will be made with regard to the mounting hardware for the All-in-One (AIO) boxes. Instead, all hardware and bracketry will be installed using existing holes or brackets on the ship. Additional hardware, provided by the Massachusetts Institute of Technology Research Laboratory of Electronics (MIT RLE), will be custom-built and modified for the AIO boxes to be mounted securely without making permanent alterations to the cutter. Figure A-8 shows the AIO box installed on the USCGC STURGEON (WPB 87336) and the same style AIO box is to be installed on USCGC WILLIAM CHADWICK (WPC 1150) The brackets will be bolted and clamped to existing structures on the cutter, which will be explained in detail in this section. Notably, semi-circular pipe straps and circular hose straps will be used as anchor points to attach the new AIO box framing to the railings. Then, the AIO boxes will mount directly to the installed bracketry for a secure fit.

A.2.1.2 AIO Box #1 Anchor Points: Engine Room Catwalk STBD Railing

The AIO box framing will be anchored at 10 points using "pipe straps" and "hose straps". Pipe straps act as semi-circular railing brackets. Hose straps act as a fully circular railing bracket, and are used to maintain railing grab area and maximize safety. The location of the AIO box placement is shown in Figure A-9. Each pipe strap is fastened with 2 bolts which attach through the framing pieces. Three brackets are to be attached to the bottom railing. Each hose strap is fastened with 1 bolt which attaches through the framing. Three hose straps are to be attached to the top railing,

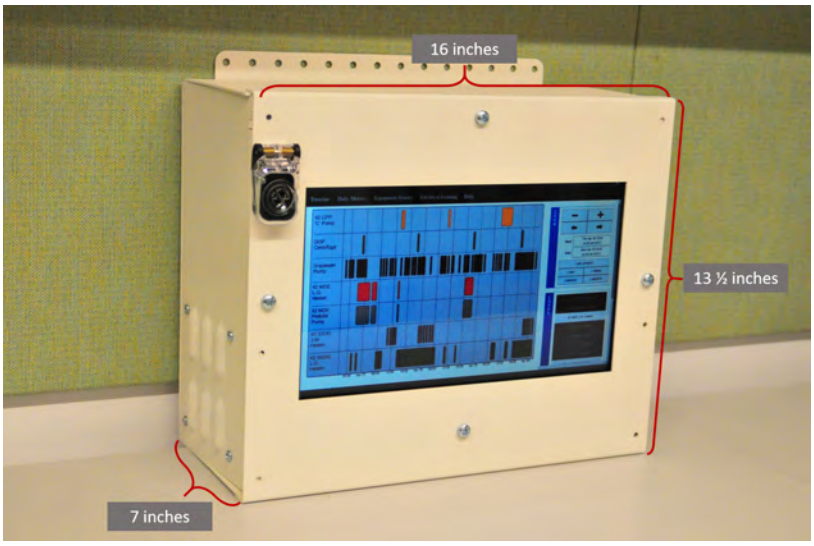

Figure A-8: Example AIO boxes installed on USCGC STURGEON (WPB 87336)

and two to each vertical railing. Three pieces of vertical framing will connect the top and bottom brackets, and two horizontal piece of framing will attach the side railings. The location and framing design is shown in Figures A-9 and A-10. Each pipe strap will have a thin piece of rubber underneath to reduce damage to the mounting system due to potential vibrations.

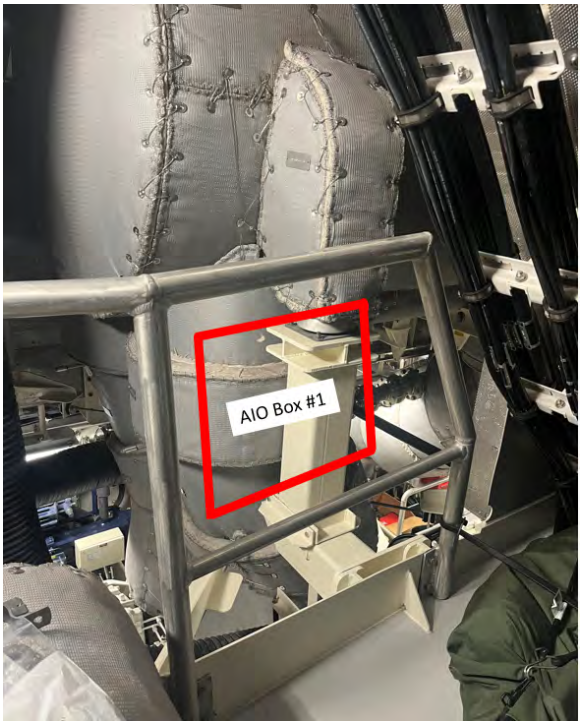

Figure A-9: Location to mount the STBD side AIO Box

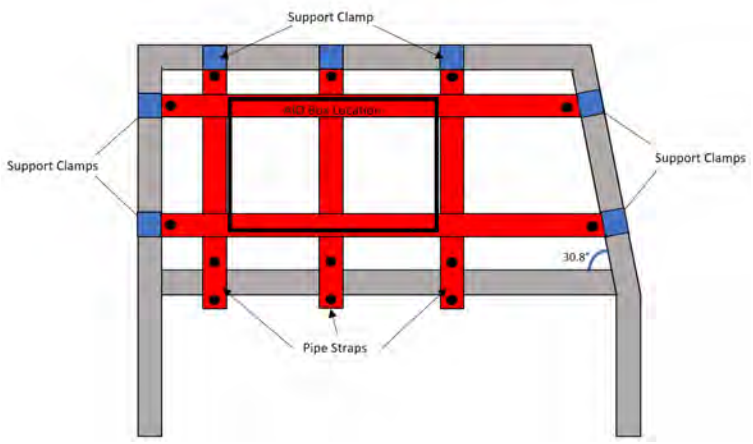

Figure A-10: Bracketry for AIO Box 1 and Box 2

A.2.1.3 AIO Box 2 Anchor Points: Engine Room Catwalk Port Railing

The AIO box framing will be anchored at 10 points using "pipe straps" and "hose straps". Pipe straps act as semi-circular railing brackets. Hose straps act as a fully circular railing bracket, and are used to maintain railing grab area and maximize safety. The location of the AIO box placement is shown in Figure A-9. Each pipe

strap is fastened with 2 bolts which attach through the framing pieces. Three brackets are to be attached to the bottom railing. Each hose strap is fastened with 1 bolt which attaches through the framing. Three hose straps are to be attached to the top railing, and two to each vertical railing. Three pieces of vertical framing will connect the top and bottom brackets, and two horizontal piece of framing will attach the side railings. The location and framing design is shown in Figures A-9 and A-10. Each pipe strap will have a thin piece of rubber underneath to reduce damage to the mounting system due to potential vibrations.

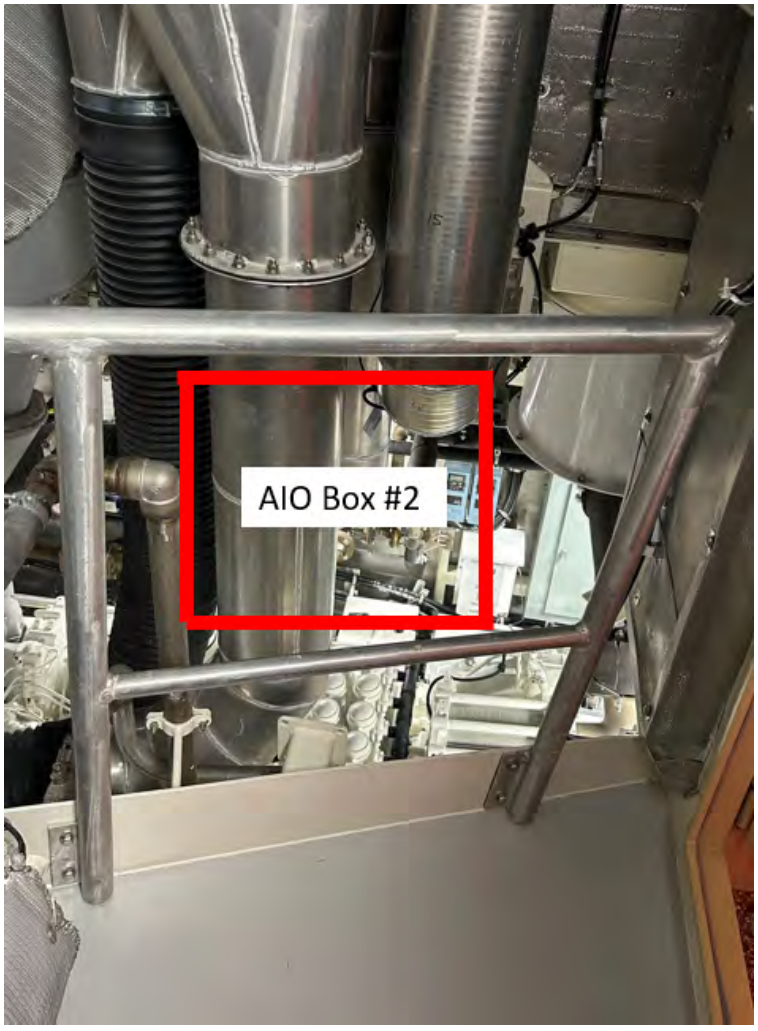

Figure A-11: Bracketry for AIO Box 1 and Box 2

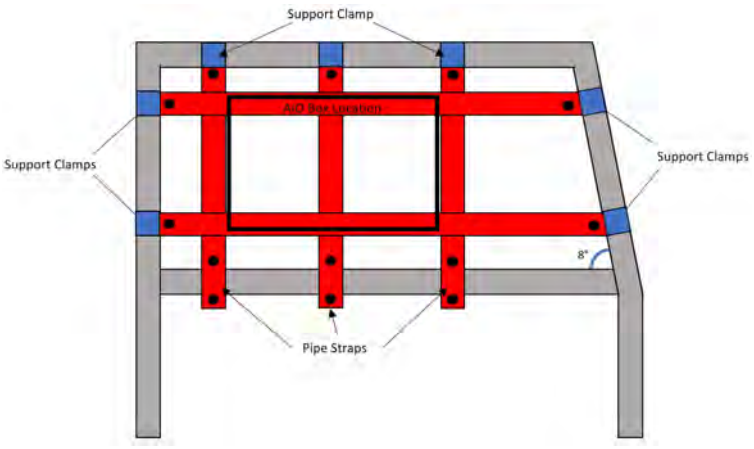

Figure A-12: Bracketry for AIO Box 2

A.2.1.4 Final Mount

The final mounting positions for the AIO Boxes are shown in Figure A-12. This shows that there is ample space for both boxes in the proposed arrangement. The two AIO boxes will be mounted in “landscape" orientation. That is, the long edge will be on the bottom while the short edge is on the side.

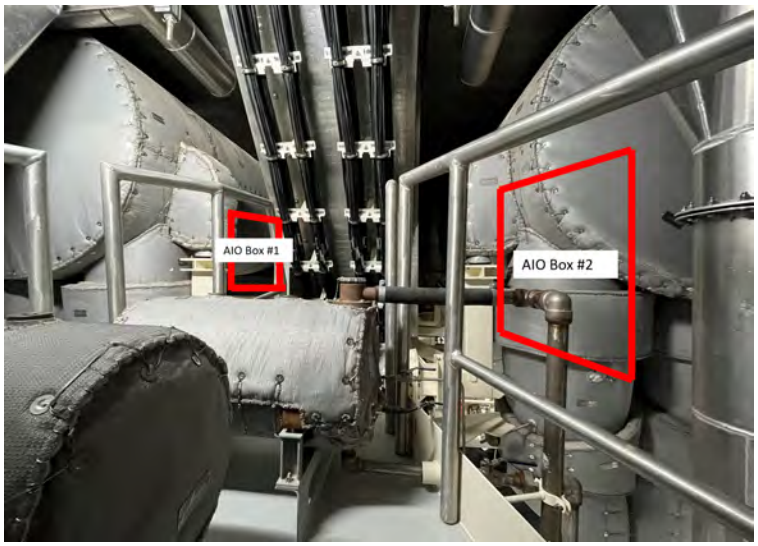

Figure A-13: Scale rendering of final location of AIO Boxes (proposed bracketry not pictured). AIO Boxes will be mounted in “Landscape" orientation.

A.2.1.5 Cable Runs

Cables will come out the side of the mounted AIO Boxes. The 3 Conxall cables and the conduit containing voltage leads for each box will be joined together by zip-ties and run forward to the large vertical “L" stiffener on the outboard bulkhead. There, they can be secured to the holes in the stiffeners referenced in Section A.2.1.2 using bolts, lock-nuts, and zip-ties. The cables will then run in the overhead cable runs to their respective panels, once again being secured along the way using zip-ties.

The IEC Power Cords will run forward to the receptacle similar to the one shown in Figure A-14. Both receptacles will be utilized to provide power to Data Acquisition Unit (DAQ).

All cords will run along existing cableways and fittings that will allow them to be secured with zip-ties. They will not impede movement of personnel or equipment in any area.

Figure A-14: Power outlet for IEC Cords.

A.2.2 Installation on Panel

This section will detail the plan for equipment installation on the electrical panel. This will include installation of the current transducers, their connection to the Conxall cables, and the wiring of the voltage leads to the spare breaker. **Prior to conducting any electrical work, equipment shall be tagged out IAW COMDTINST 9077.1 (series)**.

A.2.2.1 Cable Entry into Panel

Cables will enter into the panel via new holes that will be drilled and fitted with boot shrinks that shall maintain watertight integrity. **For the new holes to be drilled, assistance from a Ship's Force (SF) Electrician's Mate (EM) is necessary. The SF EM must Tag Out the panel installation and verify that the power is secured in accordance with (IAW) all electrical tag out and safety procedures. Then, the SF EM may proceed to drill the necessary holes in the panel.** Use of an SF EM in this step is necessary for safety and quality assurance of work. MIT RLE graduate students are not certified electricians, therefore they shall not conduct the work on the electrical panel.

For installation, two groups of cables will enter each panel: the three Conxall cables, and the voltage leads encased in conduit. The conduit used will be abrasion resistant as well as liquid tight to maintain the watertight integrity of the panel. The proposed method for both groups to enter the panel safely is to drill two 1.25" diameter holes in the top of the power panel. Then, the cables can enter into the panel via bootshrink fittings like those pictured in Figure A-15. These fittings are watertight and meet military specifications (MILSPEC) for running cables into power panels onboard ships and in engineering spaces. Later, following removal of equipment, these fittings will be fit with neoprene plugs IAW ASTM F1836M.

Other commonly used fittings include cord grips, which are shown in Figure A-15

as well. Figure 9 shows an example of the voltage leads (in conduit) as well as the Conxall cables exiting a typical power panel.

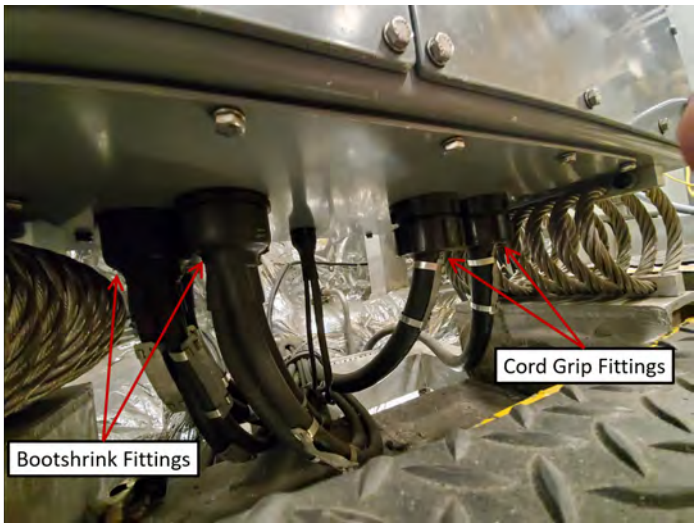

Figure A-15: Example of bootshrink and cord grip fittings feeding into power panel (from US Navy panel).

Figure A-16: Example of voltage leads (in conduit) and Conxall cables exiting from power panel.

A.2.2.2 3-27-2 Port Machinery Panel

Figure A-17 shows the top of power panel 3-27-2. NILM Conxall cables and voltage leads in conduit will enter through two new holes in this section of the panel. As can

be seen, many cords enter the panel, and cord grips are used as the watertight fittings.

Figure A-17: Cable entries into the top of power panel 2DS-4P.

A.2.2.3 3-27-1 STBD Machinery Panel

Figure A-18 shows the top of power panel 3-27-1. NILM Conxall cables and voltage leads in conduit will enter through two new holes in this section of the panel. As can be seen, many cords enter the panel, and cord grips are used as the watertight fittings.

Figure A-18: Cable entries into the top of power panel 2DS-4P.

A.2.3 Inside the Panel

This step will also require the assistance of the SF EM. **To begin, the SF EM will tag out the entire panel to be installed upon IAW the shipboard tag out and electrical safety procedures. The SF EM will then remove the front casing on the power panel, and ensure power is secured using a multi-meter IAW all shipboard electrical safety procedures.**

A.2.3.1 Current Transducer Installation

Once confirmed that power has been secured to the panel, the SF EM will remove the lugs on the power cables feeding the panel for each phase. This will allow the current transducers to be installed on each power cable by slipping them over the open lugs. Then, the SF EM will reinstall the power cable lugs.

Next, MIT RLE graduate students will secure the current transducers using zip ties and connect the Conxall cables to the current transducers. Figure A-19 shows the end result of the current transducers and Conxall cables inside the electrical panel on USCGC MARLIN (WPB 87304). As is shown, the current transducers and Conxall cables are neatly organized inside the panel and secured with zip ties. Figures 12 and 13 show the interior of the port machinery panel onboard USCGC WILLIAM CHADWICK (WPC 1150).

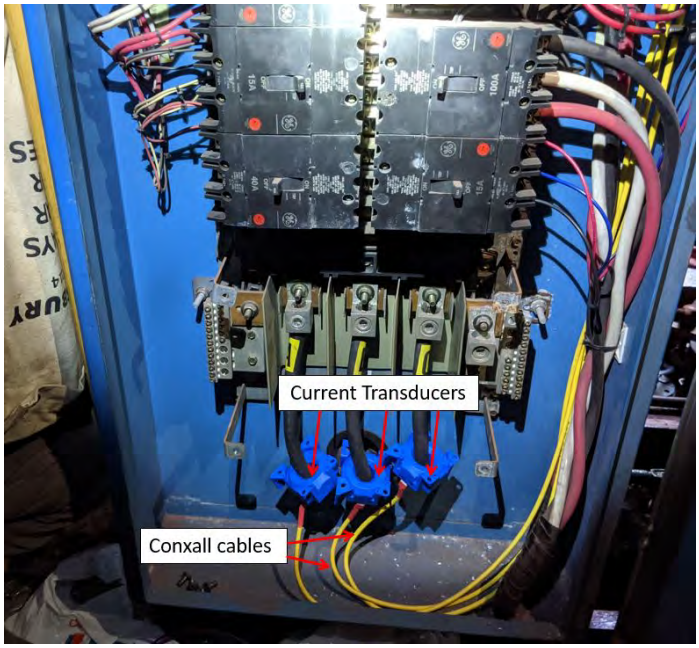

Figure A-19: Current transducers and Conxall cables installed on power cables feeding an electrical panel on USCGC MARLIN (WPB 87304).

Figure A-20: USCGC WILLIAM CHADWICK (WPC 11050) Power Panel Interior

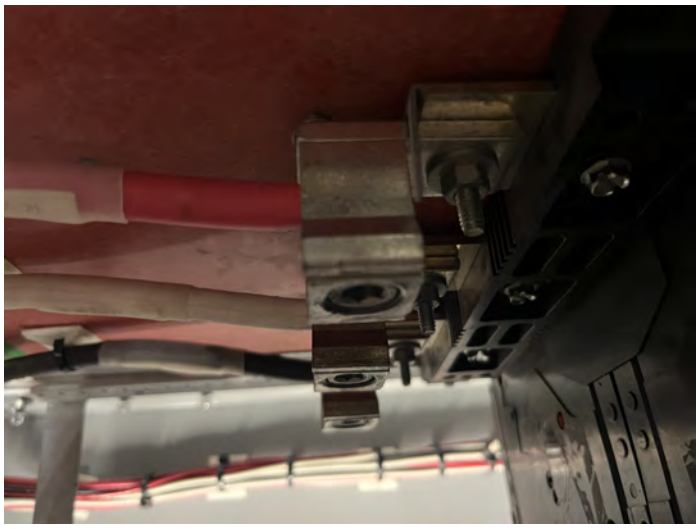

Figure A-21: USCGC WILLIAM CHADWICK (WPC 11050) Power Panel Interior

A.2.3.2 Voltage Lead Installation

The next step in the internal panel installation is to wire the voltage leads into the spare breaker. As is shown in Figure A-21, there are adequate spare breakers for installation on both panels. For the starboard panel, the MIT RLE team proposes using the (3-27-1)-4P-P spare breaker shown in the upper left corner of Figure A-22a. For the port panel, the MIT RLE team proposes using the (3-27-2)-4P-M breaker shown in the upper right corner of Figure A-22b.

(a) STBD Machinery Panel (3-27-1)

(b) Port Machinery Panel (3-27-2)

Figure A-22: USCGC WILLIAM CHADWICK (WPC 11050) Power Panels

This step requires assistance from the SF EM once again. The SF EM will need to wire the 3 voltage leads into the designated spare breaker. Each lead will wire into one power phase on the breaker. Additionally, there is a ground lead that will need to lead to an appropriate ground location as determined by the SF EM. In previous installs ground bolts inside the panels have been used. Figure A-23 shows a complete voltage lead install on a spare breaker from USCGC MARLIN (WPB 87304) and will appear nearly identically onboard USCGC WILLIAM CHADWICK.

Once the voltage leads are connected to the spare breaker, the current transduc-

ers are installed on the power cables, the Conxall cables are connected to the current transducers, the cables and wires from the NILM installation are neatly organized within the panel with zip ties, and bootshrink fittings are secured, the SF EM will close the panel and reenergize it IAW all electrical safety and tag out procedures.

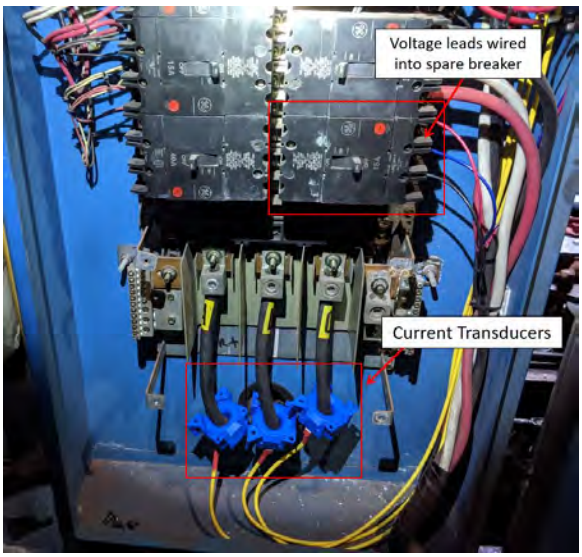

Figure A-23: Interior panel view for reference on USCGC MARLIN (WPB 87304) showing voltage leads wired into a spare breaker as well as current transducers installed on power feed cables

A.3 Equipment Testing

Following all setup steps on the panels, the MIT RLE team will work to ensure the equipment is working correctly. This will include energizing all MIT equipment, as well as the downstream loads, to ensure proper operation of NILM sensors. In the event of poor or inept readings, the panels will need to be tagged out once again and hardware be adjusted to ensure proper data capture.

Once data is capturing correctly, the MIT RLE would like to energize all downstream loads if possible. This will provide the MIT RLE team with “test data" for each piece of equipment, allowing for it to be classified individually for processing and further understanding. Acquiring this data early allows for NILM Dashboard software to be customized to work for the 154’ Patrol Cutter as quickly as possible.

A.4 Equipment Removal

A.4.1 Electrical

This step will also require the assistance of the SF EM. To begin, the SF EM will tag out the entire panel which the NILM is being removed from IAW the shipboard tag out and electrical safety procedures. The SF EM will then remove the front casing on the power panel, and ensure power is secured using a multi-meter IAW all shipboard electrical safety procedures.

A.4.1.1 Current Transducer Removal

The first step in removing the NILM is securing power to the panels. Once confirmed that power has been secured to the panel, the SF EM will remove the lugs on the powercables feeding the panel for each phase. This will allow the current transducers to be removed from each powercable by slipping them over the open lugs. Then, the

SF EM will reinstall the power cable lugs. MIT RLE Grad Students will take custody of the current transducers and remove conxall leads, zipties and any other equipment from inside the power panel. Next the SF EM will inspect the inside of the power panel to ensure it is clear of debris.

A.4.1.2 Voltage Lead Removal

The second step of the electrical uninstall is the removal of the voltage leads. This step requires assistance from the SF EM once again. The SF EM will need to unwire the 3 voltage leads from the designated spare breaker. Additionally the ground wire will need to be unwired. Once all voltage leads, current conxall cables, current transducers and zip ties are removed both MIT RLE Grad Students and SF EM will inspect the panel ensuring equipment is removed and the panel is in good working order. Upon concurrence that the panel is restored to the original condition the SF EM will close the panel and reenergize it IAW all electrical safety and tag out procedures.

A.4.1.3 Cable Holes

The bootshrink fitted holes into the panels will be sealed with bootshrink caps. This provides adequate watertightness and prevents intrusion into the energized panel. MIT RLE students will provide the caps and install caps under SF supervision.

A.4.2 Hardware

Because the mechanical portion of the supporting bracketry is temporary there will be no permanent alterations to the physical structure of the vessel. MIT RLE students will remove all associated bolts, nuts, brackets and hardware mounting under the supervision of SF. All cable runs will be removed and NILM hardware and cabling

will be removed by MIT RLE students after the electrical portion of the system has been removed.

A.5 Equipment Removal

Prior to removing any equipment from the Cutter, all equipment shall be tagged out IAW COMDTINST 9077.1 (series).

A.5.1 Electrical

This step will also require the assistance of the SF EM. **To begin, the SF EM will tag out the entire panel which the NILM is being removed from IAW the shipboard tag out and electrical safety procedures. The SF EM will then remove the front casing on the power panel, and ensure power is secured using a multi-meter IAW all shipboard electrical safety procedures.**

A.5.1.1 Current Transducer Removal

The first step in removing the NILM is securing power to the panels. Once confirmed that power has been secured to the panel, the SF EM will remove the lugs on the powercables feeding the panel for each phase. This will allow the current transducers to be removed from each powercable by slipping them over the open lugs. Then, the SF EM will reinstall the power cable lugs. MIT RLE Grad Students will take custody of the current transducers and remove conxall leads, zipties and any other equipment from inside the power panel. Next the SF EM will inspect the inside of the power panel to ensure it is clear of debris.

A.5.1.2 Voltage Lead Removal

The second step of the electrical uninstall is the removal of the voltage leads. This step requires assistance from the SF EM once again. The SF EM will need to unwire the 3 voltage leads from the designated spare breaker. Additionally the ground wire will need to be unwired. Once all voltage leads, current conxall cables, current transducers and zip ties are removed both MIT RLE Grad Students and SF EM will inspect the panel ensuring equipment is removed and the panel is in good working order. Upon concurrence that the panel is restored to the original condition the SF EM will close the panel and reenergize it IAW all electrical safety and tag out procedures.

A.5.1.3 Cable Holes

The bootshrink fitted holes into the panels will be sealed with bootshrink caps. This provides adequate watertightness and prevents intrusion into the energized panel. MIT RLE students will provide the caps and install caps under SF supervision. All holes will be sealed prior to re-energizing the electrical circuits IAW COMDTINST 9077.1 (series).

A.5.1.4 Hardware

Because the mechanical portion of the supporting bracketry is temporary there will be no permanent alterations to the physical structure of the vessel. MIT RLE students will remove all associated bolts, nuts, brackets and hardware mounting under the supervision of SF. All cable runs will be removed and NILM hardware and cabling will be removed by MIT RLE students after the electrical portion of the system has been removed.

A.6 Cybersecurity

The installation of the AIO box will conform with all applicable US Coast Guard Command, Control, Communications, Computers, Cyber, and Intelligence (C5I) policies

and directives. The AIO box is a self-contained data acquisition unit that will not be connected to any external network. All of the power stream data collected by the unit will be stored locally and internally inside the armored AIO box. The only way to retrieve this data will be through a manual download using a manually connected cable connection to the AIO box.

A.7 Conclusion

This document summarizes the steps necessary for the MIT RLE NILM installation onboard USCGC WILLIAM CHADWICK (WPC 1150). Further information regarding the nature of this project can be found by contacting the US Coast Guard graduate students at MIT (listed below). The details of the project proposal can be found in the Research Proposal. Further details regarding MIT and the Coast Guard's roles with regard to this situation can be found in the Memorandum of Agreement between MIT-RLE and SFLC-ESD. All questions should be directed to LT Isabelle Patnode (ipatnode@mit.edu), LTJG Michael Bishop (mjbishop@mit.edu), and LTJG Jacob Skimmons (jskimm10@mit.edu).

Appendix B

USCGC Sturgeon (WPB 87336 NILM Documentation)

This Appendix includes modified documentation created for use by the US Coast Guard Surface Forces Logistics Center (SFLC) Patrol Boat Product Line. The documents were submitted in order to receive appropriate authorization to install all of the aforementioned NILM equipment on USCGC Sturgeon (WPB 87336). This documentation was initially provided to the US Coast Guard in April of 2022 and the installation of all equipment was completed in July of 2022. Certain approval documentation was not classified for public release and could not be included in this Appendix.

B.1 Proposed Mounting

B.1.1 Mounting Hardware Details

The proposed installation and mounting will be set up to be temporary. That is, no permanent modifications will be made with regard to the mounting hardware for the All-in-One (AIO) boxes. Instead, all hardware and bracketry will be installed using existing holes or brackets on the ship. Additional hardware, provided by the Massachusetts Institute of Technology Research Laboratory of Electronics (MIT RLE), will be custom-built and modified for the AIO boxes to be mounted securely without making permanent alterations to the cutter.

Figure B-1a shows the proposed location of the mounting brackets to be installed in the starboard aft corner of the engine room. The brackets will be bolted and clamped to existing structures on the cutter, which will be explained in detail in this section. Then, the AIO boxes will mount directly to the installed bracketry for a secure fit.

B.1.1.1 Anchor Point #1: Unistrut Installed on Aft Bulkhead

The first anchor point for the installation will occur on the aft bulkhead. There are "L" brackets currently in this location that hold a battery charger in place as shown at the top of Figure B-1a. The Unistrut will be bolted to the "L" brackets using a flat bar and bolts, as shown in Figure B-1b. Then, it will extend downward and further be secured by being bolted to beam clamps on each horizontal beam, as can be seen in Figure B-1a.

B.1.1.2 Anchor Point #2: Flat Bar Mount

The next anchor point for the installation will occur on the outboard bulkhead. Two vertically mounted flat white brackets are welded to stiffeners on this bulkhead for

(a) Location to mount Unistrut on aft bulkhead. Unistrut will extend down from permanently mounted “L" brackets to provide anchor points for other bracketry. It will also bolt to beam clamps on horizontal stiffeners.

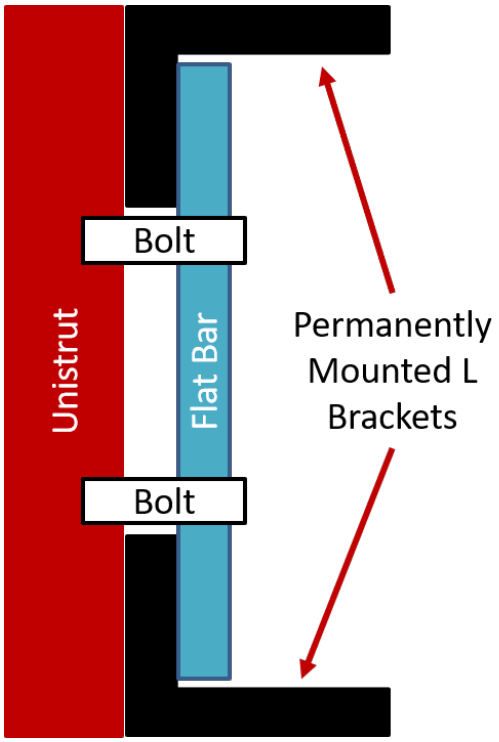

(b) Unistrut securing mock-up showing how Unistrut can be secure to the permanently mounted “L" brackets without drilling holes or permanently altering the cutter.

Figure B-1: Anchor Point #1

the FLOCS Pump controller mounting; as is shown in Figure B-2a. This allows for a flat bar to be passed behind the welded brackets. Then, another flat bar can be placed inboard of the white welded brackets and bolt to the flat bar outboard of the white welded brackets, providing a secure flat bar across the entire bulkhead.

B.1.1.3 Anchor Points #3: Holes in Stiffeners

The next anchor points will hold the main mounting bracketry on the outboard bulkhead. They will be bolt fittings, rigged with washers and lock-nuts to go through existing holes in cutter stiffeners. Figure B-3 shows an example of one of the corner fittings. This hole allows for any temporary brackets to be bolted to the stiffener through the hole with a bolt that has a washer and lock-nut on the opposite side.

(a) White welded brackets installed on outboard bulkhead stiffeners. Bracketry locations shown in red.

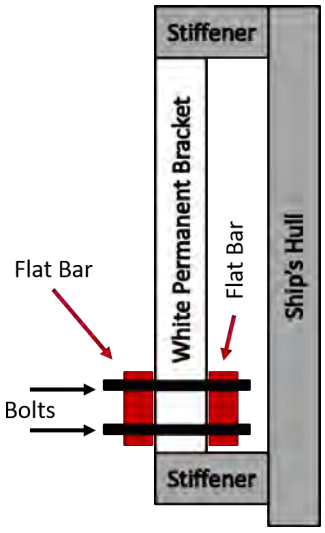

(b) Installation mock-up for Anchor Point #2. Flat bars will be bolted together over white welded brackets on outboard bulkhead.

Figure B-2: Anchor Point #2

Figure B-4 shows a mock-up of the outboard bulkhead bracketry. The flat bar referenced in Section B.1.1.2 is shown across the top of the figure, with bolts securing it at both ends. The bottom flat bar will be secured with bolts at both ends as shown as well. It will also be secured to the outboard stiffener by bolting to beam clamps onlong the stiffener as shown. The vertical brackets shown will be bolted to connect the two installed brackets, and the AIO boxes will mount directly to these brackets.

The bolt fittings in the corners will not be as strong as the other anchor points, which is why the other anchor points are included as primary, weight-bearing fittings. These fittings, as well as the beam clamp fittings, provide additional, secondary support to reduce the load on the primary anchor points and limit movement and/or vibration of the equipment.

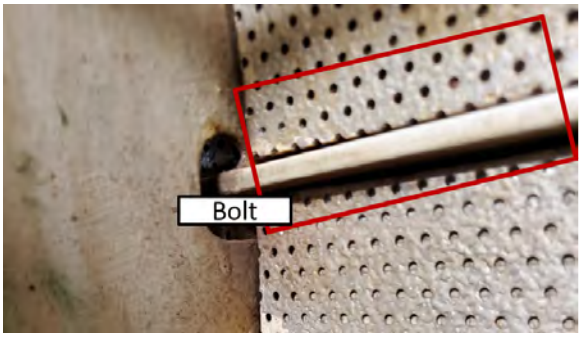

Figure B-3: Example of corner fitting with bolt overlay. Bolt will go through the open fitting in the stiffener and be secured using a washer and lock-nut on the opposite side.

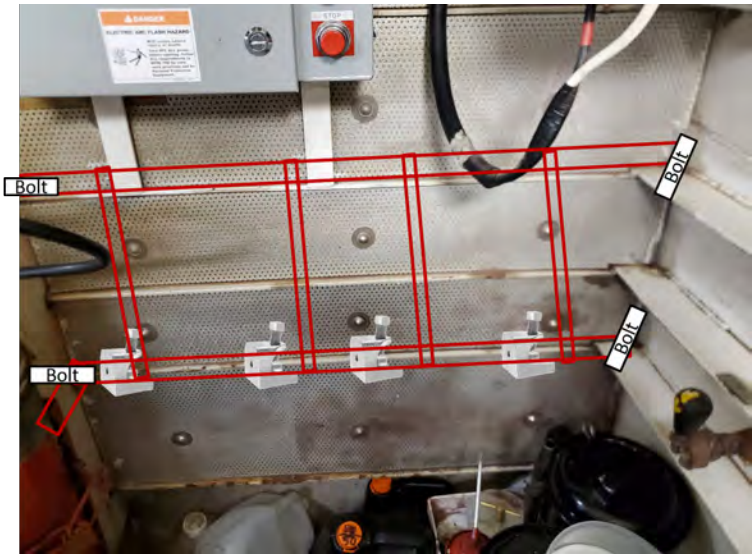

Figure B-4: Mock-up of all brackets on outboard bulkhead, with bolt locations shown in each corner.

B.1.1.4 Anchor Point #4: Lower Bracket Fabrication & Clamp

The final anchor point involves the lower bracket to be installed from Figure B-4. Because this cannot be secured by clamping to a flat bar behind permanently welded brackets like the top bar, its anchor points must be secure beyond the beam clamps and bolts depicted in Figure B-4. Figure B-5 is a schematic that shows a top-down view of the necessary bracketry and installation on the cutter. As is shown, the corner bolts will secure the bracketry through the stiffener holes as previously discussed. The beam clamps along the outboard bulkhead longitudinal stiffener are shown as well.

However, the bracketry will further be secured on both ends. On the left side of Figure B-5, a beam clamp will be applied to the “L" stiffener that is attached to the ship’s hull. Placing that beam clamp will allow the bracketry to be bolted to the “L" stiffener without drilling a hole in it. On the right side, bracketry can be connected to the unistrut referenced in Section B.1.1.1. This will provide rigid and secure mounting for the entire lower bracket.

Figure B-5: Schematic of lower bar and mounting points.

B.1.1.5 Final Mount

The final mounting positions for the AIO Boxes are shown in Figure B-6. This shows that there is ample space for both boxes in the proposed arrangement. The two AIO boxes will be mounted in “portrait" orientation. That is, the long edge will be on the side while the short edge is on the bottom. This leaves enough space for the two boxes to be mounted side by side in this location.

B.1.2 Cable Runs

Cables will come out the bottom of the mounted AIO Boxes. This will allow for easy organization. The 3 Conxall cables and the conduit containing voltage leads for each box will be joined together by zip-ties and run forward to the large vertical “L" stiffener on the outboard bulkhead. There, they can be secured to the holes in the stiffeners referenced in Section B.1.1.3 using bolts, lock-nuts, and zip-ties. The cables will then run in the overhead cable runs to their respective panels, once again being secured along the way using zip-ties.

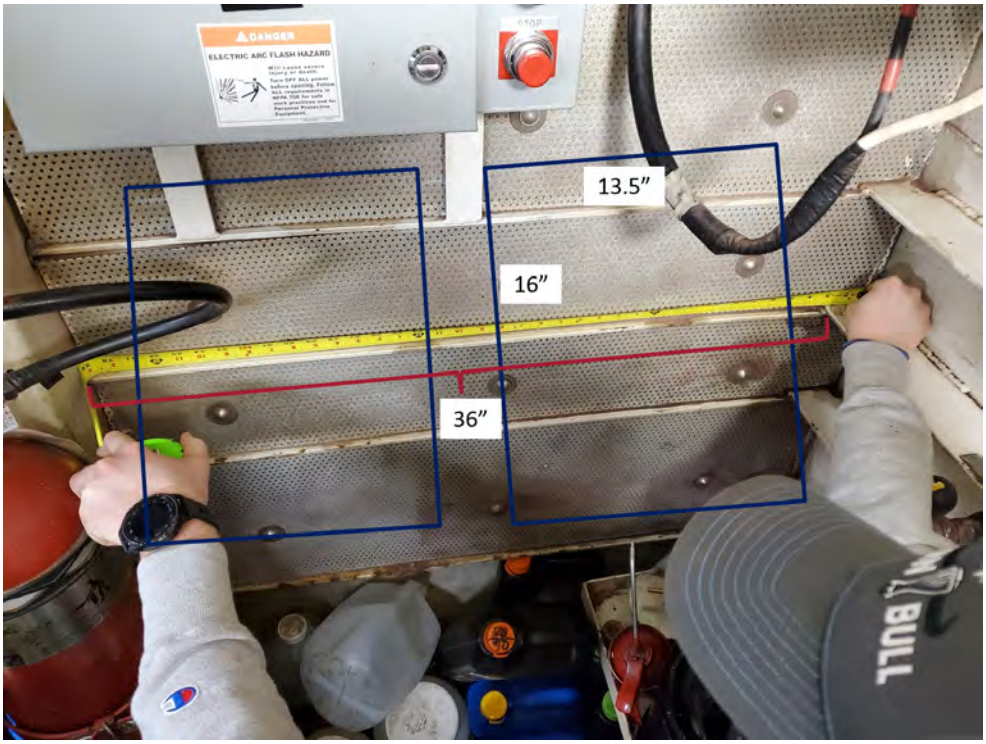

Figure B-6: Scale rendering of final location of AIO Boxes (proposed bracketry not pictured). AIO Boxes will be mounted in “Portrait" orientation.

The IEC Power Cords will run forward to the receptacle shown in Figure B-7. Both receptacles will be utilized to provide power to Data Acquisition Unit (DAQ).

All cords will run along existing cableways and fittings that will allow them to be secured with zip-ties. They will not impede movement of personnel or equipment in any area.

B.2 Installation on Panel

This section will detail the plan for equipment installation on the electrical panel. This will include installation of the current transducers, their connection to the Conxall cables, and the wiring of the voltage leads to the spare breaker.

Figure B-7: Power outlet for IEC Cords.

B.2.1 Cable Entry into Panel

Cables will enter into the panel via new holes that will be fitted with boot shrinks. **For the new holes to be drilled, assistance from a Ship's Force (SF) Electrician's Mate (EM) is necessary. The SF EM must Tag Out the panel being install on and verify that the power is secured in accordance with (IAW) all electrical tag out and safety procedures. Then, the SF EM may proceed to drill the necessary holes in the panel.** Use of an SF EM in this step is necessary for safety and quality assurance of work. MIT RLE graduate students are not certified electricians, therefore they should not conduct the work on the electrical panel.

For installation, two groups of cables will enter each panel: the three Conxall cables, and the voltage leads encased in conduit. The proposed method for both groups

to enter the panel safely is to drill two 1.25" diameter holes in the top of the power panel. Then, the cables can enter into the panel via bootshrink fittings like those pictured in Figure B-8. These fittings are watertight and meet military specifications (MILSPEC) for running cables into power panels onboard ships and in engineering spaces. Later, following removal of equipment, these fittings will be fit with neoprene plugs IAW ASTM F1836M. The running of cables into the panel and installation of bootshrink fittings will be conducted by the MIT RLE graduate students. Other commonly used fittings include cord grips, which are shown in Figure B-8 as well.

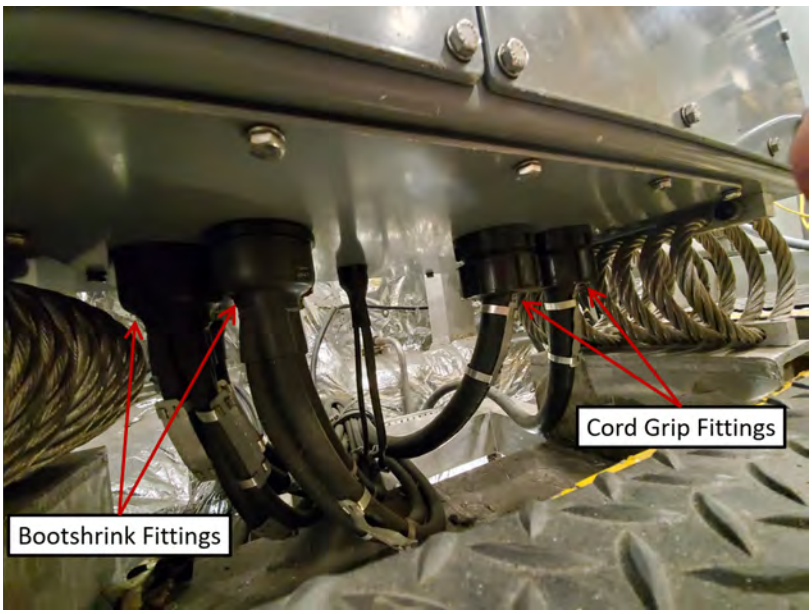

Figure B-8: Example of bootshrink and cord grip fittings feeding into power panel (from US Navy panel).

B.2.1.1 Panel 1DS-4P

Figure B-9 shows the top of power panel 1DS-4P. NILM Conxall cables and voltage leads in conduit will enter through two new holes in this section of the panel. As can be seen, many cords enter the panel, some newer than others, and cord grips are used as the watertight fittings. Though there is an empty knockout, it is not large enough for the cables or conduit to fit with an appropriate sealing fitting (bootshrink or cord grip).

Figure B-9: Cable entries into the top of power panel 1DS-4P.

B.2.1.2 Panel 2DS-4P

Figure B-10 shows the top of power panel 2DS-4P. NILM Conxall cables and voltage leads in conduit will enter through two new holes in this section of the panel. As can be seen, many cords enter the panel, some newer than others, and cord grips are used as the watertight fittings.

B.2.2 Inside the Panel

This step will also require the assistance of the SF EM. **To begin, the SF EM will tag out the entire panel to be installed upon IAW the shipboard tag out and electrical safety procedures. The SF EM will then remove the front casing on the power panel, and ensure power is secured using a multi-meter IAW all shipboard electrical safety procedures.**

Figure B-10: Cable entries into the top of power panel 2DS-4P.

B.2.2.1 Current Transducer Installation

Once confirmed that power has been secured to the panel, the SF EM will remove the lugs on the power cables feeding the panel for each phase. This will allow the current transducers to be installed on each power cable by slipping them over the open lugs. Then, the SF EM will reinstall the power cable lugs.

Next, MIT RLE graduate students will secure the current transducers using zip ties and connect the Conxall cables to the current transducers. Figure B-11 shows the end result of the current transducers and Conxall cables inside the electrical panel on USCGC SPENCER (WMEC 905). As is shown, the current transducers and Conxall cables are neatly organized inside the panel and secured with zip ties.

B.2.2.2 Voltage Lead Installation

The next step in the internal panel installation is to wire the voltage leads into the spare breaker. As is shown in Figure B-12, there are adequate spare breakers for installation on both panels. For the starboard panel, the MIT RLE team proposes using the 1DS-4P-1 spare breaker shown in the upper left corner of Figure B-12a. For

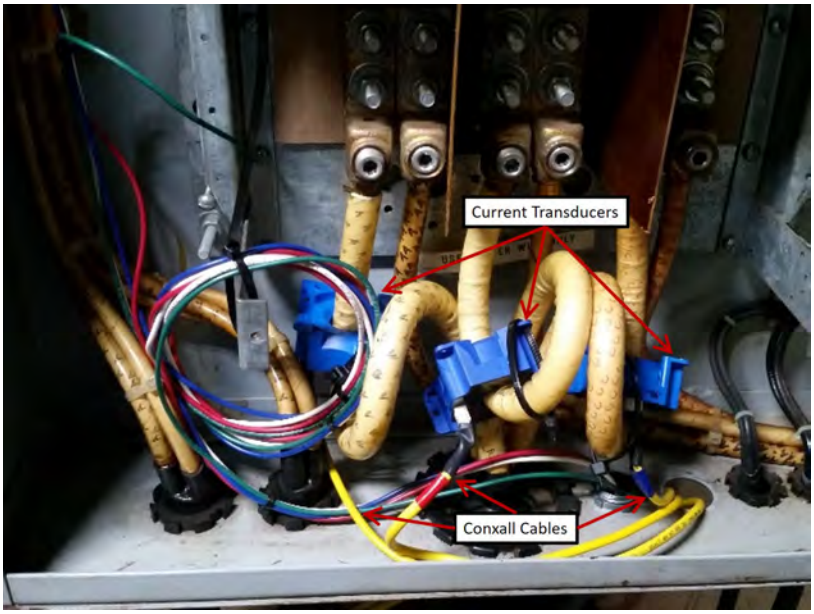

Figure B-11: Current transducers and Conxall cables installed on power cables feeding an electrical panel on USCGC SPENCER (WMEC 905).

the port panel, the MIT RLE team proposes using the 2DS-4P-4 breaker shown in the upper right corner of Figure B-12b.

This step requires assistance from the SF EM once again. The SF EM will need to wire the 3 voltage leads into the designated spare breaker. Each lead will wire into one power phase on the breaker. Additionally, there is a ground lead that will need to lead to an appropriate ground location as determined by the SF EM. In previous installs ground bolts inside the panels have been used. Figure B-13 shows a complete voltage lead install on a spare breaker from USCGC SPENCER (WMEC 905).

Once the voltage leads are connected to the spare breaker, the current transducers are installed on the power cables, the Conxall cables are connected to the current transducers, the cables and wires from the NILM installation are neatly organized within the panel with zip ties, and bootshrink fittings are secured, the SF EM will close the panel and reenergize it IAW all electrical safety and tag out procedures.

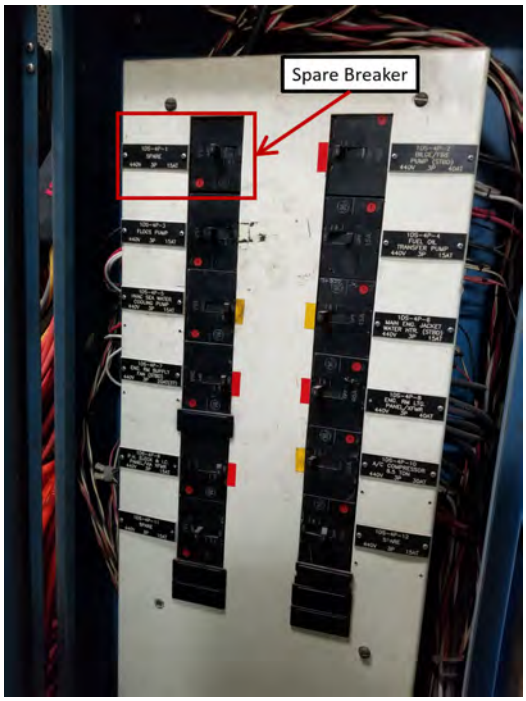

(a) 1DS-4P

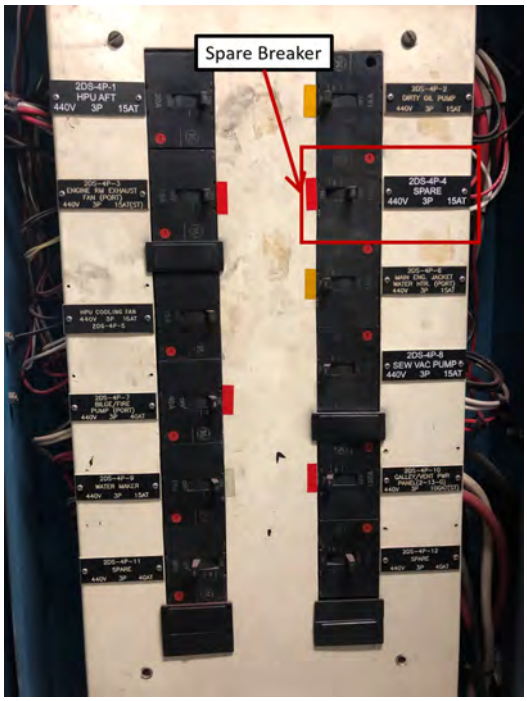

(b) 2DS-4P

Figure B-12: USCGC MARLIN (WPB 87304) Power Panels

B.3 Equipment Testing

Following all setup steps on the panels, the MIT RLE team will work to ensure the equipment is working correctly. This will include energizing all MIT equipment, as well as the downstream loads, to ensure proper operation of NILM sensors. In the event of poor or inept readings, the panels will need to be tagged out once again and hardware be adjusted to ensure proper data capture.

Once data is capturing correctly, the MIT RLE would like to energize all downstream loads if possible. This will provide the MIT RLE team with “test data" for each piece of equipment, allowing for it to be classified individually for processing and further understanding. Acquiring this data early allows for NILM Dashboard software to be customized to work for the 87’ Patrol Boat class as quickly as possible.

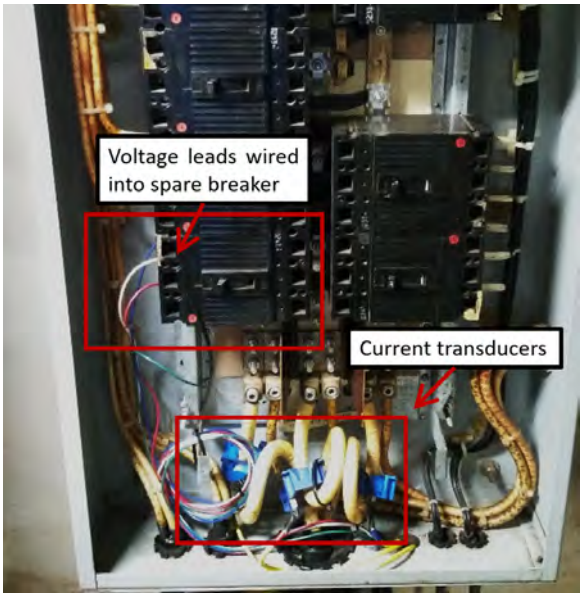

Figure B-13: Interior panel view on USCGC SPENCER (WMEC 905) showing voltage leads wired into a spare breaker as well as current transducers installed on power feed cables.

B.4 Equipment Removal

B.4.1 Electrical

This step will also require the assistance of the SF EM. To begin, the SF EM will tag out the entire panel which the NILM is being removed from IAW the shipboard tag out and electrical safety procedures. The SF EM will then remove the front casing on the power panel, and ensure power is secured using a multi-meter IAW all shipboard electrical safety procedures.

B.4.1.1 Current Transducer Removal

The first step in removing the NILM is securing power to the panels. Once confirmed that power has been secured to the panel, the SF EM will remove the lugs on the powercables feeding the panel for each phase. This will allow the current transducers to be removed from each powercable by slipping them over the open lugs. Then, the

SF EM will reinstall the power cable lugs. MIT RLE Grad Students will take custody of the current transducers and remove conxall leads, zipties and any other equipment from inside the power panel. Next the SF EM will inspect the inside of the power panel to ensure it is clear of debris.

B.4.1.2 Voltage Lead Removal

The second step of the electrical uninstall is the removal of the voltage leads. This step requires assistance from the SF EM once again. The SF EM will need to unwire the 3 voltage leads from the designated spare breaker. Additionally the ground wire will need to be unwired. Once all voltage leads, current conxall cables, current transducers and zip ties are removed both MIT RLE Grad Students and SF EM will inspect the panel ensuring equipment is removed and the panel is in good working order. Upon concurrence that the panel is restored to the original condition the SF EM will close the panel and reenergize it IAW all electrical safety and tag out procedures.

B.4.1.3 Cable Holes

The bootshrink fitted holes into the panels will be sealed with bootshrink caps. This provides adequate watertightness and prevents intrusion into the energized panel. MIT RLE students will provide the caps and install caps under SF supervision.

B.4.2 Hardware

Because the mechanical portion of the supporting bracketry is temporary there will be no permanent alterations to the physical structure of the vessel. MIT RLE students will remove all associated bolts, nuts, brackets and hardware mounting under the supervision of SF. All cable runs will be removed and NILM hardware and cabling

will be removed by MIT RLE students after the electrical portion of the system has been removed.

B.5 Conclusion

This document summarizes the steps necessary for the MIT RLE NILM installation onboard USCGC MARLIN (WPB 87304). Further information regarding the nature of this project can be found by contacting the US Coast Guard graduate students at MIT (listed below). The details of the project proposal can be found in the Research Proposal. Further details regarding MIT and the Coast Guard's roles with regard to this situation can be found in the Memorandum of Agreement between MIT-RLE and SFLC-ESD.

Appendix C

USCGC Margaret Norvell Dive Plan

This appendix outlines the steps taken by a contracted dive team to complete chapter 3 of this report. This report was given to the contracted divers and the Coast Guard members. This is a detailed description of exactly how the dive evolution was accomplished in order to gather pertinent readings in determining if the ICCP can penetrate the stern tube housing.

a. Diver enters the water

i. Connect 02 magnetic reference electrode forward and aft of the Port anode (see Figure 1)

ii. Remove one screw from each cover plate (03 screws total, see figure 2).

iii. Replace each screw with the provided plastic reference electrode screws (03 screws).

iv. Connect 03 plastic reference electrode screws to the corresponding orange extension cable (see Figure 3)

b. Diver exits the water

i. MIT Takes readings with old zincs attached without ICCP.

ii. Turn ICCP on from the Engine Room.

iii. Notify EPO and log the change.

iv. MIT takes readings with old zincs attached and ICCP turned on

v. Turn ICCP off.

vi. Notify EPO and log the change.

c. Diver enters the water

i. Mark each cover plate as to the position and orientation.

ii. Unscrew orange cable from plastic reference electrode screws

iii. Retrieve plastic reference electrode screws from the water

iv. Remove the stern tube covers.

v. Remove the stern tube anodes from each cover.

vi. Reinstall stern tube covers using old screws with one screw removed from each stern tube cover (03 screws in total).

vii. Replace the missing screws with the provided plastic reference electrode screws (03).

viii. Connect 03 plastic reference electrode screws to the corresponding orange extension cable (see photo 3)

d. Diver exits the water

i. MIT takes readings without zinc without ICCP

ii. Turn ICCP on.

iii. Notify EPO and log the change.

iv. MIT takes readings without zincs with ICCP turned on.

v. Turn ICCP off.

vi. Notify EPO and log the change.

e. Diver Enters the water

i. Unscrew orange cable from plastic reference electrode screws

ii. Remove the plastic reference electrode screw.

iii. Retrieve the plastic reference electrode screws from the water.

iv. Remove the stern tube covers and screws.

f. Diver exits the water

i. Replace zinc anodes on the stern tube covers.

g. Diver enters the water

i. Reinstall stern tube covers using 39 new stern tube cover screws, P/N: 90585A626 (one screw removed from each stern tube cover, 03 in total)

NOTE: There is no torque value required, do not over tighten.

ii. Tighten the stern tube cover screws.

iii. Replace each missing 03 screws with the plastic reference electrode screws.

iv. Connect 03 plastic reference electrode screws to the corresponding orange extension cable (see photo 3)

h. Diver exits the water

i. MIT Takes readings with new zincs attached without ICCP

ii. Turn ICCP on

iii. Notify EPO and log the change.

iv. MIT takes readings with new zincs attached and ICCP turned on

v. Turn ICCP off

vi. Notify EPO and log the change.

i. Diver enters the water

i. Remove the plastic reference electrode screws

ii. Reinstall 03 missing stern tube cover screws P/N: 90585A626 NOTE: There is no torque value required, do not over tighten.

iii. Tighten the stern tube cover screws.

iv. Remove 02 magnetic reference electrodes near the Port anode

j. Diver exits the water

Notes: Document the percentage of old stern tube anodes remaining for each anode on the sign-off sheet table for the appropriate anode. Install the 16 new stern tube anodes, P/N: Z0020202H3 REV. 0, onto each cover plate with 32 new self-locking nuts, P/N: 90715A145. WARNING FOLLOW PROPER LIFTING TECHNIQUES WHEN HANDLING HEAVY OBJECTS. OBJECTS WEIGHING OVER 50 LBS REQUIRE AT LEAST TWO PERSONNEL TO SAFELY MOVE THEM. FAILURE TO COMPLY MAY RESULT IN SERIOUS PERSONAL INJURY. Some type of aiding device may be required, at least for the fwd bearing aft covers, which weigh in excess of 100 lb each.

THIS PAGE INTENTIONALLY LEFT BLANK

Bibliography

[1] D. Faram, Mark, "The first fast response cutter," 2012.

[2] A. Zayed, Y. Garbatov, and C. Guedes Soares, "Corrosion degradation of ship hull steel plates accounting for local environmental conditions," *Ocean Engineering*, vol. 163, no. 1, pp. 299–306, 2018.

[3] United States Coast Guard, *CATHODIC PROTECTION SYSTEM - MODEL CA44227*, Department of Homeland Security, Sep 2018.

[4] B. Somerday and P. Sofronis, "Hydrogen uptake and embrittlement susceptibility of ferrite-pearlite pipeline stee.s," *ASME*, pp. 800–808, 2017.

[5] American Bureau of Shipping, *Cathodic Protection of Ships*, American Bureau of Shipping Incorporated by Act of Legislature of the State of New York 1862, 2017.

[6] United States Coast Guard, *154 WPC 161 310 Stern Tube Drawing*, Department of Homeland Security, Sep 2012.

[7] American Bureau of Shipping, *Materials and Welding*, American Bureau of Shipping Incorporated by Act of Legislature of the State of New York 1862, 2019.

[8] O. Todoshchenko, Y. Yagodzinskyy, and H. Hänninen, "Hydrogen uptake and embrittlement susceptibility of ferrite-pearlite pipeline steels," 01 2018.

[9] *Cathodic Protection of Ships*, American Bureau of Shipping, December 2017.

[10] C. C. Youngren, *Modern Marine Engineer's Manual, Vol. II.* Cornell Maritime Press, 2002, ch. 22.

[11] M. M. E. Gohary and I. S. Seddiek, "Utilization of alternative marine fuels for gas turbine power plant onboard ships," *International Journal of Naval Architecture and Ocean Engineering*, vol. 5, no. 1, pp. 21–32, 2013.

[12] D. B. Gaylo, personal communication, September 2022.

[13] C. G. Googan, *Marine corrosion and cathodic protection*, first edition. ed. Abingdon, Oxon: CRC Press, 2022.

[14] M. Bishop, "Preventing Stern Tube Corrosion Through Shipboard Cathodic Protection," Master's thesis, Massachusetts Institute of Technology, 2023.

[15] Department of Defense, *Coverings for Waterborne Main Propulsion Shafting on U.S. Naval Surface Ships and Submarines*, Department of Defense, 2020.

[16] E. Skjong, E. Rødskar, M. Molinas, T. A. Johansen, and J. Cunningham, "The marine vessel's electrical power system: From its birth to present day," *Proceedings of the IEEE*, vol. 103, no. 12, pp. 2410–2424, 2015.

[17] J. Paris, J. S. Donnal, and S. B. Leeb, "NilmDB: The non-intrusive load monitor database," *IEEE Transactions on Smart Grid*, vol. 5, no. 5, pp. 2459–2467, 2014.

[18] J. Paris, J. S. Donnal, Z. Remscrim, S. B. Leeb, and S. R. Shaw, "The sinefit spectral envelope preprocessor," *IEEE Sensors Journal*, vol. 14, no. 12, pp. 4385–4394, 2014.

[19] A. Aboulian, D. H. Green, J. F. Switzer, T. J. Kane, G. V. Bredariol, P. Lindahl, J. S. Donnal, and S. B. Leeb, "Nilm dashboard: A power system monitor for electromechanical equipment diagnostics," *IEEE Transactions on Industrial Informatics*, vol. 15, no. 3, pp. 1405–1414, 2019.

[20] S. B. Leeb, P. Lindahl, D. Green, T. Kane, J. Donnal, and S. Kidwell, "Power as predictor and protector," *Society of Naval Architects and Marine Engineers (SNAME) Marine Technology*, 2019.

[21] E. Skjong, T. A. Johansen, M. Molinas, and A. J. Sørensen, "Approaches to economic energy management in diesel–electric marine vessels," *IEEE Transactions on Transportation Electrification*, vol. 3, no. 1, pp. 22–35, 2017.

[22] B. Mills, "Solving Time-Alignment Challenges in Shipboard Non-Intrusive Load Monitoring," Master's thesis, Massachusetts Institute of Technology, 2021.

[23] S. Allen, E. Ashey, D. Gore, J. Woerner, and M. Cervi, "Marine applications of fuel cells: A multi-agency research program," *Naval Engineers Journal*, vol. 110, no. 1, pp. 93–106, 1998.

[24] N. Doerry, "Naval power systems: Integrated power systems for the continuity of the electrical power supply." *IEEE Electrification Magazine*, vol. 3, no. 2, pp. 12–21, 2015.

[25] B. T. Mills, D. H. Green, J. S. Donnal, and S. B. Leeb, "Power monitoring beyond radial distribution networks," *IEEE Transactions on Instrumentation and Measurement*, vol. 71, pp. 1–9, 2022.

[26] J. D. McDonald, *Electric power substations engineering*, 3rd ed., ser. Electrical engineering handbook. CRC Press, 2012.

[27] M. M. Islam, *Shipboard power systems design and verification fundamentals*. Piscataway, New Jersey: IEEE Press, 2018.

[28] M. D. A. Al-Falahi, T. Tarasiuk, S. G. Jayasinghe, Z. Jin, H. Enshaei, and J. M. Guerrero, "Ac ship microgrids: Control and power management optimization," *Energies*, vol. 11, no. 6, 2018.

[29] F. Chen, R. Burgos, D. Boroyevich, J. C. Vasquez, and J. M. Guerrero, "Investigation of nonlinear droop control in dc power distribution systems: Load sharing, voltage regulation, efficiency, and stability," *IEEE Transactions on Power Electronics*, vol. 34, no. 10, pp. 9404–9421, 2019.

[30] N. Doerry, "Optimal generator set loading for energy efficiency," *Naval Engineers Journal*, vol. 134, no. 2, pp. 101–111, June 2022.

[31] R. E. Cosse, M. D. Alford, M. Hajiaghajani, and E. R. Hamilton, "Turbine/-generator governor droop/isochronous fundamentals - a graphical approach," in *2011 Record of Conference Papers Industry Applications Society 58th Annual IEEE Petroleum and Chemical Industry Conference (PCIC)*, 2011, pp. 1–8.

[32] U. Orji, C. Schantz, S. B. Leeb, J. L. Kirtley, B. Sievenpiper, K. Gerhard, and T. McCoy, "Adaptive zonal protection for ring microgrids," *IEEE Transactions on Smart Grid*, vol. 8, no. 4, pp. 1843–1851, 2017.

[33] P. A. Lindahl, D. H. Green, G. Bredariol, A. Aboulian, J. S. Donnal, and S. B. Leeb, "Shipboard fault detection through nonintrusive load monitoring: A case study," *IEEE Sensors Journal*, vol. 18, no. 21, pp. 8986–8995, 2018.

[34] D. H. Green, S. R. Shaw, P. Lindahl, T. J. Kane, J. S. Donnal, and S. B. Leeb, "A multiscale framework for nonintrusive load identification," *IEEE Transactions on Industrial Informatics*, vol. 16, no. 2, pp. 992–1002, 2020.

[35] U. S. C. G. Commandant, *Reimbursable Standard Rates*, Department of Homeland Security, March 2017.

[36] T. Kane, "The NILM Dashboard: Shipboard Automatic Watchstanding and Real-Time Fault Detection using Non-intrusive Load Monitoring," Master's thesis, Massachusetts Institute of Technology, 2019.

[37] D. Green, T. Kane, S. Kidwell, P. Lindahl, J. Donnal, and S. Leeb, "NILM dashboard: Actionable feedback for condition-based maintenance," *IEEE Instrumentation Measurement Magazine*, vol. 23, no. 5, pp. 3–10, 2020.

[38] Naval Sea Systems Command 310, *DDS 310-1 Electric Power Load Analysis (EPLA) for Surface Ships*, Department of Defense, Sep 2012.

[39] Naval Sea Systems Command 200, *DDS 200-1 Calculation of Surface Ship Endurance Fuel Requirements*, Department of Defense, Oct 2011.

[40] T. Deeter, D. H. Green, S. Kidwell, T. J. Kane, J. S. Donnal, K. Vasquez, B. Sievenpiper, and S. B. Leeb, "Behavioral modeling for microgrid simulation," *IEEE Access*, vol. 9, pp. 35 633–35 645, 2021.

[41] J. V. Amy Jr., N. H. Doerry, T. J. McCoy, and E. L. Zivi, "Shipboard controls of the future," *Naval Engineers Journal*, vol. 109, no. 3, pp. 143–152, May 1997.